Development of Impedimetric Biosensors, Based on Phage-Modified Microarrays, for the Direct and Specific Detection of Bacteria

Arghavan Shabani

A Thesis

In the Department

of

Chemistry and Biochemistry

Presented in Partial Fulfillment of the Requirements
For the Degree of Doctor of Philosophy at
Concordia University

Montreal, Quebec, Canada
April 2010

Your file Votre référence
ISBN: 978-0-494-67330-0
Our file Notre référence
ISBN: 978-0-494-67330-0

Abstract

Bacteriophages (or phages) are viruses that replicate only by entering specific host bacteria. This property has facilitated their application in specific pathogen detection. This thesis will address these issues with regard to the development of phage-based methods for the detection of bacteria.

We present a novel approach for the specific detection of *E. coli K12* and *B. anthracis Sterne* bacteria, using bacteriophages as probes. We have also adapted this system to allow for separation of specific bacteria in more complex (real) samples using phage-coated magnetic beads and a simple magnetic manipulation system.

The bacteriophages were attached to electrochemically functionalized screen-printed carbon electrode (SPE) microarrays using two different methods.

In the first method, T4 phage which specifically recognizes *E. coli K12*, was immobilized onto SPE networks that were electrochemically functionalized using 1-ethyl-3-(3-dimethylaminopropyl)-carbodiimide (EDC) in acidic media. In the second method, Gamma phage that specifically recognizes *B. anthracis Sterne* was immobilized onto SPE networks that were functionalized in two steps: by electrochemically generating phenyl-amino groups at the SPE surface, followed by reaction with glutaraldehyde to act as a linker. SPE surface functionalization and phage immobilization were confirmed using XPS and TOF-SIMS analysis. The phage-modified SPEs were then used to specifically detect target bacteria. Impedance measurements in the form of Nyquist plots (imaginary impedance (Z_i) versus real impedance (Z_r)) show shifts due to binding of the bacteria to the phage. No significant

change in impedance was observed due to binding of non-target bacteria strains. The presence of surface bound bacteria was verified by scanning electron and fluorescence microscopies. Based on these results, the feasibility of using these microarrays for the direct and specific impedimetric detection of bacteria has been demonstrated.

Acknowledgements

First of all, I would like to express my great appreciation to my research supervisors, Dr. Marcus Lawrence for his excellent coaching, the best guidance and strong support throughout my academic career. Not only has he encouraged me to pursue my interest in scientific research, but he has also reinforced my ability to work independently. Thank you for your patience, support, and your good humor. I also gratefully acknowledge Dr. Rosemonde Mandeville, President and CEO of Biophage Pharma Inc., for her strong scientific support, and for allowing me to use the facilities at Biophage. I would like to sincerely thank all the people that I have had the opportunity to work with during my Ph.

I wish to thank my research committee Dr. Louis Cuccia and Dr. Christopher Wilds for their constructive criticism and advice throughout the years, and their reading of this entire piece of work. Many thanks also to my external examiners Dr. Mark Trifiro (McGill) and Dr. Paula Wood-Adams (Concordia) for agreeing to review this manuscript and for making my defense possible.

I wish to acknowledge the financial support received from the Natural Sciences and Engineering Research Council of Canada (NSERC), in the form of an Industrial Postgraduate Scholarship.

Also, I would like to thank the Laboratoire de Génie Enzymatique et Biomoléculaire, ICBMS UMR5246 - Université Lyon 1 - CNRS (Dr. C. A. Marquette and Prof. L. J. Blum) for providing the screen-printed carbon arrays.

Finally, this would not be complete without acknowledging the love and support of my family and friends both in Iran and Canada. Their help and encouragement facilitated the

work in this thesis. Leaving Iran was one of the hardest things that I've ever done (apart from writing this thesis!), but I'm glad I did because this was a great experience for me. Thank you all.

Table of Contents

List of Figures

List of Tables

List of Schemes

Lists of Abbreviations

EDC	1-Ethyl-3-(3-dimethylaminopropyl)-carbodiimide
SPEs	Screen-printed electrodes
RNA	Ribonucleic acid
DNA	Deoxyribonucleic acid
CFU	Colony forming unit
PFU	Phage forming unit
Z	Impedance
V	Potential
I	Current
Z_r	Real impedance
Z_i	Imaginary impedance
EIS	Electrochemical impedance spectroscopy
SEM	Scanning electron microscopy
XPS	X-ray photoelectron spectroscopy
GFP	Green fluorescence protein
D.L	Detection limit

CHAPTER 1
LITERATURE REVIEW

1.1 An introduction to bacteriophage

The observation of bacteriophages was first reported by British bacteriologist Frederick W. Twort in 1915. In an attempt to grow *Vaccinia virus* using agar medium, in the absence of living cells, he observed the growth of numerous micrococci colonies which he interpreted as being due to contamination of the *Vaccinia* pulp by other bacteria. Twort's publication in the journal Lancet documented this phenomenon as a "glassy transformation". He concluded that the appearance of "transparent dissolving material" might be: (i) an ultra-microscopic virus, (ii) part of the life cycle of the bacterium, or (iii) an enzyme with the power of growth [1, 2].

Two years after Twort's discovery a French Canadian bacteriologist named Felix d'Herelle, working at the Pasteur Institute in Paris, discovered a microbe that was "antagonistic" to the bacteria causing their lysis and producing clear spots in the surface of agar covered with bacteria. He was more confident as to the nature of this discovery, he believed that it was a bacteriolytic agent and termed it bacteriophage or bacteria-eater (from the Greek phago, which means 'to eat').

He reported his results in 1921 in the book entitled: *Le bactériophage: Son rôle dans l'immunité*. At the time he assumed that one single bacteriophage could be used against different bacteria species, which is not a surprising assumption when one considers that

virus classification was still in its infancy. Between 1924 and 1934, an Australian scientist named Burnett rejected d'Herelle's theory of a single bacteriophage being effective for a wide range of bacteria, and identified a variety of viruses that demonstrated different physical and biological properties, which enabled them to conserve their characteristics[3].

1.1.1 The nature of bacteriophages

Bacteriophages are small viruses that recognize specific receptors on the bacterial surface, to which they bind and then proceed to inject their genetic material. These viruses recognize target bacteria through receptors located on their tail. The target host of each phage is often narrowed to one species of bacteria but several related species can sometimes be infected by the same phage. In effect, it is now well accepted that interactions between phages and bacteria are highly specific. They are very abundant organisms on earth. They can be found in large numbers wherever their host bacteria exist, such as in the soil, in sewage and feces, and in the water [2].

As in the case of other viruses, phages are absolute parasites. They have no ability to generate energy and they have no ribosomes to produce proteins. They inject/transfer all the information for their production to an appropriate host. Each phage converts an infected bacterium into a phage-manufacturing system, which yields a large number of phage progeny. The degree to which different phages use part of the genetic machinery of the host varies. Some phages have fewer than 10 genes and they are totally dependent on

bacteria cells, while some other phages have 30 to 100 genes and they are dependent on proteins encoded by their own genetic material [4].

1.1.2 Bacteriophage structure and composition

Different types of phages vary in size and shape. The size of most phages ranges from 25 to 200 nm and the structure of the majority of phages is composed of a capsid (or head, which contains the genetic material), and a tail.

The genetic material contains the nucleic acid genome (DNA or RNA) of the specific phage, covered by a protein coating which forms the capsid. The capsid is composed of many copies of different proteins which act to protect the genetic material from harmful substances. The tail is a hollow tube surrounded by a contractile sheath through which the nucleic acid passes and ends up being injected into the bacteria. At the end of the tail, there is a base plate and fibers, which enable phages to bind to the bacteria cells. It should be reiterated however that not all phages possess the tail and sheath [2]. The structure of phage T4 is shown in Figure 1.1 as a model system.

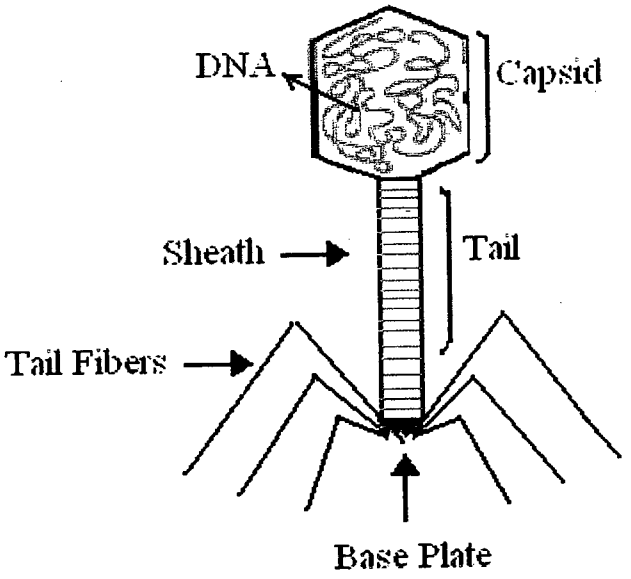

Figure 1.1 Structure of phage T4

1.1.3 Phage replication

As mentioned above, compared to other viruses, phages don't possess the internal machinery for self-replication and they rely on the host bacteria. The replication cycle differs based on the type of phage, but general commonalities exist for various phages. For example, what are referred to as the lytic cycle and lysogenic replicative cycle are used by the phage T4 and the phage lambda, respectively. The typical lytic cycle is described below.

1.1.3.1 Adsorption

Attachment occurs if the host bacteria cell surface contains specific receptors for the phages, such as cell-wall lipopolysaccharides, proteins, teichoic acids, pili or flagella [2]. In the case of T4 phage, the most studied phage, the fibers and the contractile tail are responsible for the attachment. As more of the fibers come into contact with the surface receptors of the cell, the tail of the phage settles down onto the surface. In T4-like phages there are at least three of the six long fibers that get bound to the primary receptor, then the base plate rearranges and binds irreversibly to the second receptor. Adsorption velocity and efficiency depend on the external (environmental) factors and the physiological properties of the host. The presence of specific cofactors such as calcium and magnesium (or simply any divalent cation) has a positive effect on the formation of the electrostatic bond between the tail fibers of the phage and the bacteria cell receptors and, consequently, the rate of attachment. The absence of such ions effectively prevents adsorption and phage multiplication [5].

1.1.3.2 Penetration and infection

Once the phage successfully attaches to the target bacteria, it proceeds to transfer (inject) its genetic material through the central tube into the cytoplasm of the host. In the first instance, conformational changes occur in the phage structure that cause the tail sheath to contract, forcing the central tube up against the bacteria wall and the insertion of the

DNA into the host cell. After the introduction of phage DNA into the bacteria cell, synthesis of the host DNA and protein is suppressed. This results in the host DNA production being degraded into nucleotide components, providing building blocks for the viral DNA synthesis, and preventing further host gene expression.

The viral DNA synthesis starts within 5 minutes of infection and is quickly followed by the synthesis of the capsid and other proteins, which are then assembled to form the phage structure. The number of phages that subsequently form usually varies between 50 to a 100 phages per infected bacteria cell, the number depends however on the type of phage and physiology of the host [5]. For the phage T4, it takes approximately 15 minutes for the generation of the first few phages, and another 7 minutes for bacteria lysis to occur [6].

Late, in the infection cycle, phages synthesize two types of enzyme to lyse the host cells:

(i) Holin, which degrades the cytoplasm membrane.

(ii) Lysozyme, which destroys the cell-wall peptidoglycan.

These enzymes cause the cell to burst and release the newly formed phages [7].

1.1.4 The lysogenic cycle versus the lytic cycle

Two categories of bacteriophages have been identified: lytic and temperate phages. Based on these categories, the phage follows either the lytic or lysogenic life cycle[4]. In the lytic cycle, the phage converts a bacteria host cell into a phage factory to produce more phages, effectively destroying the bacteria (lysis) and releasing newly produced phages

for the infection of other hosts. The lysogenic cycle on the other hand, is typically observed with phages containing double-stranded DNA. In this case, the phage DNA attaches itself to the host chromosome and leads to the formation of a new set of phage called a prophage. Virulent phages such as T4 usually lyse and destroy the host cells, while temperate phages, such as phage lambda, can adopt either the lytic or the lysogenic cycle [4].

The key factor dictating whether the lytic or the lysogenic pathway becomes operational is the relative expression rates of the phage repressor encoded by the *cII* gene (which promotes lysogeny) and the *cro* protein, to be able to switch off the expression of the repressor gene and initiate the lytic pathway[4]. For example, after infection of the host cells by phage lambda, a small proportion of these phages adopt the lytic pathway, while the majority of the phages enter the lysogenic cyle. These phages continue to replicate and produce clones of themselves containing phage DNA, and prevent further infection of bacteria.

1.2 Bacterial structure and shape

Bacteria are microscopic organisms which differ in size, shape, and metabolism. Bacterium cells are much smaller and simpler in structure than eukaryotic cells, and are called prokaryotic cells. In comparison to eukaryotic cells, bacteria cells lack a nuclear membrane and their chromosome structure is composed of single stranded DNA. The individual bacteria have various shapes based on the species. There are three main shapes

that bacteria cells can adopt: spherical- shaped are termed cocci (e.g. *Streptococcus*), rod-shaped (e.g. *Bacillus*), curved-shaped (e.g. *Spirillum*) [5].

1.2.1 Bacteria cell composition

The cytoplasm of bacteria is a gel-like matrix composed of water, enzymes, nutrients, and contains cell structures such as ribosomes, chromosomes, and inclusion granules (granules that store products such as glycogen and lipids). Ribosomes translate mRNA into protein. The genetic material is located in the region called nucleoid. Some species of bacteria have a capsule, which is an additional protective shell composed of polysaccharides. The most important role of the capsule is to keep the bacterium from drying out and to protect it from larger microorganisms.

Outside the cell wall there is one or more flagella, which are responsible for the mobility of the bacteria and most likely have an important role in the spread of disease. Many species of bacteria have what is called pili, a small hair-like structure outside the cell surface enabling the bacteria to attach to other cells. Without the pili bacteria are not able to attach to host cells [6]. Figure 1.2 illustrates a bacteria cell structure.

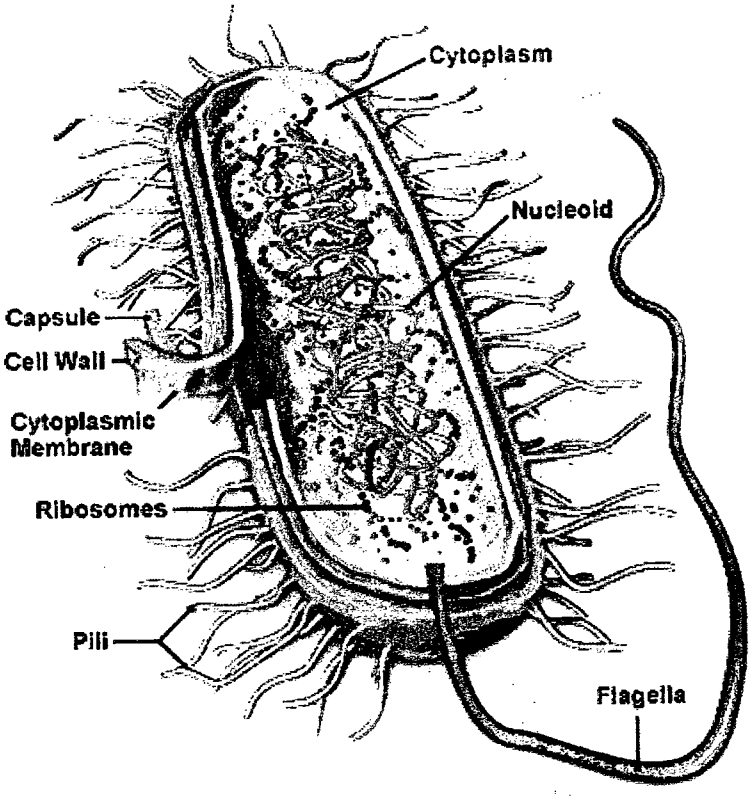

Figure 1.2 Bacteria cell structure [8]

1.2.2 Bacteria cell wall

The first layer serving to encapsulate the bacteria machinery is the cytoplasmic membrane. The cell wall lies outside the cell membrane and is made up of a special

polymer called peptidoglycan. Peptidoglycan provides for mechanical strength of the cell and is composed of *N*-acetyl glucosamine and *N*-acetyl muramic acid molecules.

Bacteria have been divided into two categories, based on the structure of the cell wall: Gram-positive and Gram-negative. The cell wall of Gram-positive bacteria contains many layers of peptidoglycan, which makes them thicker than Gram-negative bacteria. Other polymers such as teichoic acid can be found in the cell walls of Gram-positive bacteria. Figure 1.3 illustrates cell walls of Gram-positive and Gram-negative bacteria.

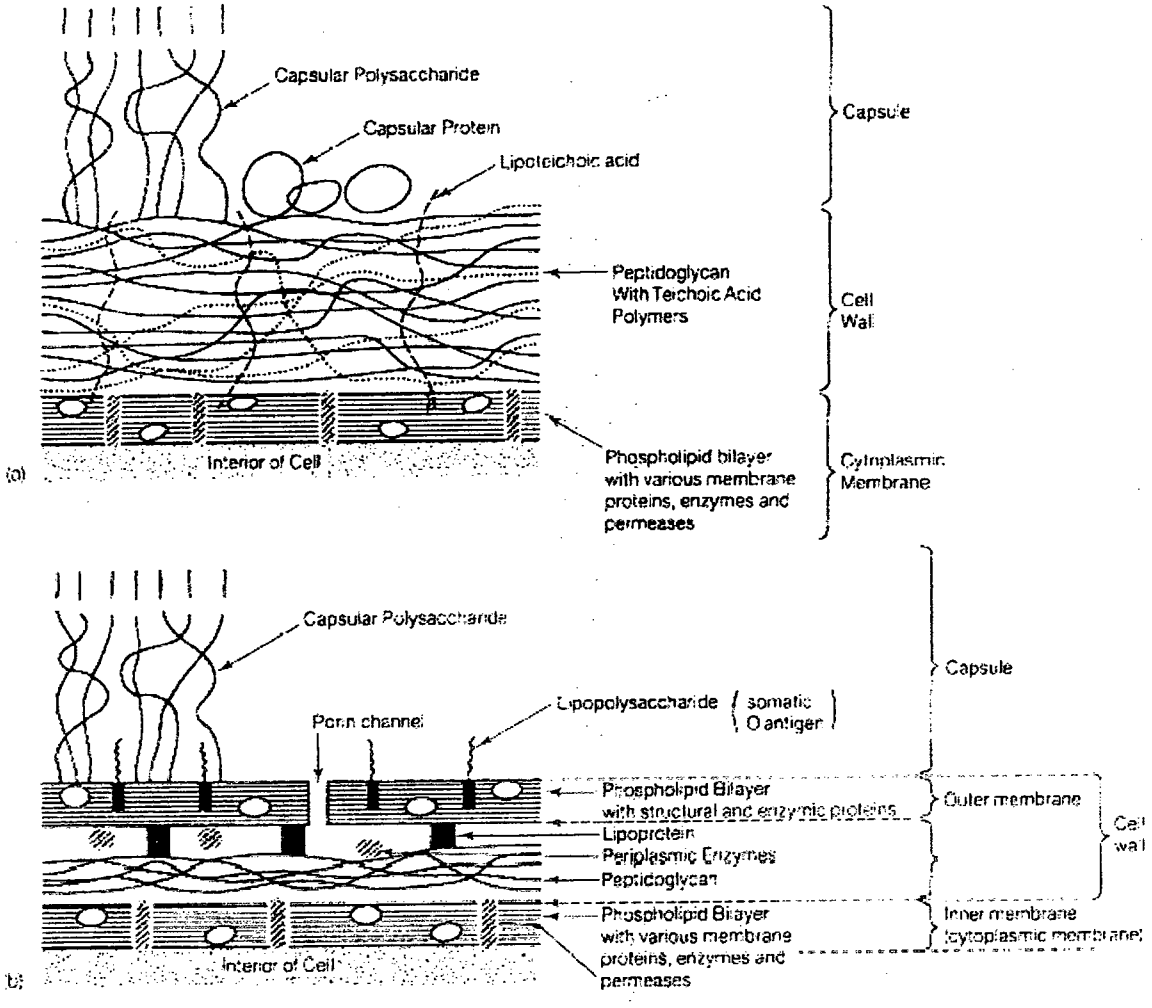

Figure 1.3 Structure of cell walls of Gram-positive (a), and Gram-negative bacteria (b) [9]

The cell wall of Gram-negative bacteria is much thinner but they are more complex. Outside the inner cytoplasmic membrane lies the cell wall which contains the peptidoglycan, in addition to lipoprotein and periplasmic enzymes. There is then a third layer, an outer membrane beyond the peptidoglycan-based cell wall, containing protein

channels (porins) that allow for easy passage of molecules. The outer side of this membrane contains lipopolysaccharides providing the antigenic property of the surface[9]. Gram staining is a method that can be used to distinguish between Gram-positive and Gram-negative bacteria. This method is based on the bacteria's ability to resist de-coloration after staining with a crystal violet-iodine dye complex in the presence of acetone or alcohol. The Gram-positive bacteria appear dark-blue or purple because the structure of their cell wall allows for trapping of the dye, whereas Gram-negative bacteria are de-colorized because the cell wall is thin and releases the dye. This technique was named after Christine Gram who developed it in 1884 [10].

1.3 Bacteria contamination and disease

Bacteria are microorganisms that can spread easily and rapidly in a moist environment at favorable temperatures. They may affect animals and humans, causing a variety of infectious diseases. Many infectious diseases result from food and water contamination by pathogenic bacteria and they are the major cause of illness and death in many countries. Some types of bacteria are resistant to changes in environmental conditions and the disease they cause may result in a high fatality rate. It should be noted also that some of these pathogenic bacteria are considered to be potential biological warfare agents. Table 1.1 provides a list of more commonly known pathogenic bacteria, and for some of them, the infection they cause.

Bacterium	Site of infection / clinical syndrome
Bacillus anthracis	anthrax
Bacillus cereus	food poisoning / food-borne enteritis
Bacteroides sp.	abdominal sepsis, abscesses (including cerebral)
Bordetella pertussis	whooping cough
Campylobacter sp.	food-borne enteritis
Chlamydia pneumoniae	respiratory tract (atypical pneumonia)
Chlamydia trachomatis	genital tract, eye
Clostridium botulinum	botulism
Clostridium difficile	antibiotic-associated diarrhoea (inc pseudomembranous colitis)
Clostridium perfringens	gas gangrene, abdominal sepsis, food poisoning
Clostridium tetani	tetanus
Corynebacterium diphtheriae	diphtheria
other Corynebacterium sp.	urinary tract, 'line' colonisation / infection
Enterococcus spp. (formerly Streptococcus)	urinary tract, 'line' colonisation / infection, abdominal sepsis
Escherichia coli	urinary tract, abdominal sepsis, neonatal septicaemia / meningitis
Haemophilus influenzae	non-capsulate: respiratory tract (inc exacerbation COAD, middle ear)
Helicobacter pylori	atrophic gastritis, peptic ulcer disease
Klebsiella sp.	urinary tract, abdominal sepsis
Legionella pneumophila	Legionnaires disease (Pontiac fever, 'atypical' pneumonia)
Listeria monocytogenes	septicaemia / meningitis (esp neonates & immunosuppressed)
Moraxella catarrhalis	respiratory tract (inc exacerbation COAD, middle ear)
Mycobacterium leprae	leprosy
Mycobacterium tuberculosis	tuberculosis
other Mycobacterium sp.	rarely tuberculosis, possibly other infections in immunosuppressed
Mycoplasma pneumoniae	respiratory tract ('atypical' pneumonia)
Neisseria gonorrhoeae	gonnorhoea
Neisseria meningitidis	septicaemia / meningitis
Proteus sp.	urinary tract, abdominal sepsis

Pseudomonas aeruginosa	urinary tract, abdominal sepsis, respiratory tract in cystic fibrosis patients
other Pseudomonas sp.	'line'; colonisation / infection
Salmonella typhi /paratyphi	typhoid fever
other Salmonella sp.	food-borne enteritis
Shigella sp.	food-borne enteritis
Staphylococcus aureus	skin & soft tissue (eg abscess / cellulitis / fascitis), food poisoning & other toxin-mediated disease, endocarditis, osteomyelitis
Staphylococcus epidermidis	'line' colonisation / infection (& other prostheses)
Streptococcus agalactiae (Group B -haemolytic)	neonatal septicaemia / meningitis
Streptococcus pneumoniae	respiratory tract (including lobar pneumonia, exacerbation COAD, middle ear), meningitis
Streptococcus pyogenes (Group A -haemolytic)	skin & soft tissue (eg abscess / cellulitis / fascitis), pharyngitis (rheumatic fever, glomerulonephritis)
Streptococcus viridans	bacterial endocarditis
Vibrio cholerae	food-borne enteritis including cholera

Table 1.1 A list of pathogenic bacteria and related diseases (reformatted from microbiologybytes website [11])

In the last decade, *E.coli* has become one of the most important organisms that cause disease. *E.coli* can easily spread and contaminate food such as ground beef, raw milk, and chicken. *E.coli* O157:H7, first discovered in 1982, is the strain that is the most dangerous food-born pathogen. This bacteria strain produces a large amount of potent toxin, causing several types of damage such as hemolytic uremic syndrome and hemorrhagic colitis. Both cases cause watery diarrhea, followed by bloody diarrhea, kidney failure and in

some cases death (especially in children) [12]. It has been determined that the *E.coli* O157:H7 strain is responsible for over 20,000 cases of diarrhea per year in the United States [9].

Salmonella is a Gram-negative bacteria and another food-born pathogen producing infectious diseases such as salmonellosis, typhoid fever, or other problems. Typhoid fever caused by *S. typhi* leads to 600,000 deaths annually, most cases occurring in South Asia, Africa, and South America [13]. Generally, infectious dosages by pathogenic bacteria such as *Salmonella* and *E.coli* are as low as 10 cells/mL [14], thus effective and sensitive methods for screening these microorganisms are essential.

1.4 Bacteria detection methods

The widespread incidents of bacterial contamination of our environment, mainly related to our food and water resources, demand the development of effective testing and analysis techniques that specifically target these microorganisms. Effective testing requires methods of analysis that meet a number of challenging criteria such as short detection time and selectivity. In the following section, we consider many approaches for bacteria detection, from conventional methods to biosensor-based techniques.

1.4.1 Conventional methods

The conventional approach to microbiological identification of bacteria involves plating and culturing methods, which allow a morphological evaluation of these microorganisms based on their ability to grow in various media. Almost all bacterial species can be detected using culture-based methods.

One of the media used for culture purposes is MacConky's agar, which was first used to isolate *Enterobacteriaceae* from water, food, and urine in 1905 [9] . This is a nutrient medium that contains bile salts, lactose, and an indicator. By replacing lactose in the standard MacConkey's agar with sorbitol, the agar media was used to detect *E.coli O157:H7* species by observing the formation colorless colonies. Lowenstein-Jensen (LJ) medium is another one that can be used to grow bacterial colonies. The LJ medium consists of glycerol, asparagine, some salts and egg, and was used to detect *Mycobacteria.* Blood agar and bismuth sulfate agar can also be used for the detection of *Bacillus* and *Salmonella* species, respectively.

Although plating and culturing provide reliable results, they are time consuming. Completion of all the steps can take at least a few days, to several weeks, depending on the species isolated. For example, *tubercle bacilli* produce visible growth in LJ medium in about two weeks, and adding to this the time for clinical isolation, the process can extend to eight weeks [9].

1.4.2 Instrumental methods of bacteria detection

General instrumental methods for bacteria detection include: microscopic methods, luminescence methods, flow cytometry, infra-red (IR) spectroscopy and mass spectrometry (MS). Among these methods, some have received less attention due to their limitations. For example, Rossi and Warner have reported on the identification of bacteria using IR spectroscopy in 1985 [15]. Using this approach, bacteria were introduced into the IR measurement cell and corresponding IR absorbance spectra were obtained. The main limitation of this technique is that the measurements of the chemical composition of the bacteria usually show similar (indistinguishable) results at the molecular level.

Mass spectrometry has also been used to detect *B. anthracis* [16-20] , but the method lacks sensitivity. Another drawback is that mass spectrometers are expensive, they are not portable, and the experiment cannot operate under atmospheric conditions. The infectious dose for *B. anthracis* has been reported to be approximately 10^4 spores, and few rapid detection methods using mass spectrometry can detect spore counts below 10^5 cfu/mL [21]. In contrast to IR and MS methods, microscopy and flow cytometry techniques do not provide data based on the chemical components of the microorganisms at the molecular level, thus they are more accurate and more commonly used.

In microscopy methods, by labeling the cells with a specific dye, it is possible to visualize and identify a wide range of bacteria. For example, Huang et al.[22] have successfully used fluorescence microscopy for the identification of *S. tythimium* cells.

The detection limit of the technique was reported to be 10^4 cfu/mL, with a total analysis time of 4 hours.

Luminescence-based systems have also been used for the detection of bacteria in the environment [23]. This detection approach is based on the oxidation of luciferin followed by light emission using ATP. The emission of light is proportional to the ATP concentration, and the process is catalyzed by luciferase.

Another interesting instrumental method is flow cytometry. Using a flow cytometer, cells are stained with a dye and injected into a stream of sheath fluid, and are kept at the center of the stream. The cells in the sample are accelerated and pass, individually, through a laser beam (Figure 1.4).

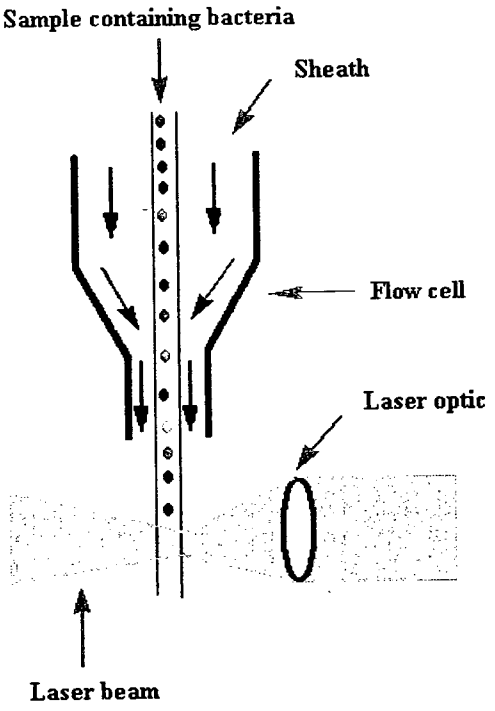

Figure 1.4 Schematic illustration of a flow cytometer

When a cell passes through the laser beam, it deflects the incident light. Light scattered from the interaction between the cell particle and the laser beam is collected by a lens and directed to the optical detectors. The detectors convert the light into an electrical signal. The light scattering gives information about cell size, shape and structure.

Forward-scattered light (FSC) is proportional to the surface area or size of a cell and side-scattered light (SSC) is proportional to the granularity or internal complexity of a cell [24] (Figure 1.5).

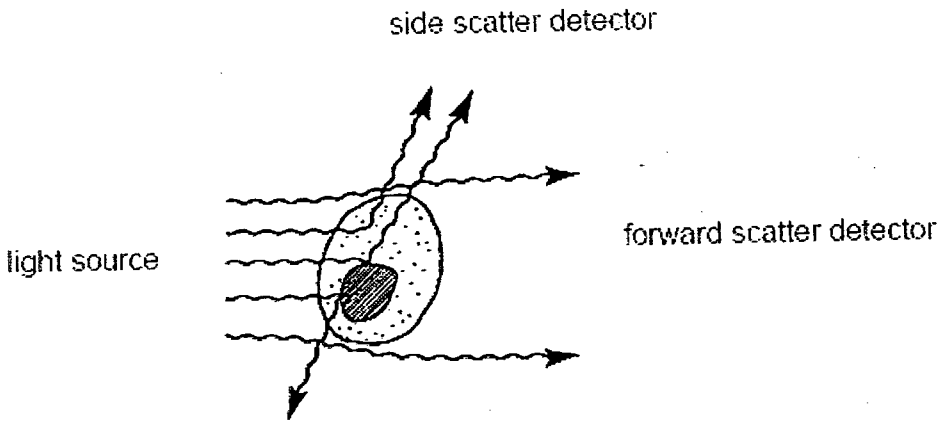

Figure 1.5 Light-scattering by a cell [24]

Flow cytometry is a practical technique for bacteria counting in clinical, environmental and industrial microbiology [25]. The method is rapid and provides the ability to perform quantitative measurements, but the disadvantage of the method remains the high cost of the instrumentation/analysis.

1.4.3 Biosensor-based detection methods

Biosensors have been defined as "analytical devices incorporating a biological material (enzyme, antibody, receptor protein, nucleic acid, etc.), a biologically derived material (engineered proteins, aptamers) or a biomimetic material (synthetic catalysis, imprinted

polymers) in intimate contact with a physicochemical transducer (electrochemical, optical, piezoelectric, etc.), or a transducing microsystem" [26, 27].

Depending on the method of signal transduction, biosensors can be classified into four major categories: optical, piezoelectric, electrochemical, and thermal sensors [28]. Each of these four sensor types can be adapted to perform either direct (label free) or indirect (labeled) detection of target species. Efforts to commercialize biosensor technology are currently widespread, but progress in this area is still slow due to problems that remain in achieving acceptable sensitivity and reproducibility. In the following section, the role of the most common biorecognition elements used in the construction of biosensors, and the improvements achieved by using optical, piezoelectric or electrochemical sensors for bacteria detection, are described.

1.4.3.1 Biological recognition elements in biosensors

The most common biorecognition elements used in biosensor technology for the detection of bacteria are antibodies, nucleic acids, aptamers, and phages.

1.4.3.1.1 Antibodies

Antibodies are used extensively as biorecognition elements. They can be used for pathogen detection or for detection of some of the pathogen components such as

enzymes, toxins, pili, and spores. Based on the method of production, antibodies are categorized as polyclonal or monoclonal, monoclonal antibodies being the more specific and more expensive recognition elements. Antibodies can easily adsorb onto the transducer surface or be immobilized by chemical conjugation or cross-linking onto the sensing surface through contact with functional groups such as amines, carboxylates, etc.

1.4.3.1.2 Nucleic acids

Single-stranded nucleic acids can also be used as recognition elements to bind with complementary DNA or RNA sequences of a target microorganism. The oligonucleotides can be deposited onto the sensor surface by different means. For example, oligonucleotides modified with NH_2 terminal groups (which are readily available commercially) can be attached to suitable functional groups at the surface of a transducer through covalent bonding [29] or, oligonucleotides modified with SH_2 terminal groups [30] can be directly self-assembled onto gold surfaces.

1.4.3.1.3 Aptamers

Aptamers, first reported on in 1990, are engineered nucleic acids that specifically bind to various targets of biological interest. The targets can be small molecules, peptides, proteins, nucleic acids or even whole cells. The advantage they offer over using antibodies or other alternative approaches is the simplicity associated with their

production and isolation. They can be created completely *in vitro* by chemical synthesis, they are easy to store, and show non-immunogenicity in therapeutic applications [31].

Aptamers immobilized as probes are more resistive than antibodies to freezing and drying reconstituting cycles, but they have a higher sensitivity to enzymatic degradation. To date work on aptamers has mainly been limited to therapeutic applications, nevertheless the number of publications on their integration with sensing devices is on the rise.

1.4.3.1.4 Phages and other bioreceptors

As we described previously, phages are bacterial viruses that bind to target bacteria through specific receptors present at the surface of host cells. They inject their genetic material inside the cells and use the cell machinery to replicate.

The fact that phages are capable of targeting specific bacteria makes them attractive candidates for use as probes in sensor devices. A few papers have reported on the use of phages as recognition elements to detect bacteria using fluorescence microscopy [32], using acoustic wave biosensors [33], or impedance spectroscopy [34].

The principle of electric cell-substrate impedance sensing (ECIS) is based on cell attachment and growth on a transducer surface producing a biofilm that behaves as an insulating layer. Infection of the bacteria by the immobilized phages then causes a change in the cells shape, or literally its destruction, thus causing a variation in the measured impedance.

Some publications have reported on the existence of peptides that are smaller than antibodies, that can specifically bind to pathogens [35] . The peptides can be produced from pathogen-binding proteins, they can also be synthesized *in vitro* following procedures similar to those used for aptamers. Fluorescent labeled peptides have been successfully used for the detection of bacterial toxin and spores [36]. Peptides have also been employed for the detection of different virus strains by ELISA and dot-plot assay [37].

1.4.3.2 Different types of biosensors

In order to detect bacteria efficiently, the analytical device needs to meet certain requirements that are outlined in Table 1.2. They should be able to specifically detect different types of bacteria, they should be able to distinguish between live and dead bacteria, their operation/manipulation should be simple and more importantly, they should be sensitive.

As mentioned previously, the main categories of biosensors are based on optical, piezoelectric, electrochemical and thermal means of detection. In the following section, these techniques are described in relation to the detection of bacteria.

Sensor Characteristics for Bacterial Detection	
Low detection limit	Ability to detect single bacteria
Assay time	5-10 min for a single test
Assay protocol	No reagent addition needed
Measurement	Direct, without pre-enrichment
Format	Highly automated format
Operator	Minimum skill required to use the assay
Viable cell count	Should discriminate between live and dead cells
Size	Compact, hand-held
Species selectivity	Ability to distinguish individual bacterial species

Table 1.2 Biosensor characteristics for bacteria detection (Reformatted from Ivnitski et al.[38])

1.4.3.2.1 Optical biosensors

Optical biosensors consist of a receptor immobilized onto a transducer, which enables the measurement of variations in light emission, refractive index, or thickness of a layer upon binding of the bacteria. Fluorimetry, surface plasmon resonance (SPR), optical fiber, and interferometry techniques are examples of this type of sensor.

Fluorimetry has been successfully used to detect bacteria. An instrument based on fluorimetric detection, the AVL BDS-240, is a noninvasive automated system for the rapid detection of bacteria as well as some fungi. This instrument has an optical unit consisting of a filtered excitation source and a photodiode detection system. Since CO_2 is a product of bacteria metabolism, CO_2 optical sensors have been chosen to detect bacteria in human blood. During the bacteria's metabolic process, the CO_2 concentration increases causing a change in fluorescence emission from a colorimetric pH indicator added to the sample [39].

An evanescent wave interferometer was also used to detect *Salmonella typhmurium* species [40]. In this case, a laser beam is directed into a wave guiding film and the light passes through the surface of the chip. The surface area functionalized with a specific receptor thus becomes the sensitive part of the chip. This system enabled the detection of 10^8-10^{10} cells/mL within 5 minutes. Although the system has a short detection time, it has a poor sensitivity.

Recently surface plasmon resonance (SPR), as an optical technique, has been wildly used for the detection of bacteria. Surface plasmons are a special mode of electromagnetic waves that propagate in a direction parallel to a metal/dielectric interface[41].

When a light beam is directed onto a metal film such as gold or silver at a fixed angle corresponding to what is called the resonance angle, oscillations of the free electrons at the metal surface are induced, which generate a sensitive area on the surface called an evanescent field. When the immobilized probe molecules bind to the targeted species, a variation in the surface plasmon oscillation frequency on the opposite side of the film occurs, which is directly proportional to the change in the amount of bound, or adsorbed target. The binding is detected by measuring the ensuing changes in the refractive index. Figure 1.6 shows a simple schematic of an SPR sensor used for the detection of *E. coli* O157:H7. A collimated polychromatic light beam is directed onto the prism at a specific angle and excites surface plasmon waves at the metal/dielectric interface. The binding of bacteria to the antibodies immobilized onto the gold film causes a change in the refractive index [42].

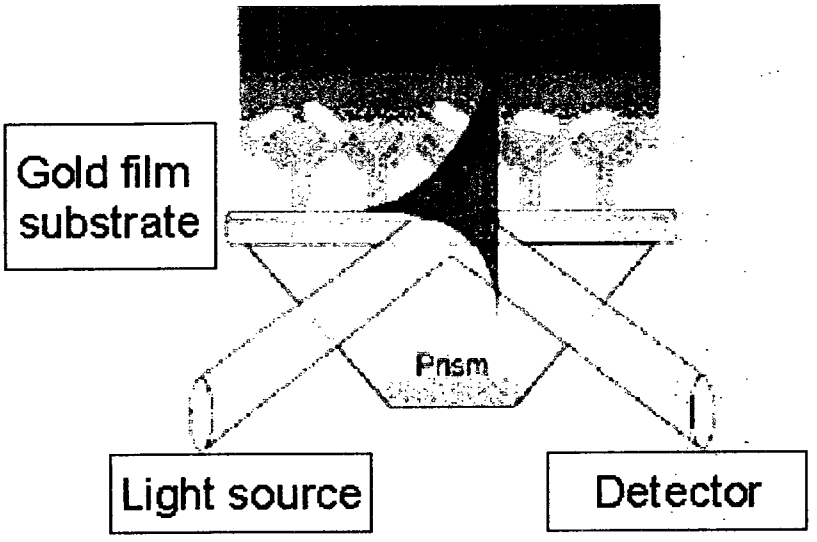

Figure 1.6 Simple schematic of an SPR sensor [42]

The first application of an SPR sensor for the detection of bacteria was reported by Fratamico et al.[43]. A sandwich assay was used to detect *E. coli* O157:H7 cells. A monoclonal antibody was immobilized onto the surface to capture the bacteria, and the captured bacteria were then further probed by a secondary antibody to increase the signal. No significant signal was observed using other (non-target) types of bacteria such as *S. typhmurium* or *Y. enterocolitica.* The sensor was able to detect 10^7 cells/mL, and the surface could be regenerated and reused for 50 measurements.

Numerous works based on using SPR for sensing purposes have been reported, and many different detection limits have been found. Obviously, many factors such as the efficiency

of probe immobilization or sample treatment methods will have an effect on the detection limit of the system. In one study, Taylor et al. compared the observed detection limits for different sample treatment methods, for the detection of *E. coli* O157:H7, and found the following [42]: 10^7 cfu/mL for an untreated live sample, 10^6 cfu/mL for a heat-killed sample, 10^6 cfu/mL for a heat-killed and ethanol soaked sample, and 10^5 cfu/mL for a heat-killed and detergent lysed sample.

The difference in detection limits can be explained by the change in size and morphology of the cells. For heat-killed samples, *E. coli* O157:H7 cells can either change from their rod shape to become spherical, or be broken up into smaller pieces. Lysis also breaks up the cells, creating smaller pieces and increasing the concentration of detectable material. This facilitates mass transport, allowing material to more easily reach the sensor surface, therefore improving the overall sensitivity.

Usually, SPR sensors have been shown to have high detection limits for the analysis of bacteria. This problem is attributed to the large dimensions of bacteria cells. Since detection with the SPR sensor depends on the ability of the analyte to reach the immobilized receptor at the surface, the large size of bacteria makes diffusion to the surface slow and limits the sensor response.

Optical fibers represent another interesting technology that has been adapted to the detection of bacteria. The structure of an optic fibre consists of polystyrene or silica glass with dopants such as Al_2O_3, B_2O_3, GeO_2. These dopants act to modify the optical properties of the fibers by raising their refractive index [44]. As illustrated in Figure 1.7, an optical fiber is composed of two main components: (i) the core with higher refractive

index and (ii) the cladding with lower refractive index. At a specific angle, incident light is transmitted through the optical fiber by total internal reflection, and a photo-detector can be used to capture the light either at the end of fiber or at the cladding.

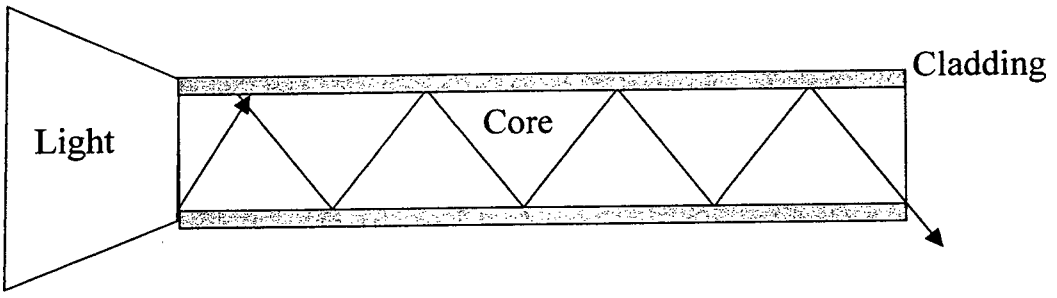

Figure 1.7 Illustration of the structure of an optic fiber

Ko et al. have used an optical fiber-based approach for the detection of *S. typhmurium* in ground beef [45]. Their fibers were functionalized using a silanization method, and labeled antibody–protein G complexes were then immobilized onto the cladding to form the evanescent wave-sensing region. The modified optic fiber was immersed into homogeneous ground beef containing *Salmonella* and the detection limit was determined to be 10^5 cfu/g, with measurements taking 5 minutes.

Geng et al. have demonstrated the use of optical fibers for the detection of *Listeria monocytogen* cells in hot-dog or bologna [46]. In this sensor, polyclonal antibodies were immobilized onto polystyrene optic fibers through biotin-streptavidin chemistry. This immunosensor was tested with other (non-target) bacteria and showed good specificity toward the *Listeria monocytogen* species. The sensitivity of the sensor was 10^3 cfu/mL in

pure culture grown at 37°C. After enrichment steps, it took approximately 24 hours to detect bacteria cells in hot-dog samples, with a detection limit of 10 to 10^3 cfu/g. In another report a fiber optic chemiluminescence biosensor, coupled with a magnetic separation system, was used for the detection of *E. coli* O157:H7 in inoculated food samples including chicken, beef, and vegetables [47]. Briefly, a sandwich immunoassay consisting of *E. coli*-antibody coated magnetic beads, *E. coli* cells, and horseradish peroxidase (HRP)-labeled anti-*E .coli* coated magnetic beads, was formed. The bacteria cells were detected by collecting, through use of a fiber optic, the HRP-catalyzed chemiluminescence emanating from the surface of the beads. The advantage of this approach is its low detection limit (10^2 cfu/mL), without any need of an enrichment step, with a detection time of 1.5 hours.

1.4.3.2.2 Piezoelectric biosensors

Piezoelectric biosensor devices are generally prepared by coating a piezoelectric transducer surface with a receptor, such as antibodies, followed by binding with bacteria. As the bacteria bind to the receptors, the mass at the surface of the piezo-sensor changes, and this is reflected by a variation of the piezoelectric crystal's resonance oscillation frequency.

The most widely used piezoelectric material is quartz because it is easily available and has good thermal stability. Piezoelectric technology has been used for the detection of a

variety of microorganisms, with a wide range of applications in the food industry, the environment, clinical diagnosis, and biotechnology in general [48, 49].

The detection of *S. enteritideis* is one example of the use of a piezoelectric device for the detection of bacteria [50]. In this sensor a piezoelectric crystal covered with layers of gold, silver, and palladium was then coated with polyethyleneimine to immobilize antibodies, allowing for recognition of the *S. enteritideis* species. Binding of the bacteria resulted in measurable changes in the crystal's resonance frequency parameter, giving a detection limit of 10^5 cfu/mL, with a detection time of 35 minutes.

In other work, *S. typhmurium* was detected using a polyclonal antibody immobilized by the Langmuir-Blodgett method onto the surface of a quartz acoustic wave sensor [51]. The detection limit of this sensor was found to be a few hundred cells/mL, with a response time of less than 100 s over the range of 10^2-10^{10} cells/mL. The sensor's response was found to be linear with bacterial concentrations ranging from 10^2 to 10^7 cells/mL.

Another piezoelectric crystal sensor using antibodies has been developed for the detection of *Salmonella, E. coli, Shigella,* and *Yersiniapestis* [52]. In this case, crystals coated with antibodies were immersed in bacteria-containing solution for 45 minutes and, after washing and drying steps, the shift in resonance frequency was measured. A linear response was observed in the concentration range of 10^6 - 10^8 cfu/mL and the authors claimed that the sensor could be reused at least 12 times.

In yet another effort, a piezoelectric device was used to detect bacteria cells in drinking water [53]. For this purpose, anti-*E. coli* were immobilized onto crystals and used to detect *E. coli K12.* An identical crystal (not modified with anti-*E. coli*) was dipped in the same

bacteria-containing solution to act as reference. The resonance frequency was measured as a function of *E. coli* concentration. The response range was found to be 10^6 - 10^9 cfu/mL. In this case it was not possible to regenerate the sensing surface. Attempts to remove the bound bacteria by washing the crystal with urea or glycin-HCl buffer resulted not only in removing the bacteria, but also the antibodies, therefore making reuse impossible.

Other similar approaches were used for bacteria detection such as the quartz crystal microbalance (QCM) for the detection of *S. typhmurium* [54] or the detection of *Chlamydia trachomatis* in urine samples [55].

The main disadvantage with piezoelectric biosensors is the numerous washing and drying steps involved and the regeneration of the sensing surface layer. However, the problem of regeneration can be solved by manufacturing small crystals at low cost, therefore making the devices disposable, but these sensors may suffer from lack of sensitivity.

1.4.3.2.3 Electrochemical biosensors

Electrochemical biosensors have some advantages over optical sensors. They are generally more sensitive, the equipment required for analysis is less sophisticated and less expensive. The electrochemical sensing electrodes are also well suited to miniaturization, making possible the development of small, portable, and potentially disposable sensors. Amperometry, potentiometry and impedance spectroscopy are the main electrochemical methods used for biosensor applications.

Amperometric biosensors typically rely on an enzyme system that catalytically converts electrochemically non-active analytes into products that can be oxidized or reduced at a working electrode. The measurement is based on the variation in current as a function of applied potential.

Neufeld et al. have reported on an amperometric method based on enzyme activity [56]. A bacteriophage is used to infect the bacteria species, causing the release of intracellular enzymes, and the activity of these enzymes is measured amperometrically. The product of the reaction between the enzyme and the substrate (*p*-aminophenyl-*β*-D-galactopyranoside) is *p*-aminophenol, which is then oxidized at a carbon electrode and the resulting current is monitored as a function of time. With this method *Staphylococcus* and *E.coli* cells were detected with a detection limit of 1 cell/100 mL, within a period of 6 to 8 hours.

Brooks et al.[57] have developed an enzyme-linked amperometric method for the detection of *S. aureus* with a detection limit of 10^4 - 10^5 cfu/mL. However, because of variations in the signals produced by the electrochemical detection step, this immunosensor suffered from lack of reproducibility.

Gehring et al. employed an immunomagnetic separation system to electrochemically detect *Salmonella* species. In this method a sandwich immunoassay was formed using super-paramagnetic beads coated with anti-*Salmonella* and anti-*Salmonella* antibodies linked with alkaline phosphate. The complex immunoassay was performed by lowering the surface of graphite ink strip electrodes into the sample using a magnet, and

voltammetry (current measured versus applied voltage) was used to detect the bacterial cells. This system was able to detect 10^3 cfu/mL within 80 min [58].

Potentiometric biosensors are another type of electrochemical sensor, which measures the variation in potential that occurs when the analyte molecules interact with the probe-modified surface. In past years, an electrochemical approach using light addressable potentiometric sensors (LAPS), has been successfully used for the detection of pathogens. A LAPS is made up of a semiconductor chip (n-type silicon), covered with a silicon-dioxide insulating layer, placed in contact with the sample solution. The potential that results from the different charge distributions that exist at the insulating layer/solution interface and the semiconductor/insulator interface, is directly influenced by the binding interactions occurring at the probe-modified insulating layer surface, and the signal is enhanced by illumination with a modulated light beam [49].

Gehring et al. have developed a LAPS system for the detection of *E. coli* O157:H7 cells in food samples using a polyclonal antibody as probe. Their system was able to detect 10^3 cells/mL [59].

The LAPS approach has also been used to detect *E. coli* DH5α in drinking water [60]. A glass cover slip was coated with primary anti-*E. coli* using a silanization method. *E. coli* in the drinking water was captured by the primary immobilized antibody, and then a secondary urease-*E. coli* antibody conjugate was used to link with the captured *E. coli*. The sample chamber was then washed with PBS, then urea was fluxed through the chamber and the reaction monitored. Urea is enzymatically converted to ammonia in proportion to the amount of bacteria cells initially present in the sample. The production

of ammonia causes a change in the redox potential which is measured. The authors have reported that this system allows the detection of 10 cells/mL. Although the LAPS technique offers improvements over the more conventional methods of potentiometric detection of bacteria, they still suffer from poor reproducibility.

1.4.4 Impedance techniques for bacteria detection

In recent years, electrochemical transduction based on impedance techniques has received increasing attention for applications in biological and biomedical detection. This is due to a number of factors such as: (i) impedance is one of the most important techniques for direct (label-free), real time detection; (ii) the electrical properties of biological cells make them attractive analytes for detection using impedance-based methods; (iii) impedance as an electronic detection system allows for the development/use of miniaturized biosensors (biochips), effectively provides access to smaller analytical devices rather than having to resort to using more cumbersome laboratory-based instruments [61].

1.4.4.1 Impedance microbiology

The simplest impedance method for identification and quantification of bacteria is growth monitoring, which is based on the changes of impedance due to actual growth of bacteria, or a reaction resulting from the bacterial growth. Impedance microbiology is the basis for

existing commercial impedimetric systems such as Bactometer® from Biomerieux, Bactrac® from Sy-Lab, and RABIT® from Don Whitley Scientific.

The major mechanism for detection based on growth makes use of the metabolic activity of the biological cells. The change in impedance is mainly caused by the release of ionic metabolites into the culture medium, as prescribed by the energetics of the live cell metabolism, which can be summarized as the consumption of oxygen and sugars by the bacteria and the generation of carbon dioxide and organic acids.

For instance, a non-ionized glucose converted to two molecules of lactic acid lead to an increase in the conductivity of the medium. Furthermore, the metabolically driven combination of lactic acid with oxygen leads to the formation of carbonic acid, yielding more mobile carbonate ions and increased conductivity [62]. Another contributing factor to changes in impedance is the possible ion exchange across the cell membrane. Ions such as K^+ and Na^+ are known to pass through ion channels in the cell membrane, which serves to adjust the osmotic difference between the interior and exterior of the cells [63]. Ion exchange causes changes in the ionic composition of the surrounding medium and therefore changes its electrical conductivity.

Even though growth-based impedance techniques are reliable and enable the detection of viable cells, they still suffer from high detection times and non-specificity. Usually, low cell numbers take a long time to grow (up to 24hours) and the method cannot be used to identify specific strains of bacteria. Therefore, antibodies, nucleic acids, or new molecules such as aptamers, phages or peptides are starting to be used consistently as probes for specific binding to target pathogens.

1.4.4.2 Impedance-based biosensors for bacteria detection

The following describes the most recent advances in the area of bacteria detection using electrochemical impedance spectroscopy (EIS). Most impedance biosensors for bacteria detection are based on using the electrically insulating properties of the cell membrane. When the cells attach to an electrode surface, the electrode surface area gradually gets covered with matter that reduces conductivity and therefore changes the impedance at the interface.

To obtain an impedance signal, the measurement can be performed in the presence or absence of redox couples such as $[Fe(CN)_6]^{3-/4-}$, which are referred to as faradaic or non-faradaic impedance measurement conditions, respectively [64]. Among the various recognition elements that were discussed previously, antibodies are the most commonly used bioreceptor for bacteria detection. Sensors based on the immobilization of antibodies require the attachment of a certain amount of bacteria cells to the electrode surface to produce a detectable signal.

When antibodies are used as probes, two types of detection processes can be distinguished; (i) in the presence of a redox couple, the detection signal corresponds to changes in the faradaic impedance due to the biological events occurring on the surface, and (ii) in the absence of a redox couple, the signal relates directly to the physical attachment of bacteria cells at the sensor surface, and the electrically insulating properties of the cell membrane [65].

Two important parameters to be considered when using EIS biosensors are the interfacial capacitance, also called the double-layer capacitance (C_{dl}), and charge-transfer resistance (R_{ct}) at the electrode surface. In certain applications, however, the key parameter of interest for detection purposes can be the conductivity of the medium (changes in solution resistance) [66].

1.4.4.2.1 Faradaic impedimetric biosensors

There are now several reports on the impedimetric detection of pathogens in media containing a redox active species, typically the $[Fe(CN)_6]^{3-/4-}$ redox couple. The detection here is based on measuring variations of the charge-transfer resistance (R_{ct}) at the electrode surface, upon attachment of bacterial cells.

Ruan et al. have reported on an electrochemical immunosensor for the detection of *E. coli* O157:H7, using $[Fe(CN)_6]^{3-/4-}$ as the electroactive redox couple in solution [67]. In this biosensor, anti-*E. coli* antibodies were immobilized onto a planner indium-tin oxide (ITO) electrode surface and used to detect *E. coli* cells. The sensor used secondary antibodies conjugated with horseradish peroxidase to generate insoluble products at the electrode surface. These insoluble products then act to prevent electron transfer at the surface and therefore cause a detectable variation in impedance.

The overall biosensing system can be interpreted by an equivalent circuit as illustrated in Figure 1.8a. The proposed equivalent circuit includes the resistance of the electrolyte

(R_s), the double-layer capacitance (C_{dl}), the charge (electron) transfer resistance (R_{ct}), and the Warburg impedance (Z_w).

Figure 1.8b shows a typical Nyquist plot of the imaginary impedance (Z_{im}) versus the real impedance (Z_{re}), measured over a range of applied ac voltage frequency, which shows a combination of a semicircle and a straight line [64]. The semicircle relates to the faster electron-transfer processes occurring at the electrode surface (it appears in the high frequency domain of the Nyquist plot), while the straight line relates to the diffusion limited, mass transfer, processes that occur near the electrode on the solution side of the interface (it appears in the low frequency domain). The intercept of the semicircle with the Z_{re} axis at high frequency yields the value of R_s, and the diameter of the semicircle is equal to R_{ct}.

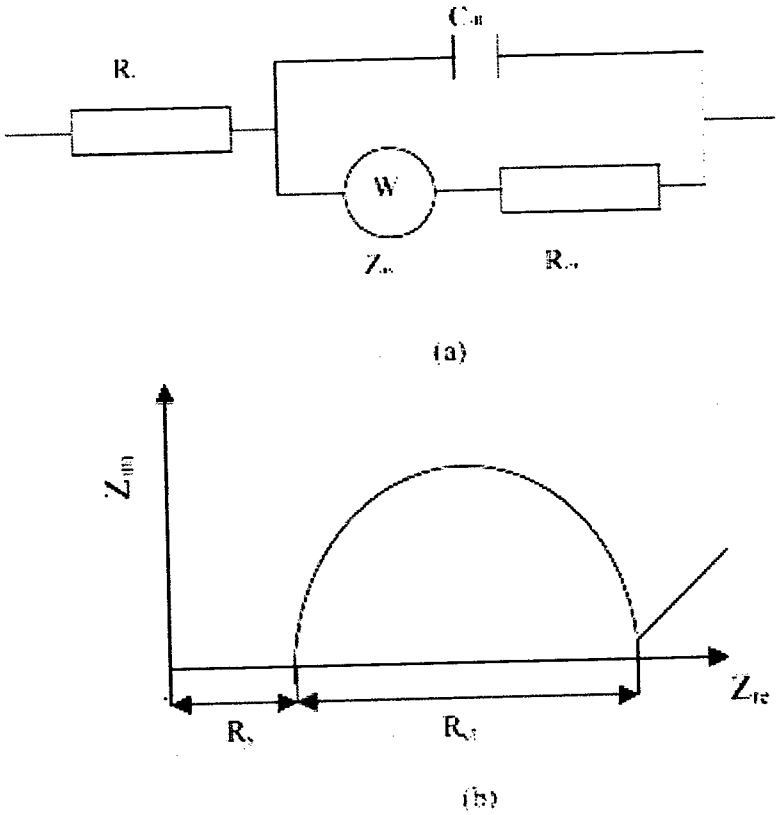

Figure 1.8 General equivalent circuit for an electrochemical cell in the presence of a redox couple **(a)** a typical Nyquist plot (Z_{im} vs Z_{re}) **(b)** used for the detection of *E. coli* O157:H7 cells [67]

Among the various parameters present in the equivalent circuit, the electron transfer resistance, R_{ct}, was identified by Ruan et al. as the main parameter being influenced by the binding of *E. coli*. After *E. coli* binding, the interfacial electron-transfer kinetics slow down and increase the electron transfer resistance. The increase in R_{ct} can be explained as bound cells inhibiting electron transfer between the electrode and he $[Fe(CN)_6]^{3-/4-}$ redox couple in solution.

Ruan et al. showed that the value of R_{ct} increased with increasing bacteria concentration. This biosensor showed a linear response in the concentration range of 10^4 to 10^7 cfu/mL, with a detection limit of 10^2 cfu/mL.

Another example of a label-free electrochemical impedance sensor using the a redox couple was reported by Yang and coworkers [68]. They developed an immunosensor for the detection of *E. coli* O157:H7, using interdigitated array microelectrodes (IDA). The sensing surface consists of indium-tin-oxide (ITO) modified with anti-*E. coli* antibodies. The antibodies were attached to the surface covalently through bonding between the carboxyl groups on the antibodies and the reactive hydroxyl groups on the ITO surface. The sample containing the target bacteria, in presence of the $[Fe(CN)_6]^{3-/4-}$ redox couple, was then deposited onto the functionalized microelectrode array. When the bacteria bind to the surface, they prevent the electron transfer between of the interdigitated electrodes and increase the electron transfer resistance (Figure 1.9).

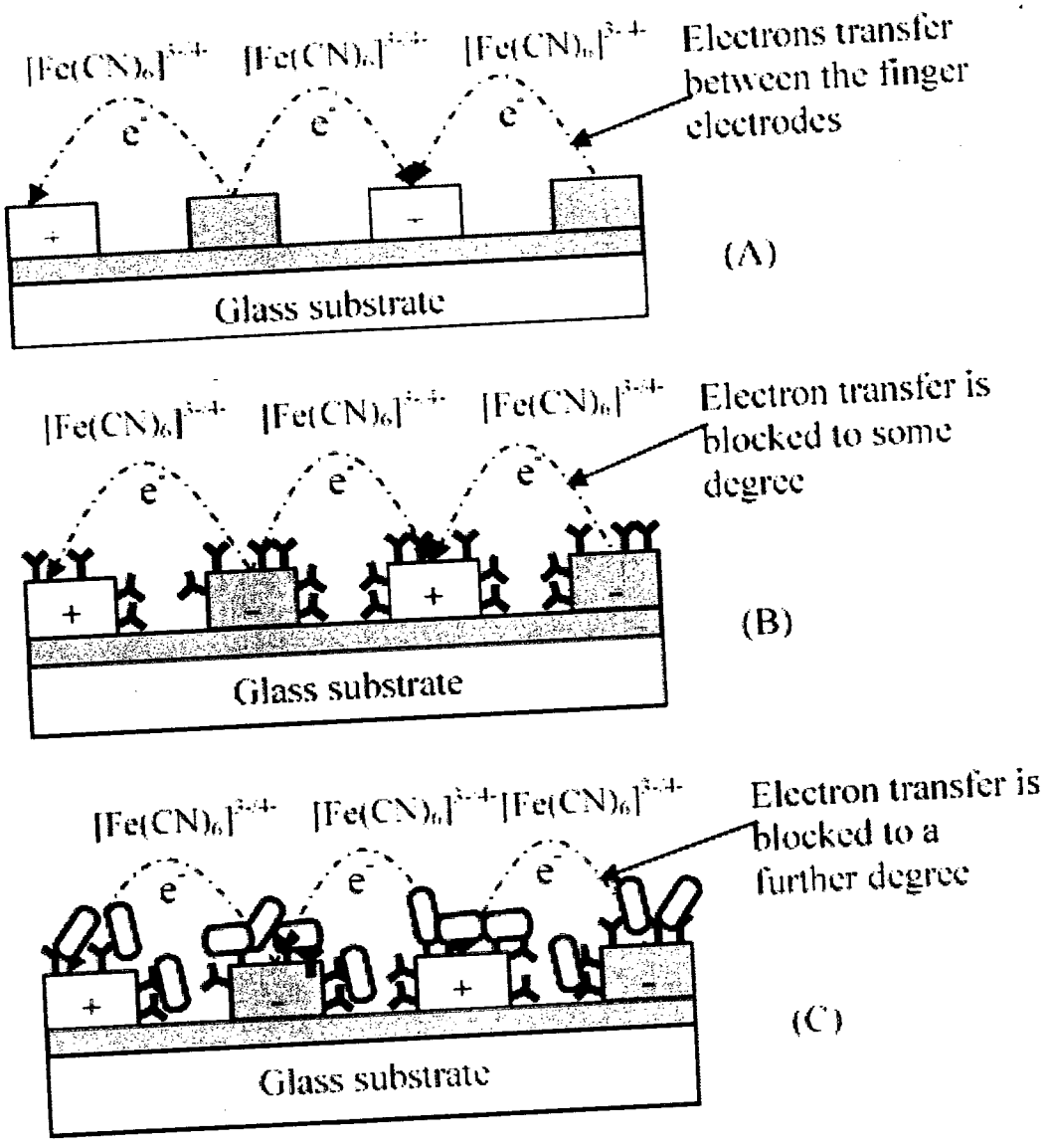

Figure 1.9 Direct impedimetric detection using interdigitated microelectrode arrays: **(A)** bare electrode; **(B)** with immobilized antibody; **(C)** with bound bacteria cells. The gray ovals are the *E. coli* O157:H7 cells; the Y shapes are the anti-*E. coli* antibody [68]

A linear dependence of the charge transfer resistance on the logarithm of bacterial concentration was observed in the range of 10^5 to 10^8 cfu/mL, with a detection limit of 10^6 cfu/mL. The detection limit for this approach is unfortunately much higher than that reported for the system used by Ruan et al., or even for ELISA, but it is comparable to other immunosensor-based methods using the quartz crystal microbalance (QCM) for the detection of *Salmonella* (with a detection limit of 10^6 cfu/mL) [69], and surface plasmon resonance (SPR) for the detection of *Salmonella enteritidis* and *L.monocytogens* (with a detection limit of 10^6 cfu/mL) [70], or the detection of *E. coli* O157:H7 (with a detection limit of 10^6 cfu/mL) [71].

1.4.4.2.2 Non-Faradaic impedimetric biosensors

Non-Faradaic impedance measurements mainly detect the attachment of bacterial cells onto the electrode surface, in the absence of a redox couple in the sample solution. Radke and Alocilja [72] have developed one such impedance sensor for the detection of *E. coli* O157:H7. The sensor was made using a high-density gold interdigitated microelectrode array, with 1700 finger electrodes. Each electrode was 3 μm in width and their separation was 4 μm, therefore providing a large sensing area. The gold microelectrode array was functionalized using 3-mercaptomethyldimethyl-ethoxysilane (MDS) followed by *N-y*-maleimidobutryloxy-succinimide ester (GMBS) acting as a cross-linker. Anti- *E. coli* were then immobilized onto the surface to detect bacteria cells. After immersing the sensor into the bacteria-containing solution, an increase in

impedance was observed over the frequency range of 100Hz-10MHz. The increase in impedance was attributed to the binding of the cells to the electrode surface (hence due to the electrically insulating property of their cell membrane). The sensor had a dose response to *E. coli* concentration from 10^4 cfu/mL to 10^7 cfu/mL.

Some researchers have developed impedimetric biosensors using microfluidic chips. An example of this type of sensor was reported by Boehm et al.[73] for the detection of *E. coli* cells. Antibodies were immobilized onto the glass surface of a microfluidic chamber, and the bacteria-containing solution was passed through the chamber causing the *E. coli* to be captured by antibodies, resulting in an increase of the measured impedance. The detection limit of this sensor was found to be 10^4 cfu/mL. In microfluidic-based sensors, injected bacteria cells tend to accumulate inside the chamber and enhance the signal, which is favorable to the detection of low bacteria concentrations [73].

1.5 Overall objective

The overall objective of this study is to develop a biosensor array system that allows rapid, specific, and quantitative detection of bacteria in field samples. This research is aimed at developing a low-cost, portable, disposable impedimetric electrochemical sensor system for efficient bacteria detection. To meet the needs for efficient bacterial diagnostics, the system should have the following characteristics.

It should:

- allow specific detection of bacteria;
- be rapid, reliable and highly sensitive;
- be low-cost (potentially disposable);
- be easy to use, even by the non-initiated;
- use the unique properties of phages as bioreceptor molecules;

CHAPTER 2

DIRECT IMPEDIMETRIC DETECTION OF *E. COLI K12*

2.1 Introduction

The rapid and specific detection of pathogenic bacteria is very important for human health safety and diagnostics. Examples of target areas where rapid intervention is required include spoilage/contamination in the food industries, quality of indoor/outdoor air and water (building ventilation, pools, beaches, city water supplies...), infection outbreaks in hospitals and the public at large, contamination in fossil and nuclear power plants, and homeland security [9, 74-77]. To meet these needs, major research efforts are currently underway to develop efficient and cost-effective sensor devices for the detection of pathogenic bacteria.

To illustrate the need for such analytical tools we refer to two noteworthy incidents that occurred in this decade. One is the major multi-bacteria water-borne outbreak that occurred in Walkerton (Ontario, Canada) in May of 2000. Contamination of the municipal water supply by *Escherichia coli* O157:H7 and *Campylobacter* species led to over 2000 reported cases of infected residents. 65 residents required hospitalization, 27 of which were treated for hemolytic uremic syndrome (HUS, a type of kidney failure), and 6 deaths were attributed to the outbreak [78]. Another major incident, the food-born outbreak caused by *Escherichia coli* that occurred in a US-based fast-food chain in late 2006, is a specific example of why rapid and accurate identification of a specific bacterial strain is

crucial. The toll for that outbreak was 71 people in five states who felt ill due to the potentially deadly strain of *E. coli* O157:H7. Of the 71 people, 53 had to be hospitalized, while 8 had developed HUS [79]. At its peak, this bacterial outbreak entailed costs of nearly $1 billion to the fast-food chain (this only included the loss of business, nothing else). These were not the only costs, as the Center for Disease Control and Prevention (CDC) estimated that the average medical cost of an *E. coli* illness can range from $26 for someone who is not in need of urgent medical care, to $6.2 million in case of death due to HUS [79]. Today, infectious diseases caused by bacteria account for as many as 40% of the 50 million annual deaths worldwide and, especially in many developing countries, microbial diseases constitute the major causes of illness and death [38, 80, 81].

Conventional microbiological methods for determining the cell counts of bacteria employ selective culture, biochemical, and serological characterization. Although these achieve sensitive and selective bacterial detection, they typically require days to weeks to yield a result. Some emerging technologies that have been used for bacterial detection include enzyme linked immunosorbent assay (ELISA) [82], polymerase chain reaction (PCR) [83-85], DNA hybridization [86, 87], flow cytometry, matrix-assisted laser desorption/ionization [88, 89], immunomagnetic techniques [90], and the combination of immunomagnetic separation and flow cytometry which enabled the detection of 10^3 cells/mL of *E. coli* O157: H7 within 1 h [91]. Pathogen detection utilizing ELISA methods for determining and quantifying pathogens in food have been well established [92] . The PCR method is extremely sensitive but requires pure sample preparation and hours of processing, along with expertise in molecular biology [81, 93]. Flow cytometry is another highly effective means for rapid

analysis of individual cells at rates up to 1000 cells/sec [94, 95], however, it has been used almost exclusively for eukaryotic cells. These detection methods are relevant for laboratory use but cannot adequately serve the needs of health practitioners and monitoring agencies in the field. Furthermore these systems are costly, require specialized training, have complicated processing steps in order to culture or extract the pathogen from food samples, and are time consuming.

Biosensors present a viable solution to these problems and technological improvements in this area continue at a rapid pace. A field-ready biosensor can be envisaged that is potentially inexpensive, easy to use, portable, sensitive and capable of providing results in minutes. In general, biosensors are composed of a biological recognition element acting as a receptor, and a transducer which converts the ensuing biological activity into a measurable signal (commonly optical or electrical in nature) [96] . A variety of biosensors has been reported in the literature for bacterial detection including piezoelectric [97-99], electrical [86, 87, 100, 101], surface plasmon resonance [43, 102, 103], and optical waveguide-based devices [104-111].

Electrochemical biosensors are particularly interesting because they are usually inexpensive, are well adapted to miniaturization, and can therefore provide disposable-type chips for field applications. Electrochemical sensors reported in the literature for detecting bacteria are mainly based on monitoring bacterial growth onto the transducer [112-114] , or the interaction between bacteria and biological recognition elements such as antibodies [101, 115, 116] and nucleic acids (DNA/RNA) [117-121]. DNA based methods (despite their good selectivity and long term stability) are unable to discriminate between viable

and non-viable cells, while antibody based biosensors on the other hand may suffer from cross-binding of other bacteria, which may result in false positives. In addition, antibodies are generally very expensive to produce.

Bacteriophages are small viruses that have recently been postulated as promising recognition elements to use in bacterial biosensors [122]. They are ubiquitous in nature, highly specific to bacteria and thus harmless to humans, much cheaper to produce than antibodies and present a far longer shelf life. In addition, they can also be immobilized onto transducing devices in pretty much the same manner as antibodies or DNA probes. For these reasons, the present work pertains to the development of a method for rapid and specific pathogen detection based on phages. Methods reported for bacteria detection using bacteriophages include amperometric detection using enzymatic activity [56, 123], bead-based electrochemical immunoassay [124], biotinylated phages [125], physical adsorption of phages onto quartz crystal microbalance [126], and surface plasmon resonance [122].

To our knowledge, the work presented in this thesis (at the time of publication in the ACS journal Analytical Chemistry in 2008) is the first example of covalent immobilization of phages onto functionalized screen-printed carbon electrodes (SPEs) as transducer surfaces, and their use for the direct impedimetric detection of *E. coli*.

2.2 Materials and Methods

2.2.1 Materials

1-(3-dimethylaminopropyl) ethylcarbodiimide hydrochloride (EDC), concentrated hydrochloric acid 37%, bovine serum albumine (BSA), sodium chloride, magnesium sulfate, gelatin, Tris (hydroxymethyl) aminomethane hydrochloride (Tris-HCl buffer pH 7.5) were purchased from Sigma-Aldrich. Luria Bertani (LB) media was purchased from Quelabs (Montreal, Canada) and prepared by dissolving 25 g of LB powder into 1L of distilled water. LB-agar medium was prepared by adding 6 g of granulated agar to 400 mL of LB media. SM buffer was prepared by mixing 5.8g NaCl, 2.0g $MgSO_4 \cdot 7H_2O$, 50 mL 1M Tris-HCl pH 7.5, and 1mL 10% (w/v) gelatin in MilliQ water. The LB medium and SM buffer were autoclaved. *E. coli K12* and T4 phages were obtained from ATCC (11303 and 11303-B4, respectively). GFP-labeled *E. coli K12* was obtained from Dr. Roland Brousseau (Biotechnology Research Institute, Montreal). *Salmonella typhimurium* DT108 bacteria was obtained from Dr. Sylvain Quessy (Faculté de Médicine Vétérinaire, University of Montreal).

2.2.2 Electrode microarray preparation

Screen printed electrodes were fabricated as previously described [127] using graphite ink (electrodag 423 SS, (Acheson, Erstein, France)) and a DEK 248 screen-printing machine (DEK, Erstein, France). The SPE platform was designed to provide multi-probe

capability, easily produced by screen- printing ink onto polyester sheets. The polyester sheets produced, each carrying 16 separate electrode arrays, were subsequently baked 10 minutes at 100 °C to dry the thermoplastic carbon ink. This was followed by printing an insulating polymer (MINICO M 7000, (Acheson, Erstein, France)) onto the microarrays, in order to define a window easily covered with a 50 μL drop of solution. This window serves to isolate the active area composed of eight 0.2 mm^2, individually addressable, working electrodes, one ring-shaped reference electrode, and one central auxiliary electrode (see Figure 2.1).

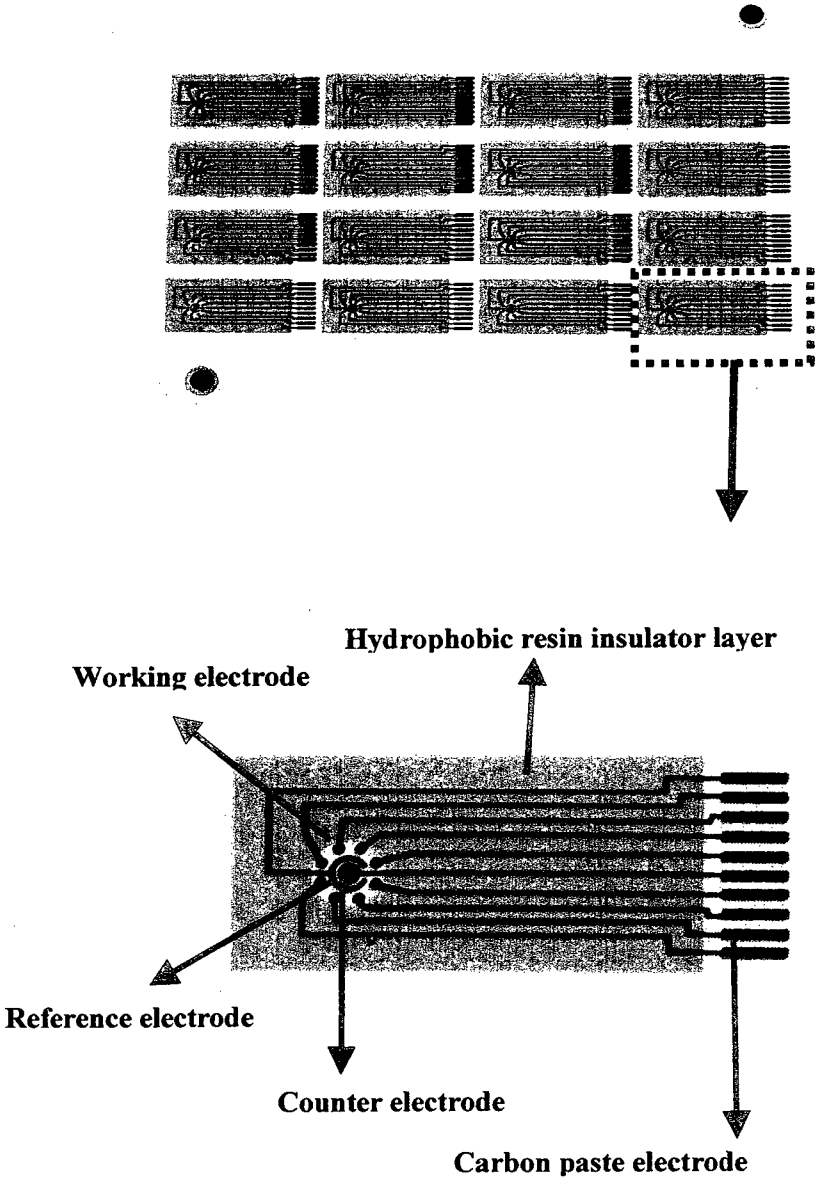

Figure 2.1 Photographic images of the screen printed carbon electrode arrays

2.2.3 Bacteriophage and bacteria preparation

T4 bacteriophage (wild type) was amplified by pipetting 100 µL 10^6 cfu/mL of *E. coli K12* and 100 µL 10^6 pfu/mL of T4 phage in a test tube and using a vortex. The mixture was incubated at room temperature for 15 min and was then added to a 20 mL tube containing LB media. The mixture was incubated for 6 hours at 37°C in a shaking incubator. The solution was then centrifuged at 2500 g for 20 min, followed by filtering the supernatant with 0.22 µm Millex filter (Millipore) to remove any remaining bacteria. After that, the supernatant was centrifuged at high speed (12000 g) for one hour followed by removing the supernatant and resuspending the phage pellet in 1mL of SM buffer. Phage counting was performed using soft agar plate and expressed in pfu/mL [128]. *E. coli K12* cells were grown at 37°C in 4 mL LB media using an incubator-shaker for 3 hours, followed by 3 centrifugations at 2500 g for 20 min, in order to exchange the media with SM buffer. Enumeration of bacteria was performed by the plate count technique and expressed in cfu/mL.

2.2.4 Electrode functionalization and phage immobilization

The SPEs were functionalized with 50 µL of 0.1 M 1-(3-dimethylaminopropyl) ethylcarbodiimide hydrochloride (EDC) in 0.12 N HCl, through chronoamperometry for 10 minutes. A potential of +2.2 V was applied to oxidize the carbon and generate

carboxyl groups to react with the EDC [129]. The electrodes were subsequently washed thoroughly with deionized water and air-dried. After the electrode functionalization, the SPEs were rinsed with deionized water and immersed in 2 mL of T4 bacteriophage solution (10^8 pfu/mL in SM buffer solution, pH 7.5), and left on a shaker for two hours. The SPEs were subsequently washed with SM buffer (pH 7.5) several times and dipped in 2 mL BSA solution (1mg/mL) and shaken for 40 min. Then the chips were rinsed with SM buffer for 5 min followed by covering the electrodes with 50 µL of *E. coli K12* (10^8 cfu/mL) suspension in SM buffer pH 7.5 for 20 min. After rinsing with buffer, the electrode arrays were covered with SM buffer to perform impedance measurements. Control experiments were performed by covalently immobilizing T4 phage on the electrodes and testing the sensor response in the presence of SM buffer only (without bacteria) and SM buffer containing *Salmonella typhimurium*. To determine the limit of detection, 7-fold serial dilutions (10^2- 10^8cfu/mL) of *E. coli K12* were incubated over the immobilized T4 phages.

2.2.5 Scanning electron microscopy (SEM)

Phages immobilized on substrates were washed several times with SM buffer. Then 50 µL of host or control bacteria (10^8 cfu/mL) were placed on the SPE surface for 15 minutes and washed with SM buffer. The images were obtained with the SEM instrument, model Hitachi S-4700 (Tokyo, Japan).

2.2.6 Time-of-flight secondary ion mass spectrometry (TOF-SIMS) analysis

TOF-SIMS studies were carried out with an ION-TOF SIMS IV (ION-TOF GmbH, Muenster, Germany). The instrument has an operating pressure of 5 x 10^{-9} Torr. Samples were bombarded with a pulsed liquid metal ion source ($^{69}Ga^{+}$), at an energy of 15 KeV. The gun was operated with a 27 ns pulse width and a 1.02 pA pulsed ion current for a dosage lower than 5 x 10^{11} ions cm^{-2}, well below the threshold level of 1 x 10^{13} ions cm^{-2} for static SIMS. Secondary ion spectra were acquired from an area of 40 x 40 μm, with 128 x 128 pixels (1 pulse per pixel), using at least 3 different positions per electrode. A chemical mapping was done on a surface of 40 μm x 40 μm.

2.2.7 Fluorescence measurements

The electrodes were washed several times with SM buffer after T4 phage immobilization. Then 10 μL of GFP-labeled *E. coli K12* bacteria (10^{8} cfu/mL) suspension were incubated over the immobilized phages and fluorescence images were recorded every 10 minutes up to 60 minutes to monitor the effect of phages on the bacteria. Fluorescence microscopy was performed using a Zeiss Axioplan- Fluorescence Microscope (Carl Zeiss AG, Oberkochen, Germany) equipped with a spot insight 2 megapixel color digital camera. Images were obtained using a 40x objective, using a blue filter with 450-490 nm excitation range and 515-565 nm emission range.

2.2.8 Impedance measurements

A three-carbon electrode setup was used to perform the impedance measurements. A dc potential of 400 mV, with a superimposed ac voltage of 20 mV amplitude at frequencies ranging from 100 kHz to 100 Hz, was applied to the working electrode. Results obtained under these measurement conditions showed good reproducibility (no adverse effects were observed due to the use of the centrally located ring-shaped carbon electrode of the array as pseudo-reference). All Nyquist curves were run from the high ac voltage frequency limit, to the low frequency limit (corresponding curves in Figure 7 thus being generated from left to right). All measurements were performed in SM buffer (pH 7.5) using a Voltalab electrochemical workstation (model PGZ 301 by Radiometer, Copenhagen, Denmark). The Voltamaster computer program (version 4.0) was used to run the electrochemical experiments and collect the data.

2.3 Results and Discussion

2.3.1 Bacteriophage immobilization and TOF-SIMS characterization

In this part we describe the covalent immobilization of phages onto functionalized SPEs and characterization of the surface, which will be used for the detection of *E. coli* using impedance spectroscopy, as shown in Figure 2.2.

The electrochemical approach to functionalize the SPEs used in this work involves performing chronoamperometry in the presence of EDC, by applying a potential of +2.2 V. The outer carbon ring electrode and inner spherical electrode were used as pseudo reference and counter electrode, respectively. This oxidation of the carbon generates carboxyl groups on the surface, as described before elsewhere [129] .

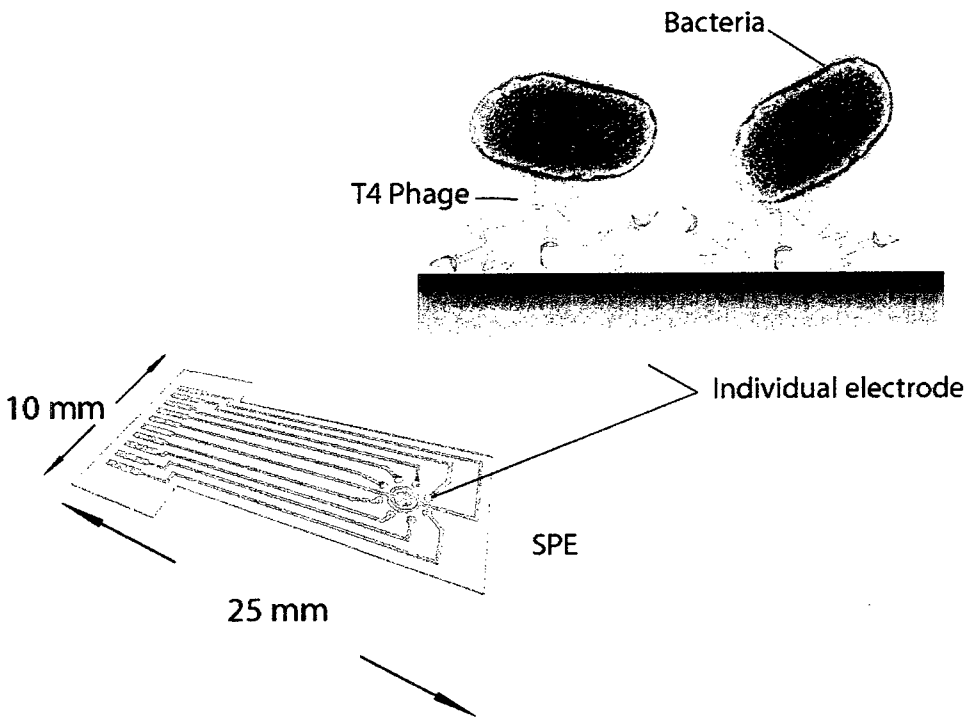

Figure 2.2 Schematic diagram for the assay using phages immobilized on electrode surfaces

The carboxyl groups react with the EDC and produce an ester intermediate that can then react with species carrying amino groups, resulting in their covalent attachment at the surface. Due to the fact that the outer membrane of a phage consists of protein, they can bind to the activated carboxylic groups, resulting in the attachment of phage to the surface through formation of amide bonds. This approach was used in this work to covalently attach T4 bacteriophage (wild type), in order to specifically detect target bacteria *E. coli K12*.

The attachment of the phage has been investigated using time-of-flight secondary ion mass spectrometry (TOF-SIMS). The chemical mapping (secondary ion spectra) was acquired from an area of 40 μm x 40 μm, using at least 3 different positions per electrode, to verify the immobilization process and confirm the attachment of phage at the electrode surface. Figure 2.3A provides the means for monitoring the reaction since it reveals two distinct high-intensity negative ion fragments at m/u = 26.0 and m/u = 41.9, indicating the presence of CN^- and CNO^- fragments after surface modification with EDC and the T4 immobilization. As shown in Figure 2.3A, the peak intensities for CNO^- (1) and CN^- (2) show a clear increase for a functionalized surface, compared to that of a bare electrode. This increase becomes drastically greater (by approximately a factor of 10) after phage immobilization due to the formation of amide bonds (EDC-T4, Figure 2.2A).

A

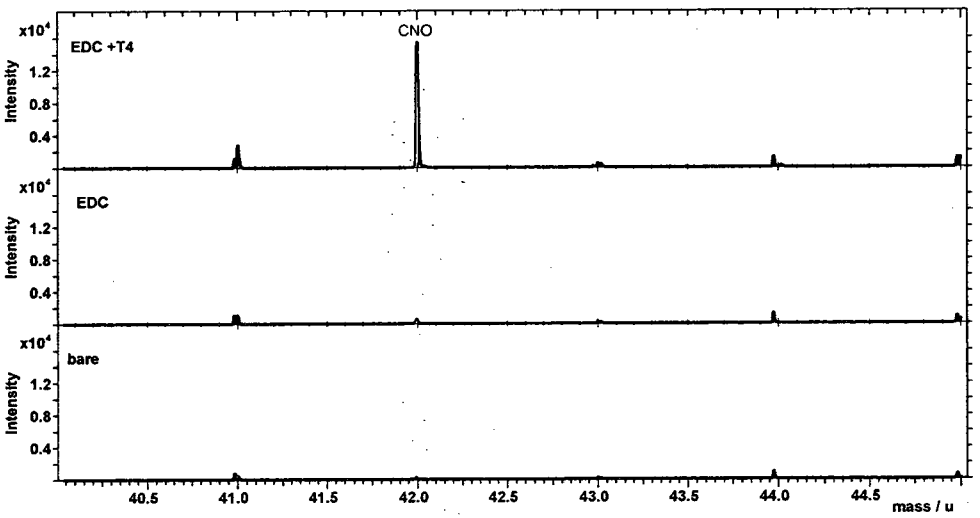
CNO
EDC +T4
EDC
bare
Intensity
x10⁴
1.2
0.8
0.4
40.5
41.0
41.5
42.0
42.5
43.0
43.5
44.0
44.5
mass / u

(1)

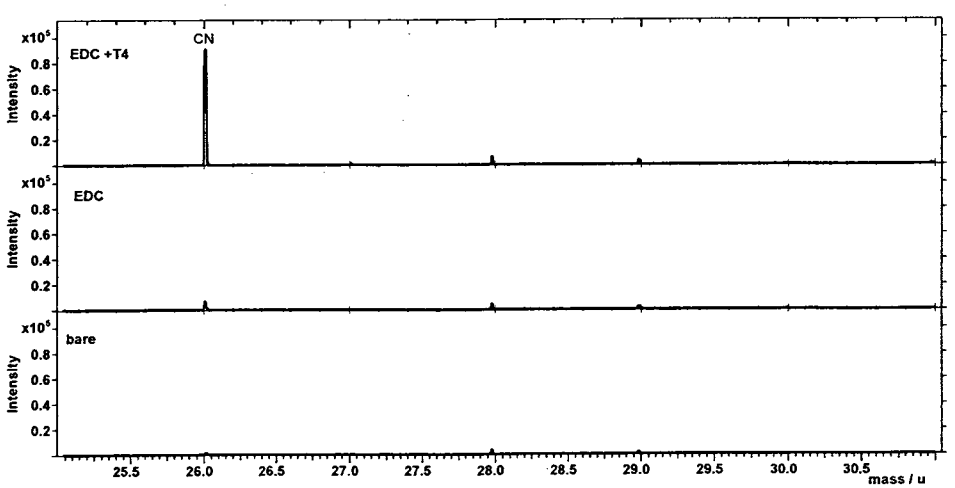
CN
EDC +T4
EDC
bare
Intensity
x10⁵
0.8
0.6
0.4
0.2
25.5
26.0
26.5
27.0
27.5
28.0
28.5
29.0
29.5
30.0
30.5
mass / u

(2)

B

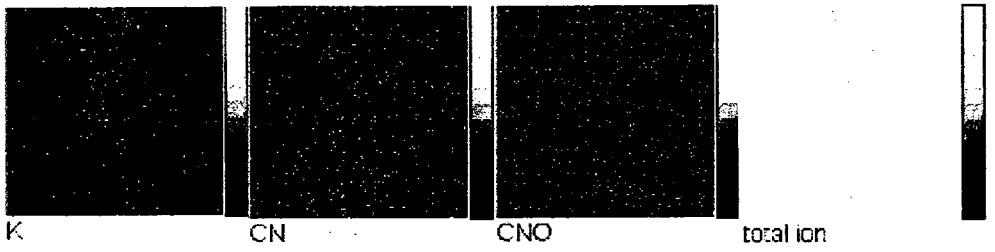

Surface 1

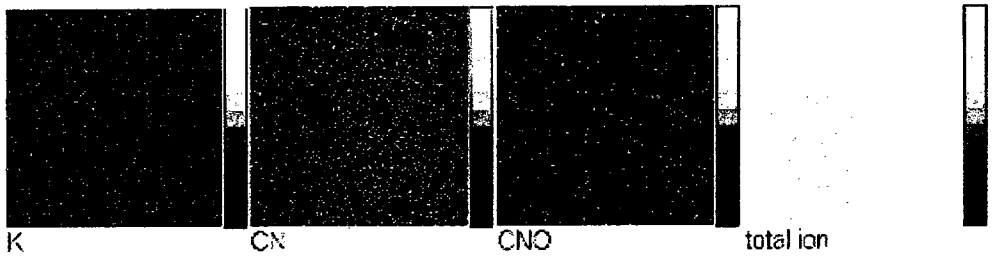

Surface 2

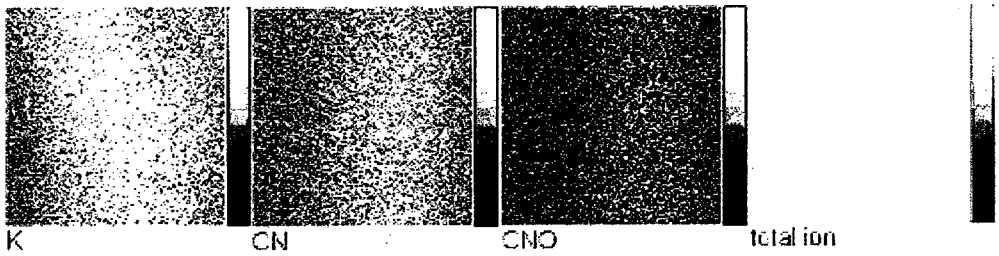

Surface 3

Figure 2.3 (A) TOF-SIMS spectrum for the bare, EDC-modified, and phage immobilized surfaces, for CNO^- (1) and CN^- (2). **(B)** Intensity maps of various positive and negative ions from each surface during the modification process, bare (surface 1), EDC (surface 2), phage T4 (surface 3). Ion intensity is scaled individually to show maximum counts as white and zero counts in black.

Figure 2.2B shows 40 x 40 μm^2 intensity maps of negative and positive fragments. It is clear from the intensity map that CN^- and CNO^- fragments are present on the EDC and T4 modified surface, showing gradually higher intensities. Also, the presence of K^+ is a good indication of the presence of biological entities such as cells and viruses [130], which is only observed after T4 immobilization. The relative intensity map for total ion reflects a homogeneous distribution for each surface following the modification processes.

2.3.2 Fluorescence and SEM imaging of bacteria at T4-modified electrode surfaces

GFP-labeled *E. coli K12* was incubated with the immobilized T4 phages on the electrode surface to study the lysis effect as a function of time. The fluorescence intensity of the bacterial cells was monitored from 0 to 40 min, and the acquired fluorescence microscope images are presented in Figure 2.4A. At time zero (immediately after adding the drop of bacteria on the surface) the fluorescence intensity is maximum, and active bacteria cells can be distinguished as bright green spots. From there, the fluorescence intensity is seen to decrease with time (a distinct decrease is already visible at 20 minutes) indicating an increasing number of *E. coli K12* cells being lysed by the immobilized T4. Very little fluorescent bacteria are visible after 40 minutes, and the process is essentially complete at 60 minutes (result at 60 minutes not shown in Figure 2.4A, but can be seen in 2.4B).

A

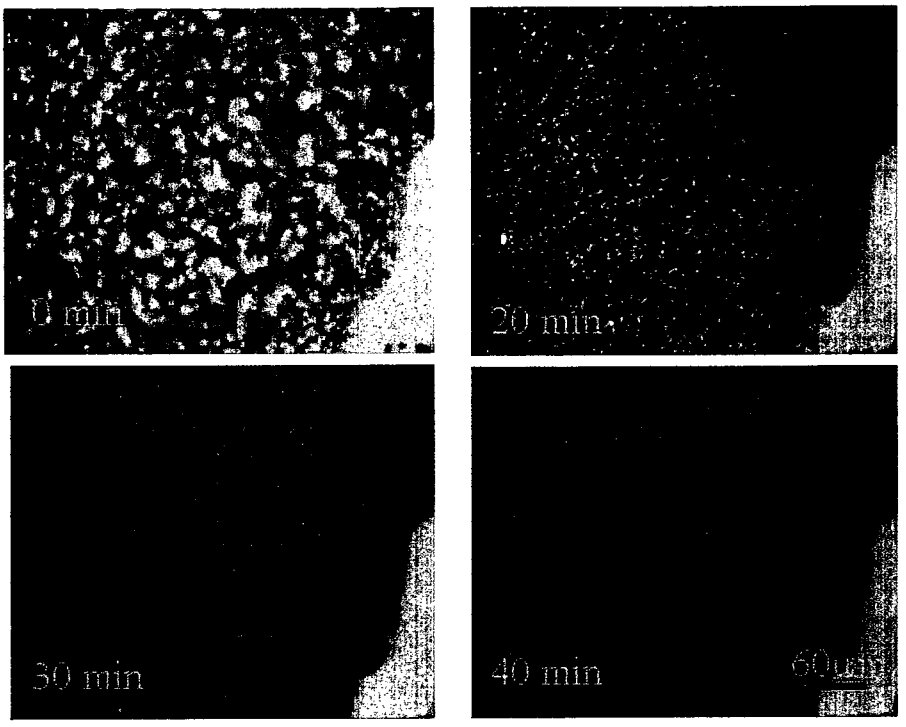

B

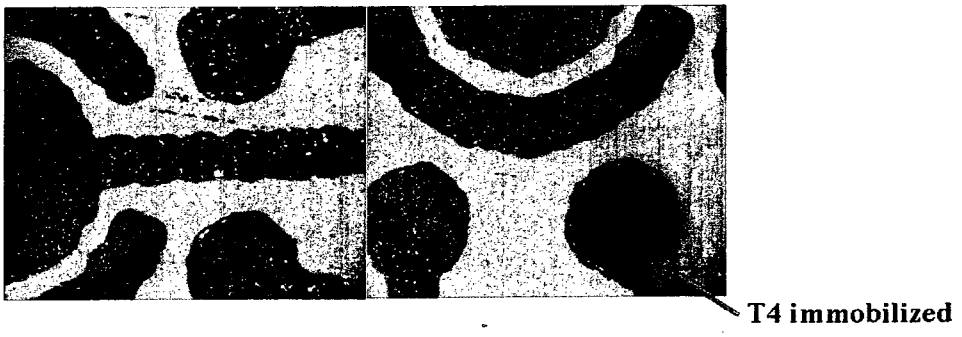

Figure 2.3 (A) Fluorescence images of T4-modified SPEs at specific times following contact with GFP-labeled *E. coli K12* solution. Magnification was the same for all four images, 400x. **(B)** Fluorescence images of T4-modified SPE (arrow), compared to non-modified SPEs on the same chip, following 60 minutes contact with GFP-labeled *E. coli K12* solution (left photo shows no T4-modified electrode). Magnification was the same for the two images, 100x. All working electrodes (as the one being pointed at) have a surface area of ~ 0.2 mm^2.

The electrochemical array approach under study presents the advantage of allowing each electrode of the same array to be addressed individually. The array carries eight similar 0.2 mm^2 working electrodes around the inner ring and larger central circular electrode. A control experiment was then performed by electrochemically functionalizing (addressing) a single working electrode of an array, while leaving the other seven working electrodes of the same array non-functionalized (without T4), and GFP-labeled *E. coli K12* was incubated on the array surface. The left image in Figure 2.4B depicts two of the seven non-functionalized working electrodes, after 60 minutes of incubation time, and intact bacteria are clearly visible. The right image in Figure 2.3B clearly shows that cell lysis has occurred only on the single T4-modified working electrode of the array (indicated with arrow), no fluorescent bacteria are observed, as compared to the adjacent non-addressed electrode.

Additionally, scanning electron microscopy (SEM) was used to verify binding of bacteria to phages immobilized on the electrode surface, after rinsing in SM buffer (Figure 2.5). SEM images were taken after phage immobilization (Figure 2.5A) and following the binding of bacteria (Figure 2.5B and 2.5C). There was no distinguishable change observed in the image following phage immobilization, mainly due to the roughness of the carbon surface compared to the nanometer size of phages. After phage immobilization, 50 μL of bacteria (10^8 cfu/mL) was incubated on the electrode surface for 10-15 min, followed by rinsing with SM buffer and acquisition of the SEM image. Figure 2.5B is a higher magnification image showing one single bacteria captured by

immobilized phage, and Figure 2.5C is a lower magnification image showing a number of bacteria on the same electrode surface. No bacteria were observed to bind to the immobilized T4 phages on the sensor surface when *Salmonella typhimurium* was used as a control experiment.

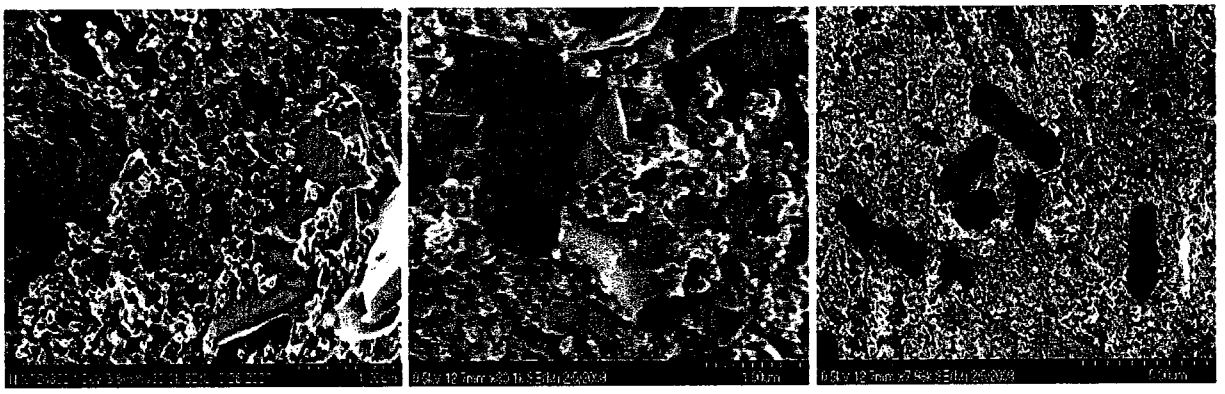

Figure 2.4 SEM images of bacteria bound to the phage-modified SPE surface. **(A)** T4 phage immobilized onto surface, **(B)** bacteria bound to immobilized T4 phage (high resolution), **(C)** bacteria bound to immobilized T4 phage (low resolution)

2.3.3 *E.coli* detection by electrochemical impedance spectroscopy (EIS)

The fluorescence imaging data presented in Figure 2.4 indicate that signs of lysis begin to appear at 20 minutes, and that the immobilized phages effectively lyse the bacteria within a period of approximately 40 to 60 minutes. As an initial experiment, this time dependent

behavior was studied with the electrochemical impedance detection approach, using T4 modified SPEs. After phage immobilization, the electrodes were washed with buffer solution and covered with 50 μL of 10^8 cfu/mL of *E. coli* cells, and the shifts in impedance were recorded at different times following the incubation of the bacteria suspension. Figure 2.6 shows the shifts in impedance observed from 10 to 60 min following deposition of the bacteria solution onto the electrode surface. First measurements were taken at 10 min to insure proper equilibration of the sensor device (for thermal equilibration and settling of the bacteria at the electrode surface).

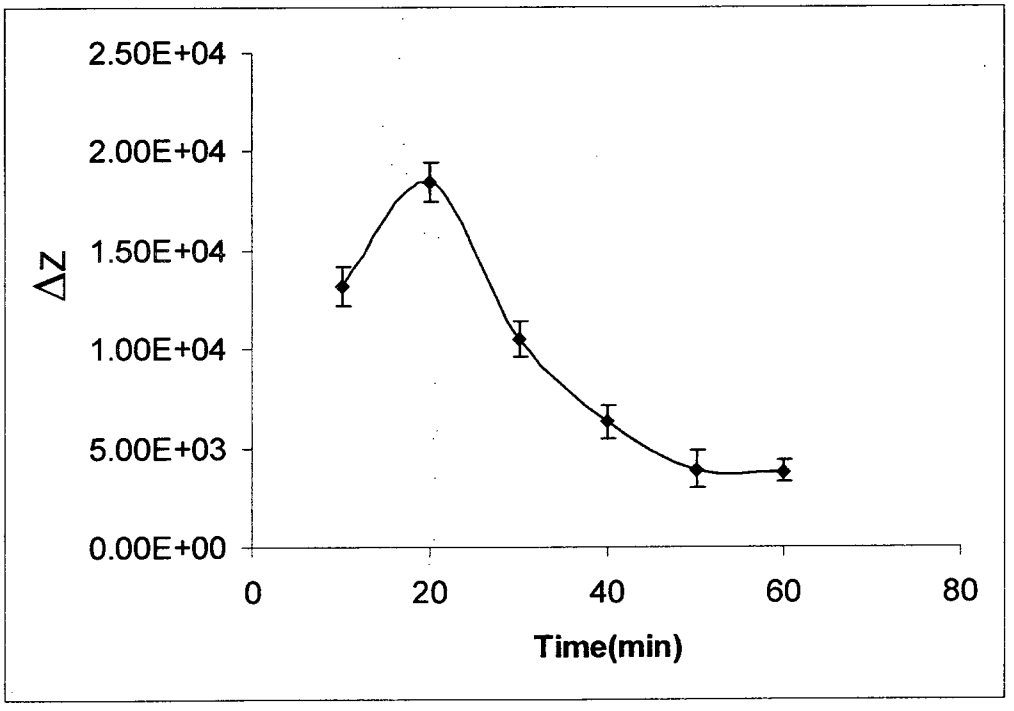

Figure 2.5 Shift in impedance at specific times following contact of *E. coli* solution with T4 modified SPE

The results show an initial increase in impedance shift, attributed to the arrival of intact bacteria at the phage modified electrode surface, which reaches a maximum value of ~ 1.9 x 10^4 Ohms at 20 min. Figure 2.6 also shows that the rate of shift gradually decreases after 20 min, providing an indication that the infection of the *E. coli* and the lytic cycle starts to occur within approximately 20 min at 37°C (approximately 35 min at room temperature), and levels off after 50 min.

The fluorescence imaging experiments (Figure 2.4) tend to confirm the time-response for bacterial decay, as monitored by electrochemical impedance. The images presented in Figure 2.4A show a progressive decrease in fluorescence intensity due to lysis of intact cells after 20 min, and Figure 2.4B indicates that essentially all of the bacterial cells have lysed after 60 min.

Figure 2.7 shows the impedance results (Nyquist plots) obtained when bacteria suspensions with different concentrations (10^2 to 10^8 cfu/mL) were placed on the bacteriophage-modified surface. Attachment of the T4 phage was typically observed to cause the Nyquist curve to shift positively by approximately 3 x 10^4 Ohms (looking at the extrapolation of the straight line portion of the Nyquist plot, onto the Z_r axis), relative to its position when the surface is modified with EDC only (curve not shown for clarity). To insure that a maximum impedance signal was measured, the Nyquist plots were taken at 25 min of incubation with the bacteria (after lysis has begun according to Figures 2.4A and 2.6), with each measurement (complete curve) taking 3 min to acquire. The equivalent circuit typically used to interpret the impedance results observed with this system is also shown in Figure 2.7. It is the same as the one presented in Figure 1.8, but

here we have simply adopted a different notation for the various circuit components. It consists of the resistance of the electrolyte (R_A), the charge transfer resistance (R_B), the double layer capacitance (C_d) and the impedance due to mass transfer (Z_a). In the high frequency domain, the Nyquist plots are expressed by the following equation:

$$(Z_r - R_A - R_B/2)^2 + Z_i^2 = (R_B/2)^2 \qquad (1)$$

corresponding to a half–circle plot starting at R_A and having a radius value equal to $R_B/2$. Z_r and Z_i are the real and imaginary impedances, respectively. In the low frequency domain, the plots show a straight line given by the following equation:

$$Z_i = Z_r - R_A - R_B + 2\sigma^2 C_d \qquad (2)$$

where σ is a diffusion-dependent term which is inversely proportional to the concentration of electroactive species in solution near the electrode surface [64].

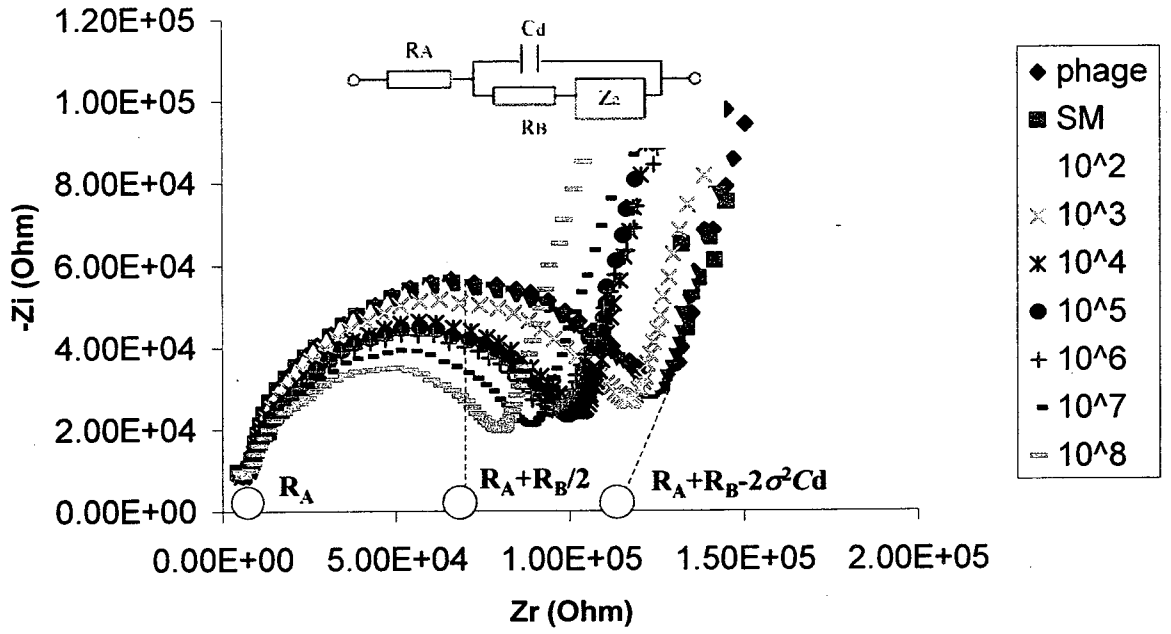

Figure 2.6 Nyquist plots for T4-modified SPE in the presence of *E. coli* at different concentrations

The numerical values of the equivalent circuit components were thus extracted from the data shown in Figure 2.7, and are summarized in Table 2.1.

E.coli Concentration (cfu/mL)	R_A (kΩ)	R_B (kΩ)	$2\sigma^2 Cd$ (kΩ)	($R_A + R_B - 2\sigma^2 C_d$) (kΩ)
0	5.67	121.22	15.13	111.76
10^2	5.70	117.71	12.75	110.66
10^3	5.75	113.99	10.69	109.05
10^4	5.88	102.39	9.32	98.95
10^5	5.85	102.57	13.55	94.871
10^6	5.83	91.93	8.36	89.39
10^7	5.94	89.64	13.78	81.80
10^8	5.96	88.28	18.30	75.94

Table 2.1 Values of equivalent circuit components as a function of bacteria concentration

Table 2.1 shows that R_A increases by approximately 290 Ohms for *E. coli* concentrations ranging from 10^2 to 10^8 cfu/mL, which is basically a consequence of an increasing introduction of non-conducting bacteria (intact bacteria having insulating membranes) in the electrolyte solution. Interestingly, the results (Figure 2.7 and Table 2.1) clearly indicate that the semicircle diameter, which relates directly to the value of the charge transfer resistance (R_B), undergoes a decrease with increasing bacteria concentration. This effect is contrary to what is usually observed for simple attachment of intact bacteria

cells to an electrode surface (i.e. an increase of charge transfer resistance, of impedance, with increasing concentration of intact bacteria at the surface) [77]. The reverse behavior presented in Figure 2.7 can be readily attributed to the fact that the measurements here are being performed during lysis of the bacteria, after 20 min, following surface attachment. Lysis involves the breakup of the bacterial cells and the release of highly mobile ionic material (such as K^+ and Na^+), thus increasing the conductivity of the media near the electrode surface. Correspondingly, the values related to charge transfer resistance (R_B) show a clear decrease with increasing concentration of *E. coli* cells.

The effect of increased bacteria concentration on the double layer capacitance and diffusion controlled processes at the surface, as expressed by the $2\sigma^2 C_d$ values obtained from the straight line portions of the curves shown in Figure 2.7, is also reported in Table 2.1. It should be noted that although the degree of roughness of the screen-printed carbon surfaces used in this study may preclude the formation/consideration of a double layer as described by strict theoretical formalism, the Nyquist plots however do show very good compliance with the behavior prescribed by the equivalent circuit (with C_d and Z_a) shown in Figure 2.7. The values for the $2\sigma^2 C_d$ factor appear to follow an initial decrease from 0 to 10^4 cfu/mL, followed by an increase (except for the result at 10^6cfu/mL) at higher concentration. Although this factor has much less influence than R_B on the overall variation in impedance, the trend can also be attributed to the lysis of bacteria at the surface. On the one hand an increase in the concentration of ionic species at the electrode surface is reflected by a decrease in the diffusion-dependent component, σ. On the other

hand, it increases the dielectric permittivity and decreases the thickness of the double layer, resulting in an expected gradual increase in C_d (hence a decrease in impedance) [77]. The overall effect on the variation in impedance is given in the last column of Table 2.1 which reports the values of $Z_r = R_A+R_B-2\sigma^2C_d$. No significant change in these values was observed for a concentration of 10 cfu/mL (compared to 0 cfu/mL), and therefore a concentration of 10 cfu/mL could not be detected by this system. It should be noted however that very small aliquots (50 μL) were used in these studies, which corresponds to a theoretical detection limit of 20 cfu/mL, confirming that 10 cfu/mL could not be detected.

2.3.4 Dose response

Control experiments in dose response were also performed with buffer solution only, and the non-target bacteria *Salmonella typhimurium*, and no significant impedance shifts were observed. Figure 2.8 shows a log-log plot for the impedance shifts (given as ΔZ, corresponding to the $\Delta(R_A +R_B -2\sigma^2C_d)$ between the curves in Figure 2.7), observed as a function of *E. coli* and *Salmonella typhimurium* concentrations ranging from 10^2 to 10^8 cfu/mL. For the specific target bacteria *E. coli*, the dose response was found to be nearly linear over seven decades of bacterial concentration, using three replicates of eight assays. The detection limit was found to be 2×10^4 cfu/mL when 50 μL of the bacteria sample was incubated for 25 min with the immobilized T4 phages. The detection limit

has been calculated from the slope of the calibration curve according to the following equation:

$$D.L. = k\sigma / m \qquad (3)$$

where k = 3, σ = noise of blank, and m = slope of calibration curve. The same detection experiments preformed with samples containing non-specific *Salmonella typhimurium* show comparatively minor variation over the same concentration range.

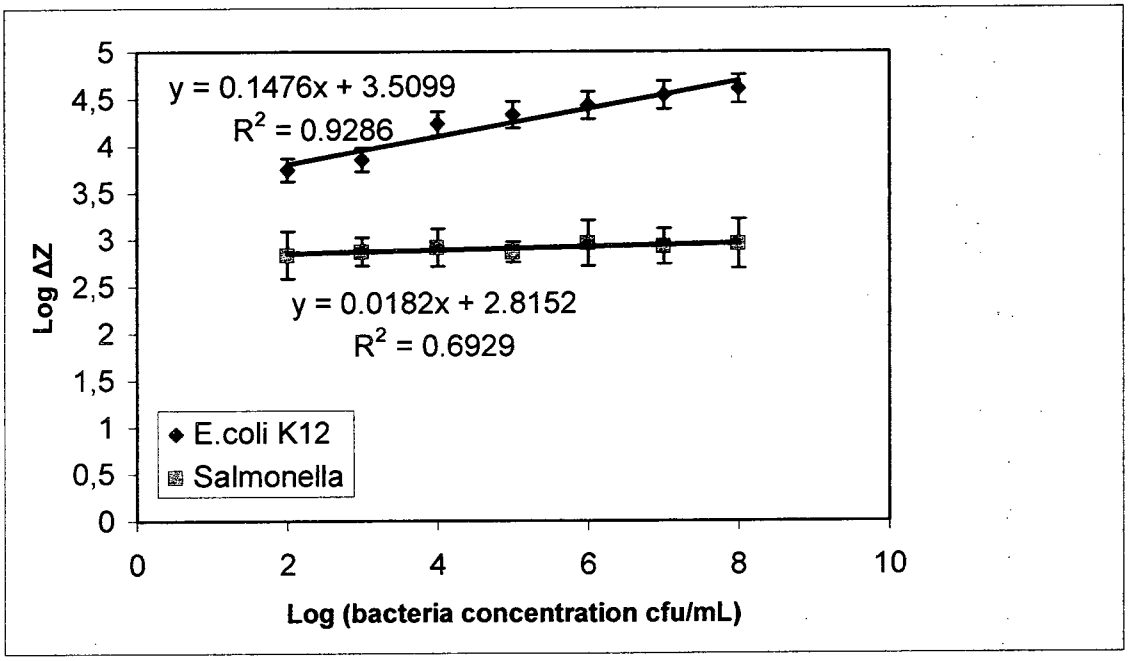

Figure 2.7 Dose response for different bacteria concentrations. $\Delta Z = \Delta(R_A + R_B - 2\sigma^2 C_d)$

The detection approach described herein has been shown to be fast and efficient in comparison with other phage-based methods reported for bacterial detection. For

example, the methods described by Goodridge et al. [131, 132], or Van Poucke and Nelis [133], are either time consuming (requiring 9-10 h) or require fluorescence labeling. Another approach published for identification of *E. coli* O157:H7, using the phage PPO1, requires genetic modification of the phage genome [134].

2.3.5 Conclusion

Low-cost, versatile, and robust screen-printed carbon electrode arrays have been used as the base transducers to successfully immobilize the lytic phage, T4, to act as a recognition element for the detection of *E. coli K12* cells. The impedance measurements performed with these arrays have been shown to provide a rapid, direct and label-free means of detecting specific bacteria using a simple phage-based approach. The Nyquist plots show significant changes in the high frequency range, corresponding mainly to a decrease in charge-transfer resistance due to lysis of *E. coli* by T4 at the electrode surface. TOF-SIMS analysis provides solid support for the successful immobilization of the bacteriophage, and fluorescence microscopy also indicates that specific bacteria lysis is occurring only at functionalized addressable electrodes of choice. Finally, comparison of the observed impedance response in the presence of non-specific *Salmonella typhimurium* demonstrates this approaches potential for direct and specific detection of bacteria.

CHAPTER 3

CARBON MICROAARAYS FOR THE DIRECT IMPEDIMETRIC DETECTION OF *BACILLUS ANTHRACIS* USING *GAMMA* PHAGE AS PROBE

3.1 Introduction

Bacterial contamination of food and water resources requires continued research world wide to develop rapid and specific methods to detect the various pathogens involved. In recent years this has led to important progress in the field of biosensors, resulting in the development of more rapid, analyte-specific, robust, and cost-effective devices by incorporating emerging technologies from various disciplines [9, 14, 38, 77, 135].

In addition, the potential threats to population and territorial security associated to some of these bacterial agents, is another aspect justifying the need to develop immediate means of identification and intervention. Biological warfare agents may include microorganisms such as bacteria, viruses, fungi, or toxins causing death or disease in humans, animals or plants [136]. Some of the bacterial pathogens that have been classified as potential bioterrorism agents include *Bacillus anthracis* (anthrax bacteria), *botulinum* toxin, *staphylococcal enterotoxin* B (SEB) and *Yersinia pestis* [137]. Among these the most common is the gram-positive *B. anthracis*, which causes a highly lethal infection. In most cases these organisms enter through skin wounds, but they may also be inhaled or ingested.

The genus *Bacillus* includes three species, *B. anthracis, B. thuringiensis* and *B. cereus* that are of primary interest because of their ability to produce toxins. Endospores are ideal delivery vehicles for the distribution

of toxin-producing species into the environment, because their extreme resilience enables them to survive in bioaerosols for extended periods. The most ominous use of endospore-formers is the release of *B. anthracis* as a bio-weapon [138, 139] with devastating health, psychological, and economic impacts [140]. In 1998-1999, an outbreak due to the release of anthrax in the United States led to the infection of 6000 people. In 2001, 22 suspected cases of bio-terrorism related to anthrax were reported in the United States [139]. Most cases were postal workers in New Jersey and Washington DC, where letters were contaminated with anthrax. According to a study performed by the Centers of Disease Control and Prevention (CDC), the release of anthrax in a US city could cost from $477.8 million to 26.2 billion per 100,000 people exposed. The prevention of disease propagation by biological threat agents such as *B. anthracis* in clinical medicine, food products and other environments, has therefore driven major efforts to develop portable, field-ready, inexpensive sensor devices for rapid detection [141]. To date techniques for identification of anthrax are mainly based on nucleic acid detection [142-148]. Although these methods are highly sensitive, they have the disadvantage of requiring several reagents to conduct the assay, and spores need to be germinated prior to the assay. Another type of method being used is immuno-detection [16, 17, 149-152], which again requires multiple reagents, and performing the assay takes more than 30 min. Additionally, this method suffers from cross-reactivity of antibodies and non-specific binding. Mass spectrometry

has also been used to detect *B. anthracis* [18- 21, 153] , but the method is not as sensitive as antibody or nucleic acid detection. An additional drawback is that mass spectrometers are expensive and are not portable.

The infectious dose for *B. anthracis* has been reported to be around 10^4 spores and few rapid detection methods can detect spore counts below 10^5 [154]. ELISA has been used extensively for the detection of *B. anthracis*. The detection limit of typical ELISA for endospore and whole cell detection is usually in the range of 10^4–10^6 bacteria [110, 155]. ELISA involves several steps that are time consuming, it relies on reagents that have a short shelf life, and it can be prone to cross-reactivity therefore limiting its use. ELISA has been somewhat improved in recent years to increase its sensitivity and shorten the detection time. ELISA-based immunoassay has been performed in a capillary to produce a portable detection system [156]. Magnetic bead-based ELISA is rapid and sensitive, and was developed for the detection of *B. anthracis* endospores [157]. The reported detection limit in this case was 2.6×10^3 spores/mL, with detection being achieved in 30 min. The detection limit of ELISA was further improved 20-fold when cooled ultrasonic cavitation was applied to bacterial spores [158].

Several lateral-flow immunoassay-based test kits, for endospore detection using the naked eye, are on the market and include the SMART-II Anthrax Spore test kit, (New Horizons Diagnostics, Columbia, Md.), the Anthrax BioThreat Alert Kit (Tetracore, Gaithersburg, Md.), and the BioWarfare Agent Detection Devices (Osborne Scientific, Lakeside, Ariz.). These test systems can be used by personnel having minimal training, and give results within 3 to 15 minutes. However, the sensitivities of these kits still

remain low with a 10^5 to 10^6 endospore detection range [159]. The RAMP System, developed by Response Biomedical Corp., can detect as few as 4000 *B. anthracis* spores in 15 minutes using fluorescent magnetic beads and a portable scanning fluorescence reader. Immunomagnetic electrochemiluminescence was employed for the detection of *B. anthracis* in a phosphate buffer, with a detection limit of as few as 100 spores within 30 to 90 min [160, 161], and the detection limits were reduced by 3 orders of magnitude in soil suspensions [160].

Flow cytometry has been successfully adapted as a detection method for immune-based assays for *B. anthracis*. Stopa et al. achieved detection of *B. anthracis* spores in 5 minutes by simply allowing fluorescein-labeled antibodies to incubate with a sample of endospores before analysis on a flow cytometer [162]. The reported detection limit was approximately 10^3 spores/mL. The use of specific capture peptides conjugated with fluorescent quantum dots has also been reported for the detection of *B. anthracis* spores [163]. A membrane filter microchip-based flow cell system was developed to detect *B. globigii* spores as a model for *B. anthracis* [164]. This system has a sensitivity of 500 spores and gives results within 5 min.

Mass sensitive devices such as the quartz crystal microbalance (QCM), magnetoelastic sensors and piezoelectric cantilevers have also been employed for *B. anthracis* detection. The QCM approach was able to detect concentrations as low as 10^3 cfu/mL, in less than 30 min, using polyclonal antibody [165]. Magnetoelastic biosensors, as mass sensitive devices, have been used successfully for the detection of *B. anthracis* using filamentous bacteriophage. A detection limit of 10^3 cfu/mL, with a sensitivity of 6.5 kHz/decade, was

achieved [166-168]. Piezoelectric-excited millimeter-sized cantilever sensors consisting of a piezoelectric and a borosilicate glass layer, with a sensing area of 2.48 mm^2, enabled the detection of *B. anthracis* using antibodies as probes. The detection limit was 300 spores/mL in Bain phosphate buffer [169]. The same system was used for the detection of *B. anthracis* in air samples, after concentration in phosphate buffer. The results showed that detection of 38 *B. anthracis* spores/L of air was achievable with an estimated lower limit of detection of ~ 5 spores/L of air in the configuration tested [170].

To date a great number of different types of optical biological sensors have been reported, employing surface plasmon resonance (SPR), fluorescent evanescent planar waveguides, interferometric [171] and fiber optical techniques. To highlight a few and going back to year 2000, we have Perkins and Squirrell that worked on developing a sensor device to detect *Bacillus subtilis*, based on simultaneously measuring the scattering of light and change in refractive index, caused by captured spores. The scattering signal enabled detection of spores at a level of 10^7 mL^{-1}, but no significant response was obtained in relation to changes of refractive index (the SPR aspect of the detection process) [103]. A fluorescence-based biosensor using a planar waveguide with a patterned array of antibodies was developed to detect biothreat bacteria such as *B. anthracis* and *Franciscella tularensis* [172, 173]. Using this evanescent wave sensor, detection limits of 10^3 to 10^6 cfu/mL were achieved for bacterial analytes. Tims and Lin demonstrated the feasibility of using an evanescent wave fiber-optic sensor (Analyte 2000) to detect *B. anthracis* spores in various powder samples with minimal preparation [174]. Biotinylated capture-antibodies were immobilized on tapered polystyrene fibers and used with Cy5-

labelled anti-*B. anthracis* antibodies in a sandwich assay format. Spores were detected at a level of 3.2×10^5 spores/mg, with no false positives, in less than 1 hour [174]. Hang et al. have reported a detection limit of 10^3 spores for *B. anthracis* using an integrated waveguide biosensor followed by a method for the rapid release and germination of immuno-captured spores [175]. Zourob and coworkers have developed a system using a metal-clad leaky waveguide (MCLW) to extend the evanescent field penetration at the sensors surface to sense more of the cells volume and improve the sensitivity [104, 176]. The detection limit using refractive index variations was 8×10^4 cfu/mL and 1×10^4 cfu/mL using scattering, with results collected in 20 min. They were able to integrate the waveguide with an electric field [177], and with ultrasound waves [178], to deposit the cells rapidly onto the immobilized antibodies of the sensor surface to improve the sensitivity and shorten the analysis time. The group was able to reach a detection limit of 10^3 cfu/mL, with measurements achieved in 2 min [104].

In the area of electrochemical techniques of detection, Yemini et al. used an amperometric, phage-based biosensor for the detection of as low as 10 viable cells/mL of *Bacillus cereus* and *Mycobacterium smegmatis* in 8 hours [179]. Pal et al. have reported on a direct charge-transfer conductometric polyaniline-based nano-wire biosensor, for the detection of *Bacillus cereus* using a sandwich assay for various food samples. In their study, the biosensor was able to detect cell concentrations in the range of 35–88 cfu/mL in food samples, with a detection time of 6 min [180, 181]. The same group used an electrically active, polyaniline-coated magnetic nanoparticle-based biosensor, for the immunocapturing and detection of *Bacillus anthracis* endospores in lettuce, ground beef,

and whole milk samples. The detection limit for this approach was as low as 4.2×10^2 spores/mL, with procedures performed in 16 min [182].

In this work we describe the development of a phage-modified microarray, for the direct and rapid impedimetric detection of *B. anthracis*. The method was adapted from the previous work on the detection of *E. coli K12* using phage T4 as probe [34]. Here *Gamma* phage is used as probe and we report on an alternate electrochemical functionalization approach for the attachment of the phage at electrode surfaces. The detection approach is also electrochemical in nature, it is inexpensive and can provide the basis for a sensitive and portable device.

3.2 Experimental Methods

3.2.1 Surface functionalization and phage immobilization

Cyclic voltammetry was performed using 2mM 4-nitrobenzenediazonium tetrafluoroborate in an aqueous solution containing 0.1 M H_2SO_4. The nitro groups were then reduced to amino groups in 0.1M KCl (90:10 H_2O-EtOH) solution using cyclic voltammetry. For all cyclic voltammetric scans, the potential range was varied from 0.4V to -1.7 V, at a scan rate of 200 mV/sec. All cyclic voltammograms were obtained with a computer-controlled Voltalab electrochemical workstation (model PGZ 301 by Radiometer, Copenhagen). After the electrochemical modification, the chips were rinsed with distilled-deionized water and dried under a flow of air. The chips were subsequently treated with 50 μL of 25% glutaraldehyde solution for 30 minutes prior to immobilization

of the bacteriophage probes. The glutaraldehyde acts as a linker to attach the phage to the surface. After treatment with glutaraldehyde, the chips were rinsed with distilled-deionized water and immersed in 2 mL of bacteriophage gamma solution (10^8 pfu/mL in SM buffer solution pH = 7.4) for two hours with shaking. The modified chips were then treated with glycine (dipped in 0.1 M aqueous glycine solution for 20 min) to cap off any unreacted aldehyde groups remaining after phage immobilization.

3.2.2 XPS analysis

XPS studies were performed on a VG ESCALAB 3 MKII (VG, Thermo Electron Corporation, UK). The instrument has an operating pressure below 5 x 10^{-9} Torr. Samples were irradiated using an MgK_α source. The power of the source was 206 W (energy = 12 kV, emission current = 18 mA). The analyzed surface was 0.2 mm, at a take-off angle of 0° (i.e., perpendicular); consequently, the depth sampled was around 60-100 Å. On the survey scan each peak corresponds to a binding energy associated to a specific chemical element. The relative atomic percentages of relevant chemical bonds were determined from the deconvoluted peak intensities.

3.2.3 TOF-SIMS analysis

TOF-SIMS studies were carried out with an ION-TOF SIMS IV (ION-TOF GmbH, Muenster, Germany). The instrument has an operating pressure of 5 x 10^{-9} Torr. Samples

were bombarded with a pulsed liquid metal ion source ($^{69}Ga^{+}$), at an energy of 15 KeV. The gun was operated with a 27 ns pulse width and a 1.02 pA pulsed ion current for a dosage lower than 5 x 10^{11} ions cm^{-2}, well below the threshold level of 1 x 10^{13} ions cm^{-2} for static SIMS. Secondary ion spectra were acquired from an area of 40 x 40 μm, with 128 x 128 pixels (1 pulse per pixel), using at least 3 different positions per electrode. A chemical mapping was done on a surface of 40 μm x 40 μm.

3.2.4 Impedimetric detection

A three-electrode setup was used to perform the electrochemical measurements. Impedance measurements were performed with 40 μL aqueous samples composed of 10 mM potassium hexaferricyanide/potassium hexaferrocyanide (1:1) mixture in 0.1 M KCl. Impedance was measured at a dc potential of 400 mV, with a superimposed ac voltage of 20 mV amplitude at frequencies ranging from 100 kHz to 100 Hz, applied to the working electrode. Results obtained under these measurement conditions showed good reproducibility (no adverse effects were observed due to the use of the centrally located ring-shaped carbon electrode of the array as pseudo-reference). All Nyquist curves were run from the high ac voltage frequency limit, to the low frequency limit. All measurements were performed with a Voltalab electrochemical workstation (model PGZ 301 by Radiometer, Copenhagen). The Voltamaster computer program (version 4.0) was used to run the experiments, acquire, and process the data of the Nyquist plots (imaginary impedance (Z_i) versus real impedance (Z_r)).

3.3 Results and Discussion

3.3.1 Surface modification of carbon using a diazonium salt

The first step for chemical functionalization of the carbon SPEs was carried out using cyclic voltammetry in contact with an aqueous 2 mM tetrafluoroborate 4-nitrobenzene diazonium solution in 0.1 M H_2SO_4. The initial cyclic-voltammetric scan in Figure 3.1 (blue curve) shows a broad and irreversible cathodic wave at around – 0.7 V, which upon a second scan displays a flat, near zero, cathodic current profile (red curve) indicating good coverage of the surface and little further redox activity. The reduction process of the diazonium moiety at the carbon surface can be described by the following simplified reaction (Scheme 3.1) [183].

Scheme 3.1 Chemical functionalization of carbon surface using nitrobenzene diazonium moiety

The next step in surface functionalization, is the cyclic voltammetric reduction of nitro groups to amino groups in the presence of a 0.1M KCl, (90:10 H_2O-EtOH) solution (Scheme 3.2), indicated by the cathodic wave seen in Figure 3.2 at around – 1.1V.

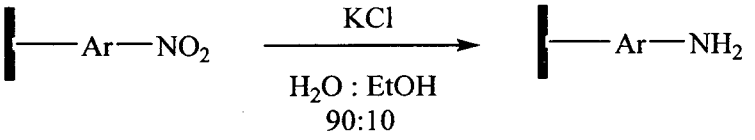

Scheme 3.2 Electrochemical reduction of nitro groups to amino groups

The reduction of the nitro groups to amino groups is known to be a 6-electron process, as described in the literature [184]. It should be noted however, that reports focused on the modification of glassy carbon surfaces using this electrochemical approach have revealed that the reduction is only partial, resulting in a small fraction of NO_2 groups undergoing a 4-electron reduction to form NHOH rather than NH_2 [183] . This aspect was further investigated herein by x-ray photoelectron spectroscopy (XPS) measurements.

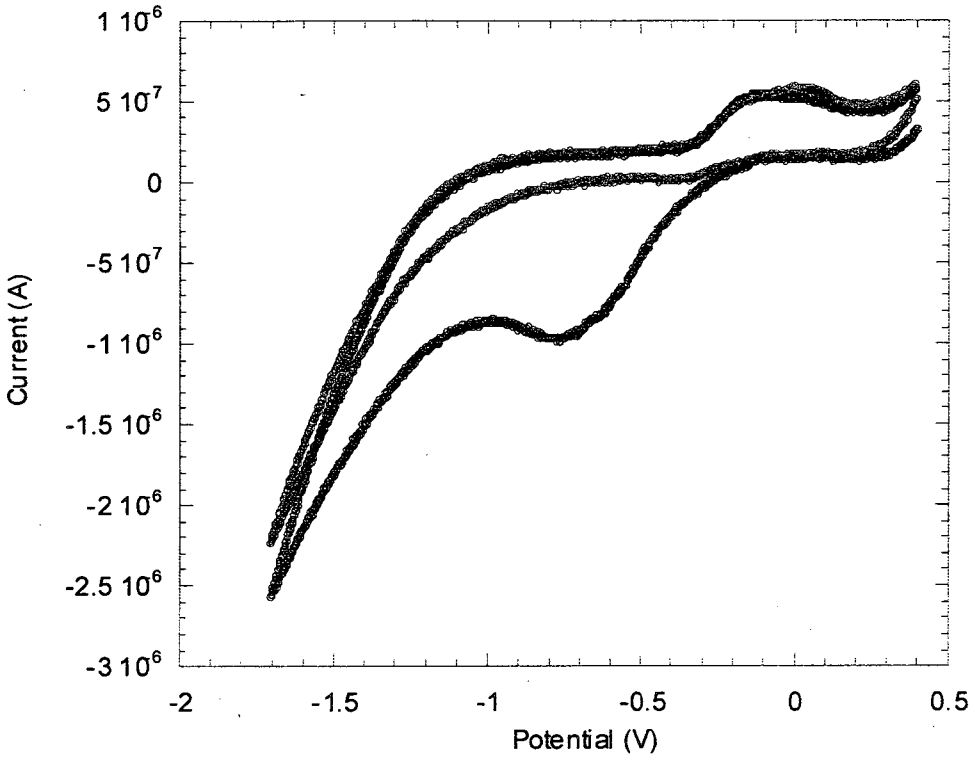

Figure 3.1 Cyclic voltammetric functionalization of carbon electrodes in contact with 2 mM BF_4-N_2 (C_6H_4)-NO_2 in 0.1 M H_2SO_4 aqueous media.

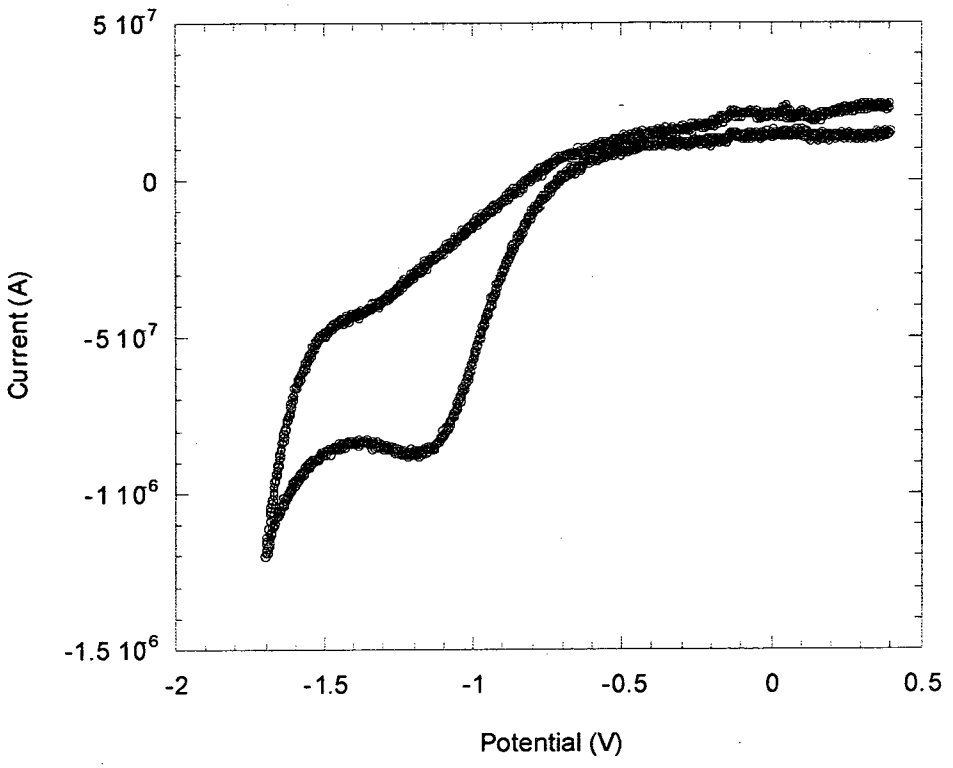

Figure 3.2 Cyclic voltammogram of the reduction of nitro groups to amino groups in 0.1M KCl (90:10 H_2O-EtOH) solution

3.3.2 XPS characterization

X-Ray photoelectron spectroscopy survey scans of bare and functionalized microarrays are presented in Figure 3.3. Figure 3.3 curve A indicates the presence of the carbon 1s (C 1s) and oxygen 1s (O 1s) peaks at the surface of the bare screen-printed carbon electrodes.

Upon electrochemical functionalization with the nitro-aryl moiety (Figure 3.3 curve B), and further reduction of the nitro groups to amino groups (Figures 3.3 curve C), a decrease in the C 1s peak intensity is observed, accompanied by the appearance of peaks due to nitrogen 1s (N 1s) in the 400 eV region.

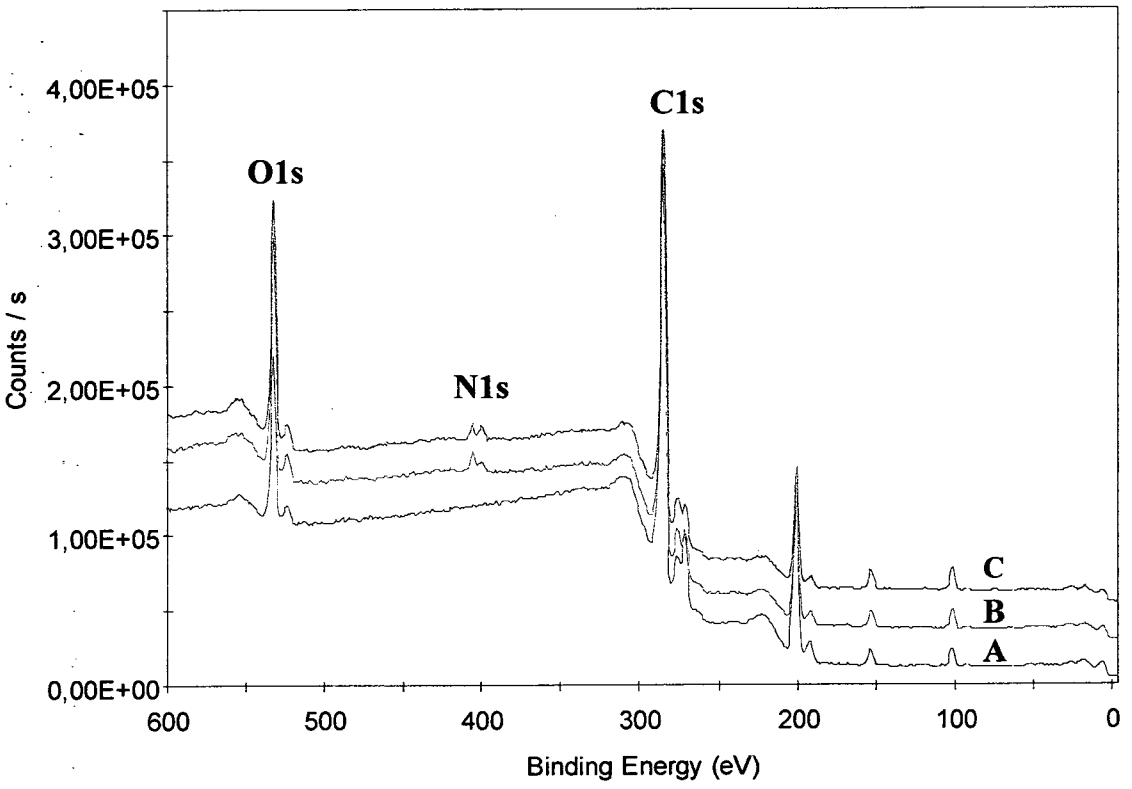

Figure 3.3 XPS survey spectra for **(A)** the bare carbon surface, **(B)** carbon functionalized with aryl-nitro groups, and **(C)** the reduction of nitro groups to amino groups

The binding energies at which peaks appear provide means of identifying different chemical elements involved in surface bonding and therefore higher resolution scans were taken to focus on elements of interest. The binding energy values were calibrated with the hydrocarbon C 1s peak situated at 285.0 eV, and the overall results (bond type and assigned percentages) are presented in Table 3.1.

Surface	**C 1s** **BE (eV); %, assignment**	**N 1s** **BE (eV); %, assignment**	**O1s** **BE (eV); %, assignment**
Bare			
	284.6 (46.4), C=C		532.1(11.1),O=C
	286.5 (21.1), C-O		533.1(4.3), O-C
Nito group			
	284.6 (26.7), C=C	399.9(0.7), C-N	532.1(11.8),O=C
	285.4 (32.0), C-NH	400.9(0.6),-NH_x	533.1(9.3), O-C
	286.5 (15.3), C-O	402.5(0.3),-N(CH_x)	533.9(2.4), O-N
		406.2(2.4), NO_2	534.9(0.9), NO_2
Amino group			
	284.6 (28.2), C=C	399.9(0.5), C-N	532.1(10.2),O=C
	285.4 (31.5), C-NH	400.9(1.0),-NH_x	533.1(8.1), O-C
	286.5 (16.2), C-O	402.5(0.3),-N(CH_x)	533.9(1.4), O-N
		406.2(1.7), NO_2	

Table 3.1 Summary of the XPS binding energies for C 1s, N 1s, and O 1s, after each modification step.

As shown in Figure 3.4, the deconvoluted C 1s peak for surfaces following the aryl-NO_2 to aryl-NH_2 reduction step, presents three distinct contributions (peaks A, B, C). The first peak at 284.6 eV is attributable to the C=C bonds of the aryl component. The second and

third peaks, centered at 285.4 eV and 286.5 eV are indicative of C-NH and C-O bond-types [185].

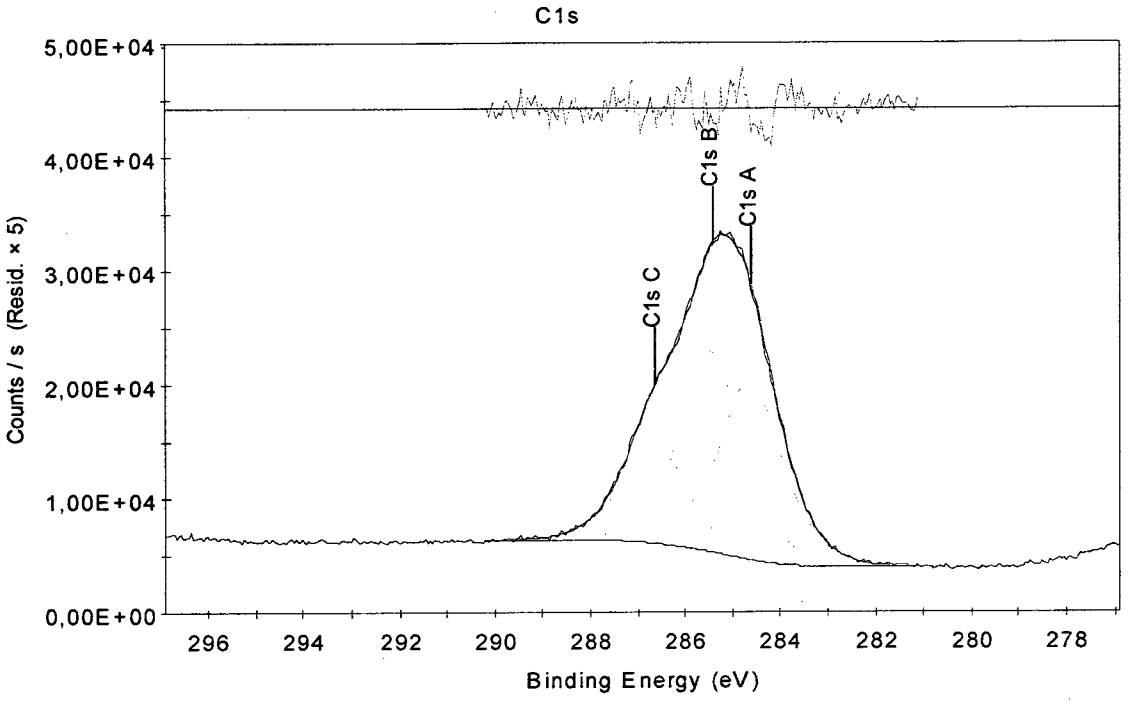

Figure 3.4 High-resolution, deconvoluted C 1s peak of the XPS spectrum for SPEs following reduction of nitro groups to amino groups

In Figure 3.5, the deconvolution of two peaks corresponding to the N 1s energy yields four separate bonding interactions at 399.9 (A), 400.9 (B), 402.5 (C), and 406.2 eV (D). In most applications involving amino-functionalized surfaces, the amino groups are oriented outward and available for reaction with other molecules coming in contact. The presence of these free

reactive primary amines is indicated by the peak at 400.9 eV (N 1s B), and is supported by the peak centered at 399.9 eV corresponding to C-N bonding. The peak at 402.5 eV is attributed to hydrogen bonding expected to occur between the amino groups [186] . The peak at 406.2 eV corresponds to NO_2 species and tends to indicate that a low fraction of nitro groups are still present following the final electrochemical reduction process (with NH_2 functional groups more likely near the surface and NO_2 groups more likely present toward the bulk of the layer formed during the initial reduction step).

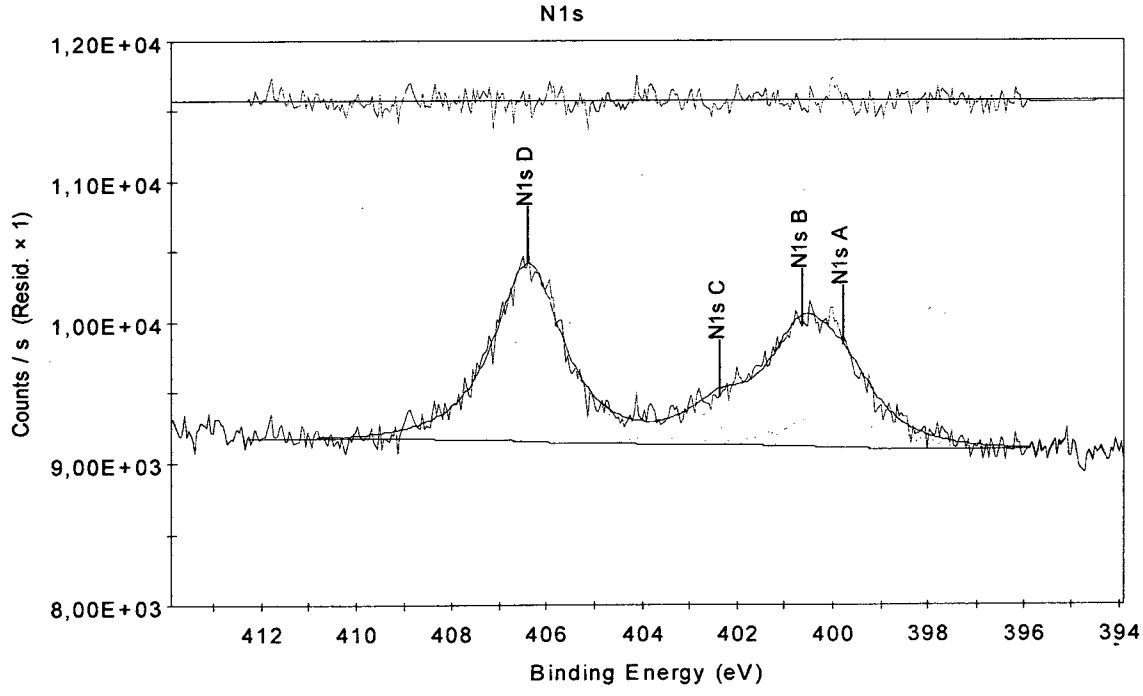

Figure 3.5 High-resolution, deconvoluted XPS spectrum of the N 1s peak for SPEs following reduction of nitro groups to amino groups

3.3.3 TOF-SIMS characterization of the surface after phage immobilization

Phage immobilization onto the SPE surface was performed using glutaraldehyde as a linker (Scheme 3.3).

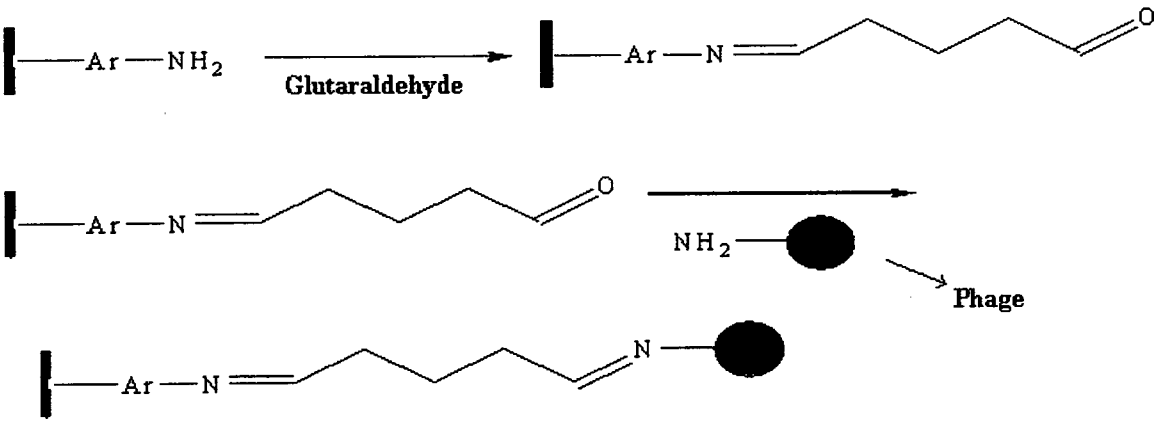

Scheme 3.3 Phage immobilization using glutaraldehyde as linker

The attachment of the phage was then investigated using time-of-flight secondary ion mass spectrometry (TOF-SIMS). Figure 3.6 reveals the appearance of a distinct high-intensity peak at m/u = 26.0, after immobilization of *Gamma* phage onto the glutaraldehyde-modified surface, corresponding to the negative ion fragment CN^-. This provides evidence for the binding reaction of the aldehyde groups with the amino groups of the phage.

presence of K^+ provides a good indication of the presence of biological entities such as cells and viruses, and further supports the conclusion that the attachment of *Gamma* phage was successful.

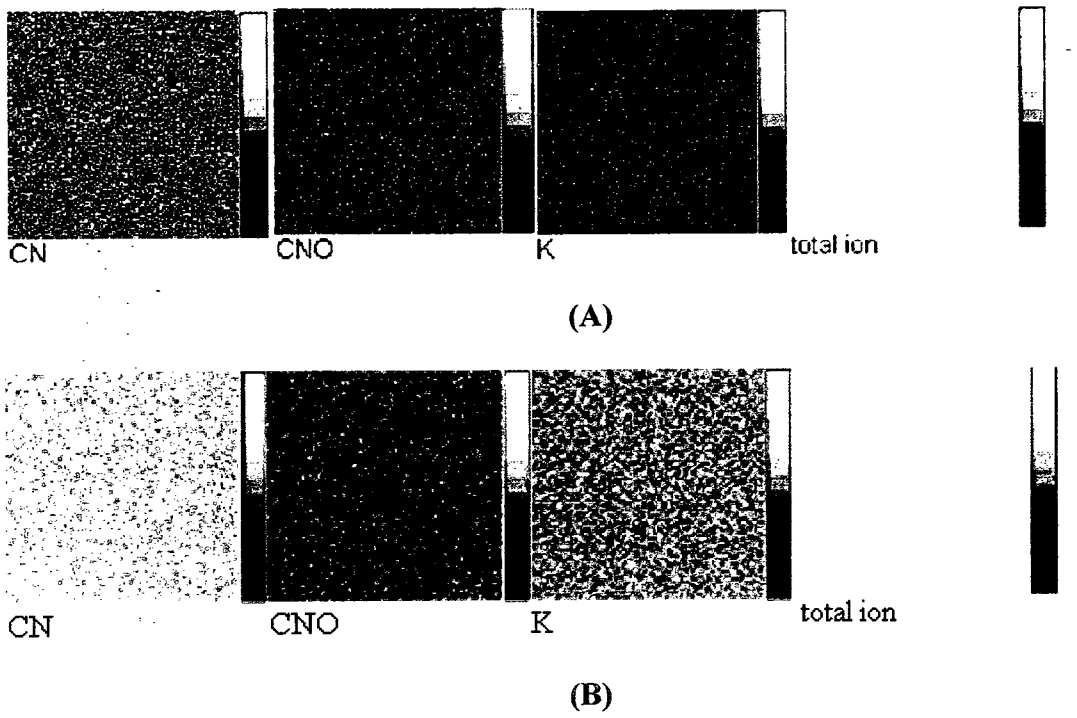

Figure 3.7 Intensity maps of ions following the modification with glutaraldehyde (A) and *Gamma* phage (B). Ion intensity is scaled individually to show maximum counts as white and zero counts as black.

3.3.4 *Anthracis* detection and concentration dependence using Faradaic impedance

The basic impedimetric detection principle using the phage-bacteria complex is illustrated in schematic 3.4.

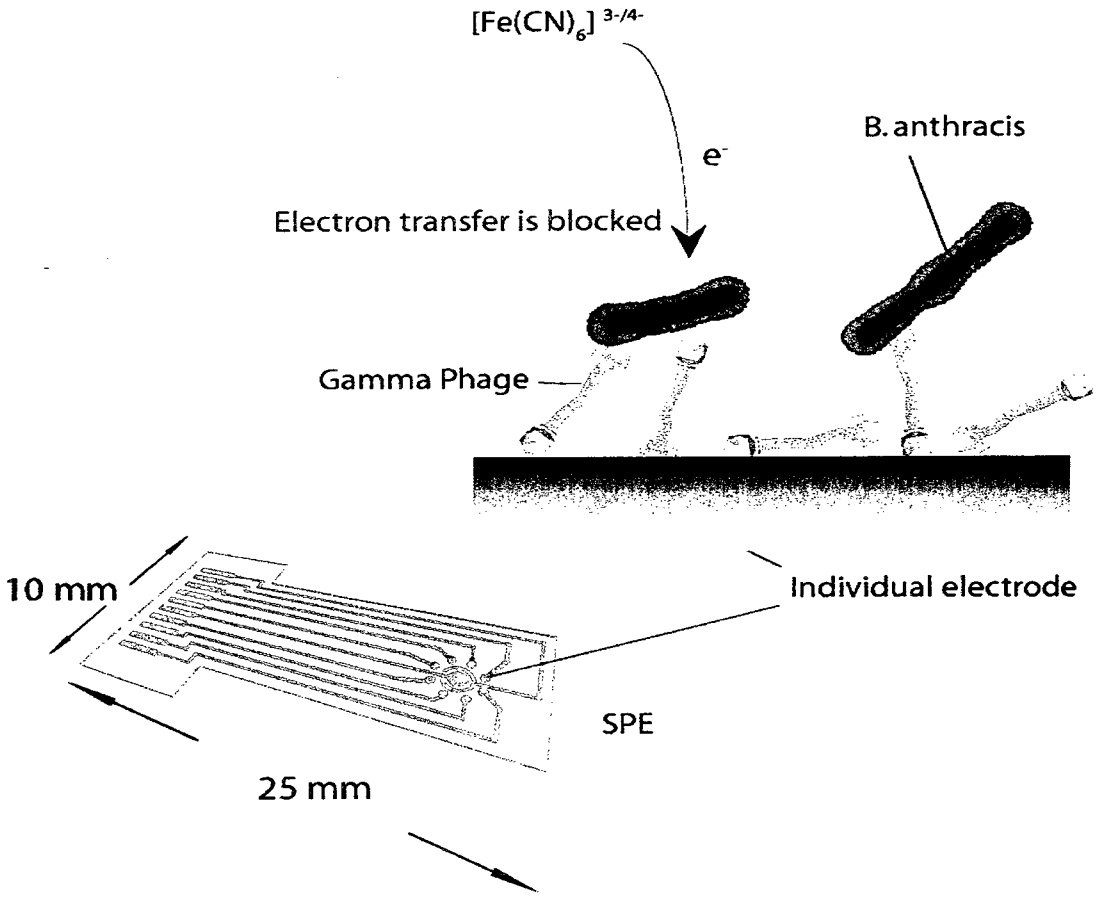

Scheme 3.4 Faradaic impedance detection of *B. anthracis*

Faradaic impedance has been measured using the hexacyanoferrate redox couple (10 mM $[Fe(CN)_6]^{3-/4-}$ (1:1 mixture) in 0.1 M KCl solution as electrolyte). The typical equivalent circuit used to interpret the impedance results (Nyquist plots) observed with this system is based on the Randles model (Figure 3.8A). As described previously it consists of the resistance of the electrolyte (R_s), the charge transfer resistance (R_{ct}), the double layer

capacitance (C_d), and the Warburg impedance (Z_w). R_s and Z_w represent the bulk resistive property of the electrolyte solution and the diffusion controlled transport of redox species near the electrode surface, respectively.

Figure 3.8 B illustrates the shape of Nyquist plots that result from the equivalent circuit given in figure 3.8A, and the associated parameters. R_s and R_{ct} correspond to the Z_r values obtained by extrapolation of the half circle (to the Z_r axis at $-Z_i = 0$), at the high frequency and low frequency ends, respectively. The value of Z_r, obtained by extrapolating the straight-line portion of the plot (to $-Z_i = 0$) in the low frequency range, is given by the following equation [64].

$$Z_r = R_s + R_{ct} - 2\sigma^2 C_d \qquad \textbf{(3.1)}$$

The Nyquist plots were acquired at 40 min of incubation with bacteria concentrations ranging from 0 to 10^8 cfu/mL, with each measurement (complete curve) taking 3 min to acquire. Figure 3.9A shows the typical shift in Nyquist plots observed when bacteria suspensions of 10^8 cfu/mL were placed on the bacteriophage-modified surface (plots for intermediate concentrations are not shown for the purpose of clarity). These results show that the semicircle portions of the Nyquist plots, from which the values of R_s and R_{ct} are determined, clearly overlap indicating that these resistances are not significantly affected by contact with the bacteria.

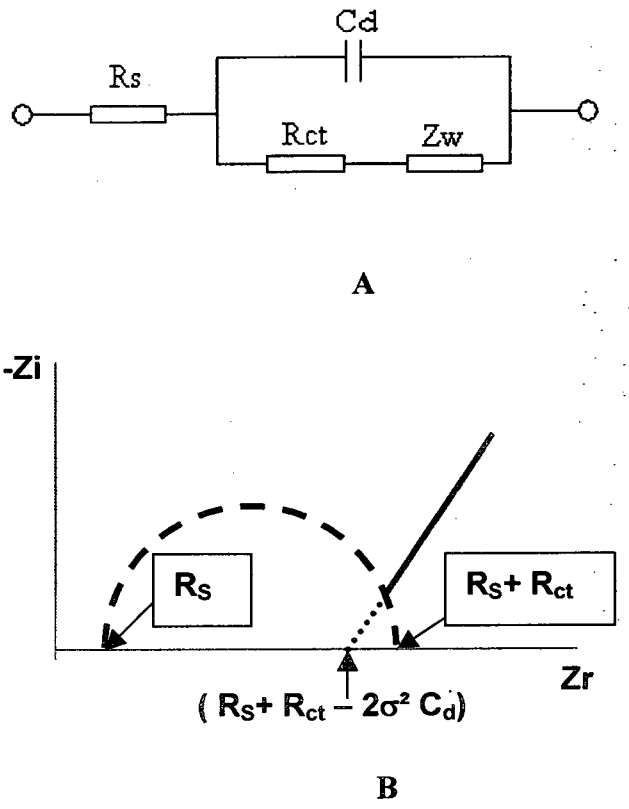

Figure 3.8 Diagram of the equivalent circuit used to interpret the impedance measurements **(A),** and corresponding theoretical Nyquist plot highlighting where relevant data is acquired **(B)**

The same behavior was observed for the range of bacteria concentrations used, and the values of R_s and R_{ct} were estimated to be 5 x 10^3 Ω and 8 x 10^4 Ω, respectively. On the other hand, the Z_r value obtained by extrapolating the straight line in the low frequency domain of the Nyquist plots (corresponding to equation 3.1), which reflects the dependence of Z_r on mass transfer/diffusion controlled processes near the electrode

surface, shows a significant positive shift with increasing *B. anthracis* concentration. These variations are associated with the Warburg impedance of the equivalent circuit (Z_w in Figure 3.8A), and correspond to a decrease in the $2\sigma^2 C_d$ component of Equation 1 (see Table 3.2).

This behavior is in general agreement with what is usually observed for simple attachment of intact bacteria cells to an electrode (i.e. an increase of impedance with increasing concentration of intact bacteria) [77]. This response however is in contrast to our previous results on the detection of *E. coli K12* with T4 phage. The detection measurements in presence of *E. coli K12* were actually conducted after lysis of the bacteria bound to the T4 phage had begun (at 20 minutes of incubation time), resulting in a decrease of the overall impedance due to release of highly conducting ions (K^+ and Na^+) near the surface. In the case of *B. anthracis*, the situation is quite different. These cells take a long time (hours) to be lysed by the *Gamma* phage, and therefore the results show only the effect due to binding of intact bacteria to the phage, and no effect due to lysis. The Nyquist plots obtained for measurements performed in contact with non-target *E. coli K12* (at 10^8 cfu/mL concentration, Figure 3.9B) show no significant shift in the impedance spectra.

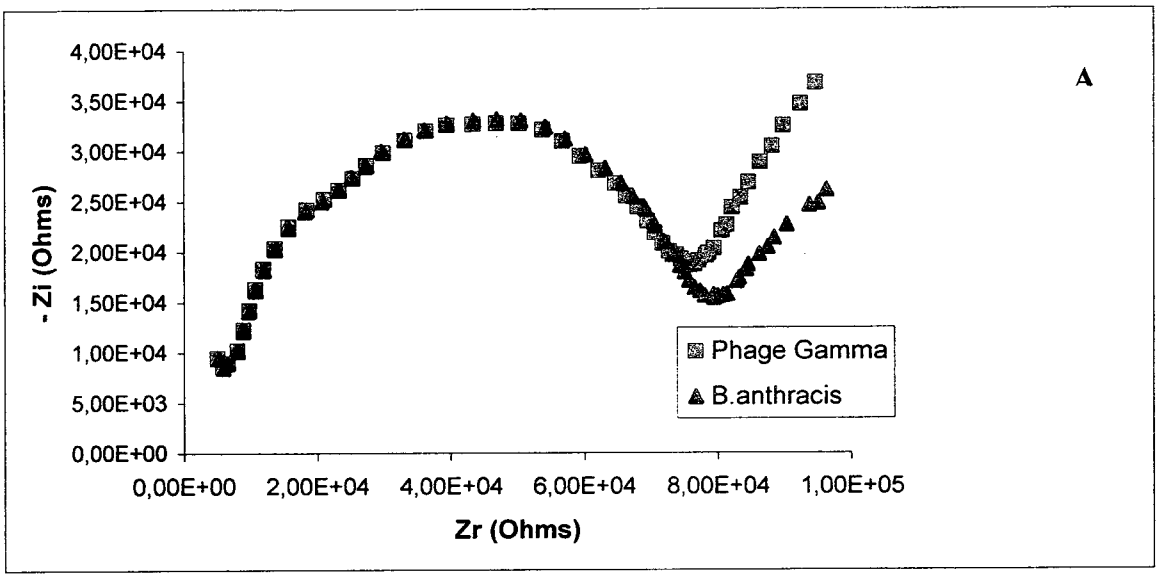

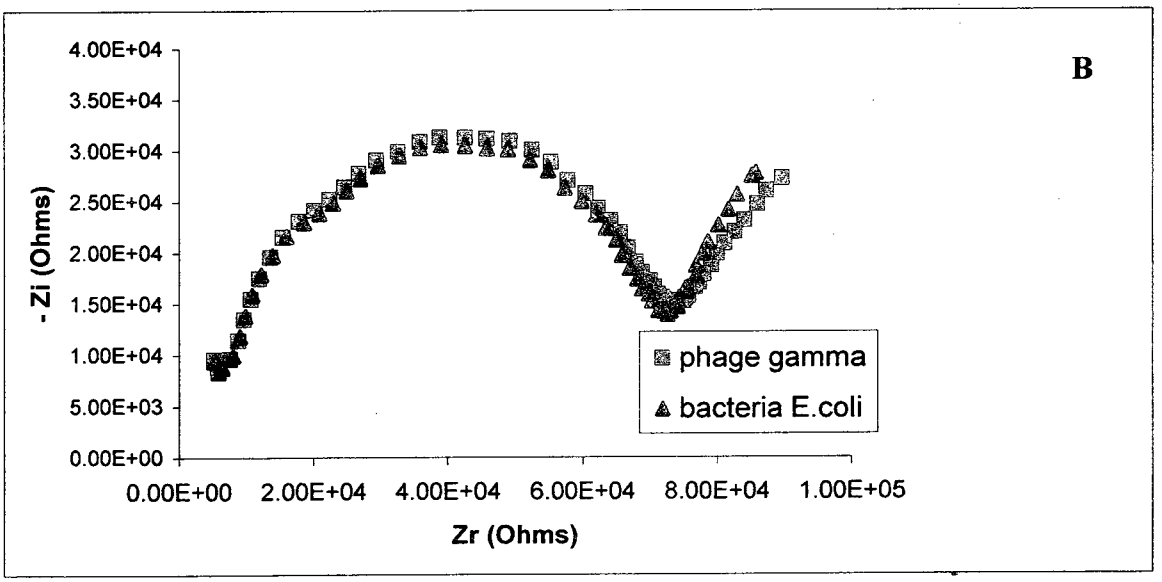

Figure 3.9 Experimental Nyquist plots for the detection of *B. anthracis* at zero concentration (red curve) and at 10^8 cfu/mL (blue curve) (A). Control experiment Nyquist plots for non-target *E. coli K12* at zero concentration (red curve) and at 10^8 cfu/mL (blue curve) (B). Measurements were taken in 0.1 M KCl aqueous solution containing 10 mM $[Fe(CN)_6]^{3-/4-}$

B. anthracis concentration (cfu/mL)	ΔZ_r (Ohms)	$2\sigma^2 Cd$ (Ohms)
0	**0**	**24.10×10^3**
10^2	**7.40×10^2**	**23.36×10^3**
10^3	**8.73×10^2**	**23.23×10^3**
10^4	**16.17×10^2**	**22.48×10^3**
10^5	**26.80×10^2**	**21.42×10^3**
10^6	**38.32×10^2**	**20.27×10^3**
10^7	**42.26×10^2**	**19.87×10^3**
10^8	**52.67×10^2**	**18.83×10^3**

Table 3.2 Summary of the ΔZ_r and $2\sigma^2 Cd$ values for *B. Anthracis* concentrations ranging from 0 to 10^8 cfu/mL

Figure 3.10 shows a log-log plot of the impedance shifts (ΔZ_r) as a function of *B. anthracis* concentration. The ΔZ_r corresponds to the difference in Z_r (obtained by extrapolating the linear portion of the Nyquist plots) between the value observed at each concentration of *B. anthracis* and that observed in absence of bacteria (see Table 3.2). For the specific target bacteria *B. anthracis*, the dose response was found to be nearly linear over seven decades of bacterial concentration. No significant change in these

values was observed for a concentration of 10 cfu/mL (compared to 0 cfu/mL), and therefore a concentration of 10 cfu/mL could not be detected by this system. The detection limit was calculated from the slope of the calibration curve according the following equation:

$$D.L. = k\sigma / m \qquad (3.2)$$

where k = 3, σ = noise of blank, and m = slope of the calibration curve. The detection limit was found to be 1 x 10^3 cfu/mL using bacteria samples of 40 µL. It should be noted that this sample size corresponds (theoretically) to only 40 bacterial cells being deposited at the sensor surface.

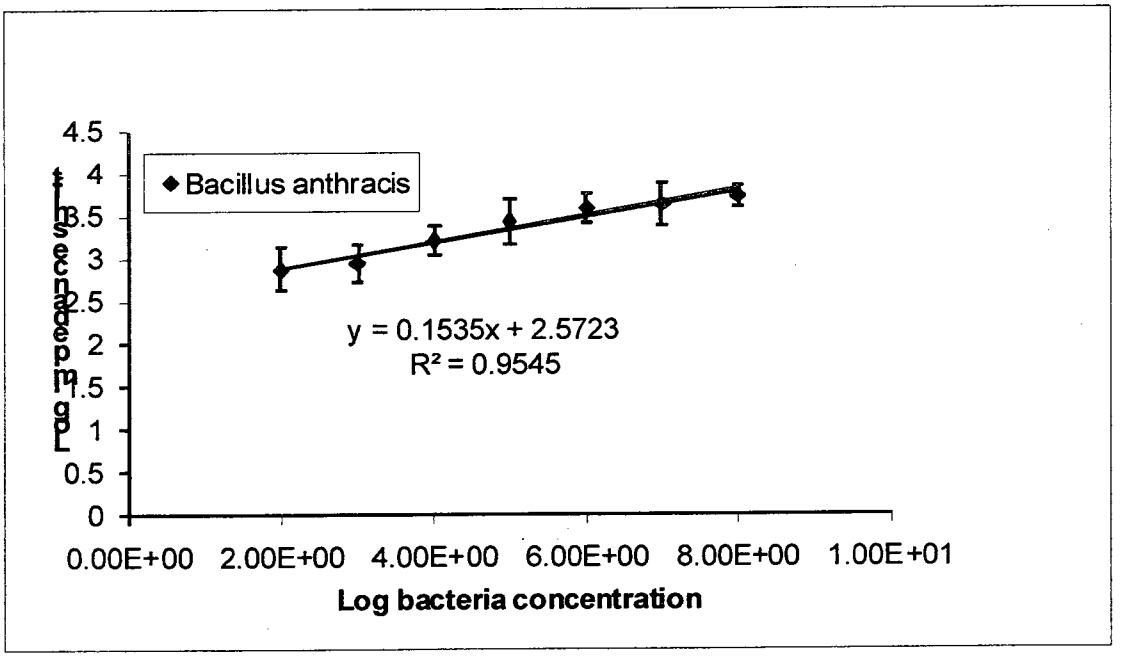

Figure 3.10 Log-log plot of ΔZ_r as a function of *B. anthracis* concentrations ranging from 0 and 10^8 cfu/mL (ΔZ_r values are reported in Table 3.2

3.4 Conclusion

Screen-printed carbon electrode arrays have been used as the base transducers to successfully immobilize *Gamma* phage to act as a recognition element for the detection of *B. anthracis Sterne* cells. XPS and TOF-SIMS analysis provide solid support for the successful functionalization of the carbon electrodes and immobilization of the bacteriophage. The impedance measurements performed with these arrays have been shown to provide a rapid, direct (label-free) means of detecting specific bacteria using a simple phage-based approach. The Nyquist plots show significant shifts due to a decrease of the mass/charge transfer dependent component in the low frequency range (the $2\ \sigma^2\ C_d$ contribution related to the Warburg impedance of the equivalent circuit), upon binding of intact *B. anthracis* cells at the electrode surface. Finally, comparison of the impedimetric detection results obtained for *B. anthracis* to those observed in the presence of non-specific *E. coli K12*, demonstrate this approaches potential for not only direct, but specific detection of bacteria. The biosensor provides rapidity, good reproducibility, sensitivity that compares favorably with current commercial and experimental techniques, and provides a very low-cost platform for direct bacterial detection.

CHAPTER 4

IMPEDIMETRIC DETECTION OF BACTERIA ASSISTED BY MAGNETIC MANIPULATION

4.1 Introduction

As mentioned in the previous chapters, bacteria contamination in different environments, especially in the food industry, causes a lot of problems and disease. Environmental, clinical, and industrial analysts are looking for inexpensive, rapid and easy-to–use methodologies to monitor the contamination caused by microorganisms [187-190].

Various techniques including biochemical tests or immunological techniques such as enzyme-linked immunosorbent assay (ELISA) have been studied [191-195]. Depending on what procedure is used, pre-enrichment of cultures or use of an optically active reagent conjugated with a secondary antibody, for example, the detection limits are known to vary. There is however one common setback to all of these techniques: high detection limits and long detection times.

Biosensors were introduced as analytical devices for the rapid detection of these microorganisms. A variety of biosensors for the detection of bacteria are based on the use of labeled–secondary antibodies. The quartz crystal microbalance (QMC) and surface plasmon resonance (SPR), as label-free (direct) biosensing devices, offer the advantage of rapidity of detection and simplicity of operation.

Impedance-based measurements, as an alternate inexpensive method, can be used for the development of label-free biosensors. Generally, impedance measurements require a three electrode set-up containing a metal foil or a wire immersed in the sample solution. In recent years, several electrode geometries and designs, such as interdigitated microarray electrodes or screen-printed electrodes, were used to improve the sensitivity of impedimetric sensors. But the problem with the majority of sensors remains the low capture efficiency of the target, especially when antibodies are used as the immobilized bioreceptor, resulting in high detection limits.

In order to overcome this problem, other interesting strategies were used to increase the sensitivity of the detection system, including the use of magnetic particles. In these approaches, instead of immobilizing antibodies onto the electrode surface, they were immobilized onto the magnetic particles. An example of this method has been reported by Varshney and Li [196]. They used magnetic beads for the detection of *E. coli* O157:H7 in samples of ground beef. The magnetic beads were immobilized with anti-*E. coli* through biotin-streptavidin interaction, and then they were mixed with bacteria solution and impedance variations were measured. The magnetic particle-bacteria complex was attracted onto the surface of an electrode using a magnetic field. The detection limit of this system was found to be 10^4 cfu/mL and 10^5cfu/mL in pure culture and ground beef, respectively.

This biosensor was further improved by the same group [197] using a microfluidic cell. A microchamber with a volume of 60 nL was made by bonding a poly-(dimethysiloxane) (PDMS) micro-channel to the gold interdigitated microelectrode array. This microfluidic

cell was used to detect bacteria in the active layer above the microelectrodes. The active layer is a sensitive region of a few micrometers above the electrode surface, where variations in impedance can be detected efficiently. The complex sample containing antibody-coated magnetic beads and bacteria was injected into the chamber, and this enabled the detection limit to be reduced to 10^2 cfu/mL and 10^3 cfu/mL, with a measurement time of 35 minutes, for the pure culture and ground beef samples, respectively. Using a thin microfluidic chamber to increase analyte proximity to the electrode surface decreases the time for the diffusion of conductive ions to the active layer, resulting in a more rapid reaction [197].

Another impedimetric approach to detect *Salmonella* cells using interdigitated microelectrodes and magnetic particles has been demonstrated by Yang et al.[198]. Magnetic beads modified with anti-*Salmonella* were used to capture bacteria cells in the media and then impedance measurements were performed. The variation in impedance in this case was found to be related to changes of the double layer capacitance. The decrease in the capacitance was observed to be due to an increase in bacterial growth. A linear relationship was found between the logarithm of bacteria concentration ranging from 10 cfu/mL to 10^6cfu/mL. For the detection of 10 cfu/mL, 8 hours were required, while the detection time for 10^6 cfu/mL of bacteria was found to be 1.5 hours.

Immunomagnetic separation is a simple and rapid method to capture and concentrate bacteria present in complex (real) samples. Techniques based on magnetic bead separation do not require centrifugation, filtration or expensive columns [199]. Also, immunomagnetic separation is not limited to impedance sensors. In order to rapidly

detect and separate of pathogens in food samples, the immunomagnetic separation approach has been coupled with various detection methods such as chemiluminescence [200] flow cystometry [191], immunoassays [201] and electrochemical methods [202, 203].

Here, we investigated the feasibility of coupling magnetic separation with our impedimetric detection system, to reduce the detection limit of our sensor.

4.2 Experimental Methods

4.2.1 Activation of magnetic, carboxylic acid-coated Dynabeads

Dynabeads are uniform particles with super-paramagnetic properties rendered by an even dispersion of magnetic materials (Fe_2O_3 and Fe_3O_4). They are coated with a polymer layer which allows the adsorption of, or the coupling with, a variety of biomolecules or cells. Beads with different surface functional groups are commercially available and they can be easily used to bind to target analytes through shaking or rotating in suspension. Their super-paramagnetic properties allow for the magnetic separation of the beads, and there remains no residual magnetism when they are removed from the magnetic field.

In order to immobilize T4 phage onto the surface of Dynabeads, the beads must first be activated with carbodiimide compound. The Dynabeads were activated according to a modified procedure adapted from a Dynabeads protocol (Figure 4.1). Briefly, 300 μL of Dynabeads (1 μm in diameter, 10 mg/mL) with a carboxylic acid coating was washed twice with the same amount (300 μL) of 0.01M NaOH for ten minutes with good mixing.

This was followed by a threefold washing with 300 μL of de-ionized water. 200 μL of 1-ethyl-3-(3-dimethyaminopropyl) carbodiimide hydrochlroride (EDC) (20mg/mL) were then added to the Dynabeads with mixing and incubation for 30 minutes with slow tilt rotation.

After incubation, the mixture was placed onto a magnet for 4 minutes and the supernatant was removed, then the beads were washed with cold de-ionized water and with 25 mM 2-[N-morpholino] ethane sulfonic acid (MES) (pH=6). At this point the Dynabeads are activated and are ready for the attachment of the phages.

4.2.2 Coating the Dynabeads with phage T4

After activation of the beads with EDC, the solution is removed and 100 μL of T4 phage (10^{10} pfu/mL) is added to coat the Dynabeads. Then, 100 μL of MES was added and incubated for 30 minutes with slow rotation at room temperature. The supernatant was removed by placing the tube on the magnet for 4 minutes. In order to quench non-reacted carboxylic groups, the beads were coated with phages incubated with 300 μL of 50 mM Tris-HCl buffer (pH=7.4) for 15 minutes at room temperature with slow rotation. Then, the solution was washed with 300 μL of 50 mM Tris-HCl buffer four times, and re-suspended into the Tris buffer and stored at 2-8°C for further use.

In order to bind the bacteria with the phage-coated magnetic beads, 20 μL of beads (10 mg/mL) was mixed with 1 mL of bacteria cells (at different concentrations) for 10 minutes with rotation at room temperature.

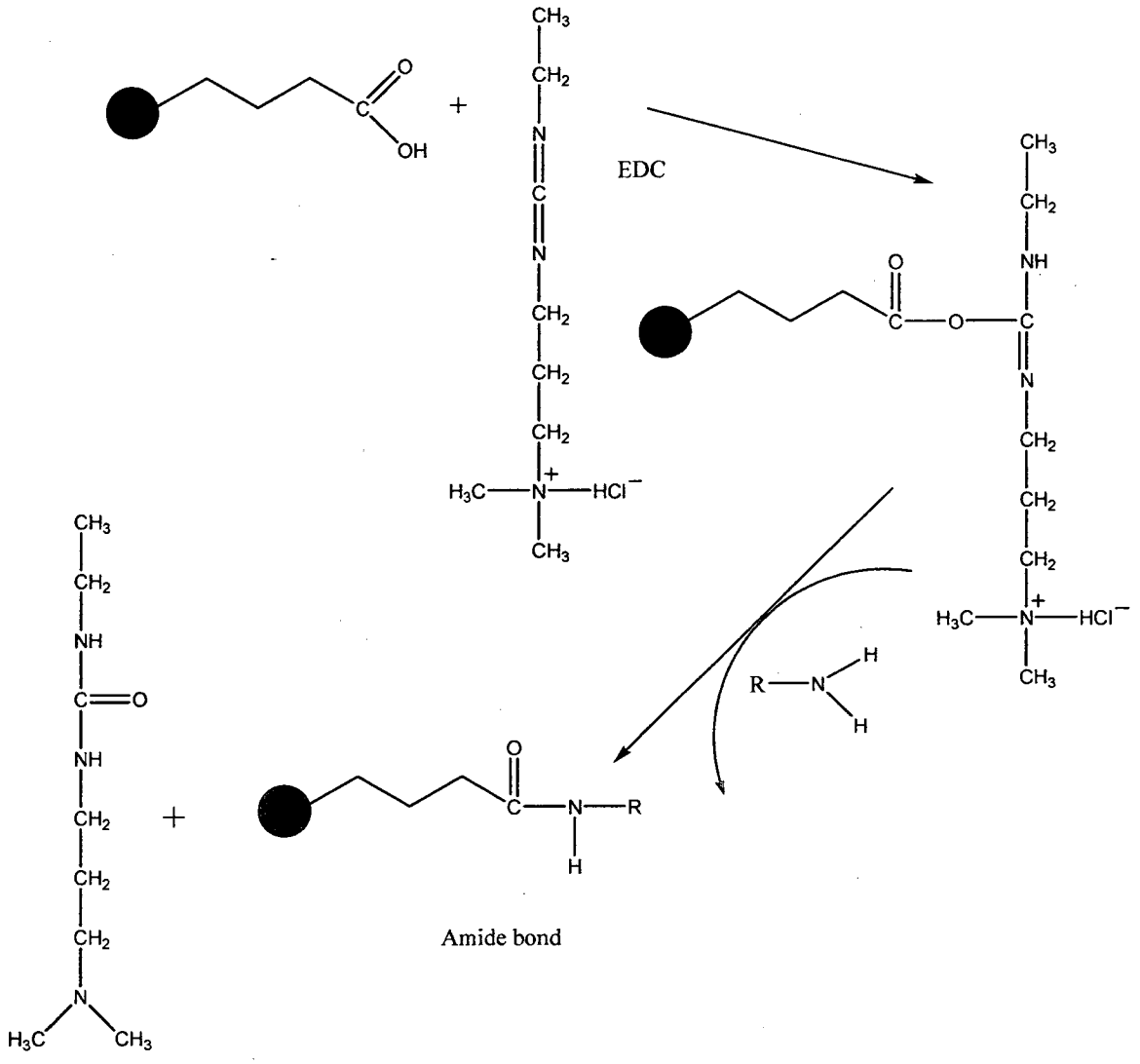

Figure 4.1 Attachment of the phage at the functionalized bead surface (R represents the phage)

4.2.3 Preparation of fluorescence-labeled bacteriophage

The phage T4 was labeled with fluorescein isothiocyanate (FTIC) according to a modified procedure found in the literature [204]. Briefly, 60 μL of phages at 10^{11} pfu /mL in SM buffer were mixed with 0.0105 g of FTIC and 2.5 mL of *N, N*-Dimethylformamide (DMF). The solution was stirred overnight at 4° C and then purified by membrane dialysis.

4.2.4 Flow Cytometry measurements

Flow cytometry analysis for GFP expression was performed on a BD LSRII(tm) flow cytometry system (Becton-Dickinson Biosciences, CA) equipped with a 488 nm argon ion laser as an excitation source. The green fluorescence emission was detected using a 530/30 nm band pass filter set.

4.2.5 Magnetic separation

10 μL of phage-coated bead solution (10 mg/mL) were mixed with 100 μL of *E. coli K12* (10^8 cfu/mL) in 2% milk, or a mixture of *Salmonella* (10^8 cfu/mL) and *E. coli* (10^8 cfu/mL) in 2% milk, and rotated at room temperature for 10 minutes. After applying a magnetic field the supernatant was removed. The beads were washed 3 times with 1 mL

of SM buffer, and re-suspended in the milk solution. 20 μL of this sample were deposited onto the phage T4-modified electrodes of the sensor for impedimetric detection.

4.3 Results and Discussion

Magnetic beads are spherical particles that can be prepared by a number of methods, and their most important feature is that they possess super paramagnetic properties, i.e. they do not aggregate spontaneously but they are attracted by a magnetic field. Accordingly, these beads can be suspended in a large volume and easily recovered in high yields afterwards just by using a simple magnet. Use of these magnetic particles to immobilize phages and specifically capture the bacteria from complex samples can be performed in a few minutes.

To determine the efficiency phage-modified magnetic beads to bind target bacteria, different concentrations of *E. coli K12* were mixed with beads modified with phage T4, and were counted using the plate method to measure the efficiency of recovery.

The binding efficiency was calculated as follows:

$$\%\text{Binding efficiency} = \frac{\text{Count before separation - Count in supernatant after separation}}{\text{Count before separation}} \times 100$$

Table 4.1 shows the binding efficiency of phage-coated magnetic beads with *E. coli* cells in pure culture.

Bacteria concentration (cfu/ml)	Count before separation	Count after separation	%Binding efficiency
10^8	1.4×10^8	2.8×10^7	80
10^7	6.2×10^7	1.5×10^7	75
10^6	1.1×10^6	2.8×10^5	74
10^5	1.6×10^5	3.5×10^4	78
10^4	1.7×10^4	4.1×10^3	75
10^3	6.5×10^3	3.2×10^3	50
10^2	2.4×10^2	2.2×10^2	8

Table 4.1 Binding efficiency of phage-coated magnetic beads with *E. coli K12*, in pure culture

The results indicate that the binding efficiency of the beads was between 70% and 80% when in contact with bacteria cell concentrations ranging from 10^4 to 10^8 cfu/mL, a percent efficiency, which remains quite constant regardless of the concentration of bacteria cells. However, for bacteria concentrations of 10^3 cfu/mL and 10^2 cfu/mL the binding efficiency decreases significantly (particularly for the 10^2 cfu/mL concentration at 8%). This is to be expected, in general the binding efficiency of magnetic beads is higher when the concentration of bacteria is high.

4.3.1 Fluorescence microscope image of phage T4 immobilized onto magnetic beads

To verify for the successful attachment of the phage to the magnetic bead surfaces, the phages were labeled and fluorescent images were taken of the magnetic beads, following immobilization of labeled phage T4. Single bright spots can be distinguished in the image shown in Figure 4.2, clearly indicating that the beads are carrying immobilized FITC-labeled phage on the surface. The images of beads with non-labeled phage showed no fluorescence intensity.

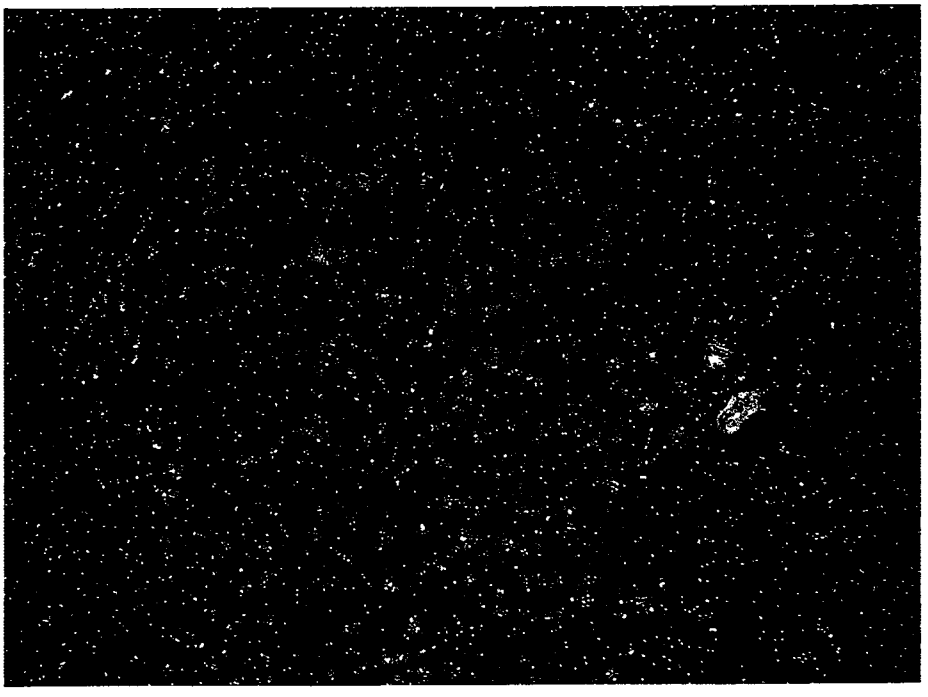

Figure 4.2 Fluorescence image of FITC-labeled phage immobilized onto magnetic beads magnification = 400X

Figure 4.3 shows a non-filtered, white-light, microscopic image of labeled phage-coated beads. This image clearly shows the beads as yellowish spots surrounded by green fluorescent phages.

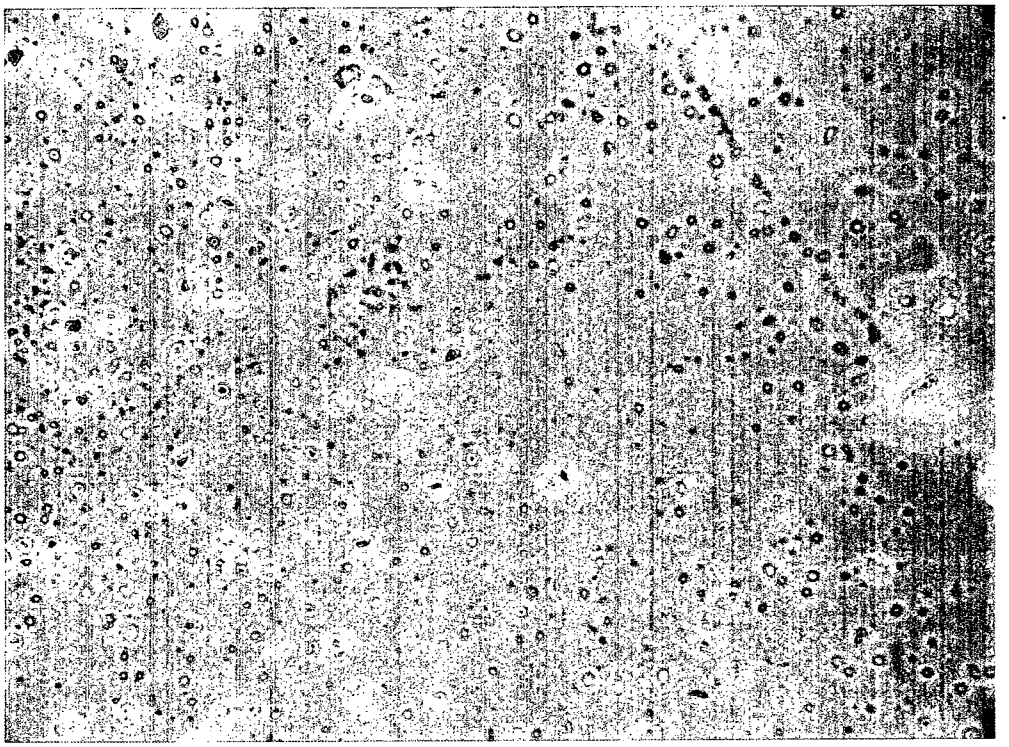

Figure 4.3 Non-filtered white-light microscopic image of labeled phage-coated magnetic beads, magnification = 1000X

4.3.2 Flow cytometry of bacteria mixed with phage-coated magnetic beads

Flow cytometry was chosen as an alternative method to verify the formation of complexes between the phage-coated beads and GFP-labeled *E .coli K12* (10^8cfu/mL).

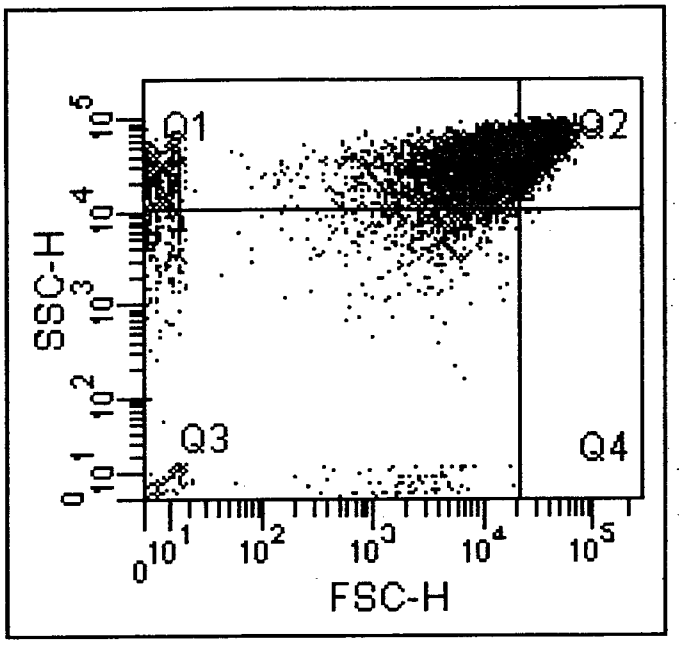
Q1
Q2
Q3
Q4
SSC-H
FSC-H
0
10^1
10^2
10^3
10^4
10^5

A

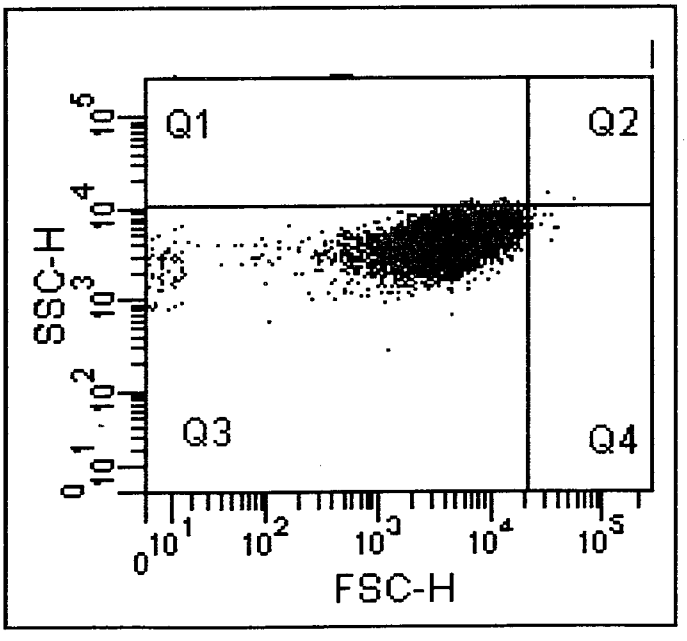
Q1
Q2
Q3
Q4
SSC-H
FSC-H
0
10^1
10^2
10^3
10^4
10^5

B

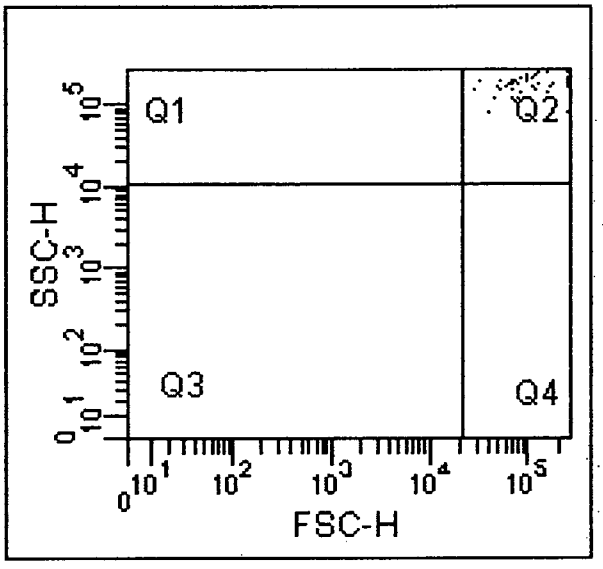

C

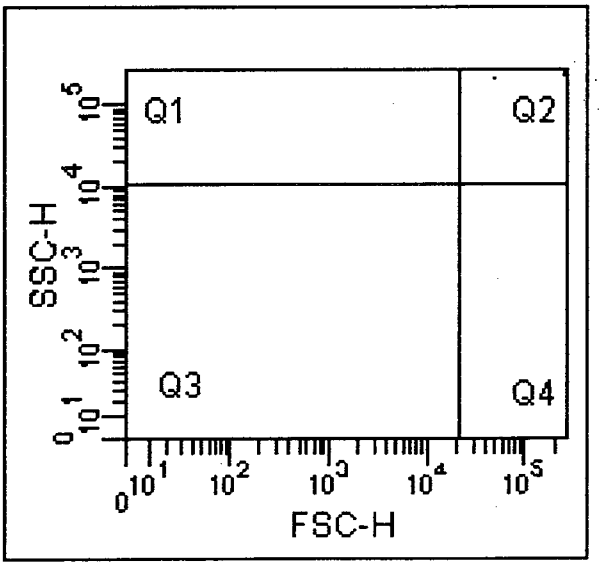

D

Figure 4.4 Dual parameter contour plot of side scattering and forward scattering for the complex of phage T4 immobilized onto beads, mixed with GFP-labeled bacteria **(A)**. A pure bacteria culture **(B)** A mixture of bead with phage only as control **(C)** SM media **(D)**

Upon analyzing the data, three distinct regions were observed due to different populations; regions Q1 to Q3 (Figure 4.4A). Region Q2 contained the particles with the largest size, indicating that phage-modified magnetic beads and the bacteria cells formed large complexes [132] . Region Q1 consists of bacteria debris only, and region Q3 is non-fluorescent debris.

Figure 4.4B shows the flow cytometry results for bacteria in a pure culture. As we can see from this Figure, a small number of populations were recorded close to the *y*-axis, which may represent subcellular particles. Comparing Figure 4.4A and 4.4B, the shift in forward and side scatter observed after mixing the bacteria with phage-modified beads indicates the formation of larger complexes, which have much larger forward and side scatter characteristics.

As a control experiment, sterile filtered SM media (Figure 4.4D), and a mixture of beads and phage (Figure 4.4C) were analyzed in the same fashion. These yielded no more than 4 events for SM media, and 45 events for the bead and phage mixture (Table 4.2).

Tube: SM media

Population	#Events	%Parent	%Total
All Events	4		100.0
Q1	0	0.0	0.0
Q2	4	100.0	100.0
Q3	0	0.0	0.0
Q4	0	0.0	0.0

A

Tube: Beads Phages

Population	#Events	%Parent	%Total
All Events	43		100.0
Q1	0	0.0	0.0
Q2	43	100.0	100.0
Q3	0	0.0	0.0
Q4	0	0.0	0.0

B

Table 4.2 Flow cytometry data analysis of the number of events for SM media **(A)**, and mixture of beads and phage **(B)**

4.3.3 Flow cytometry histogram for the binding of bacteria to phage-coated beads

The data shown in Figure 4.5 is a single parameter histogram of the number of events as a function of side scattering. The different sizes and shapes of bacterial cells and bacteria complexed with phage-coated beads cause a shift in the peaks present in the single parameter histograms of Figure 4.5A and B. This shift is most likely due to changes in the side scattering after incubation of the bacteria cells with the phage-coated beads,

indicating a change in the shape and granularity, which confirms the formation of big bacteria/bead complexes.

Another series of experiments were performed with only SM media, and a mixture of bacteria, phage and beads (without immobilizing the phage onto the beads). Figure 4.6B shows the effects of beads and phages on the light scattering properties of *E. coli* cultures; for this representative experiment, instrument and software settings were identical to those used for the experiment shown in Figure 4.5.

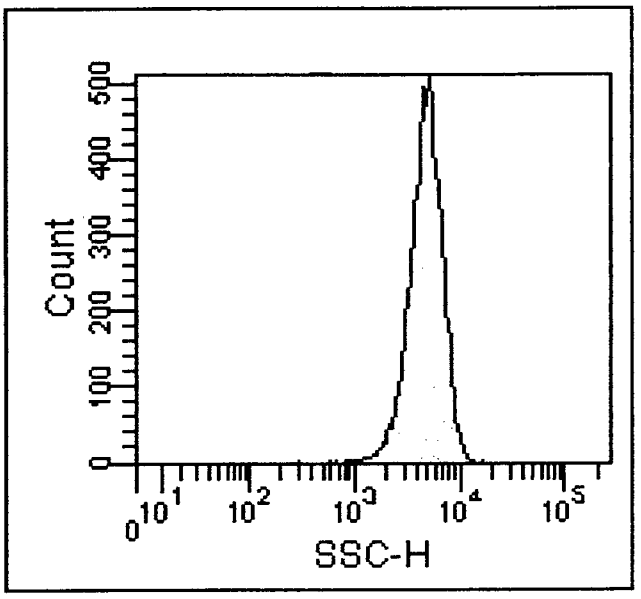

A

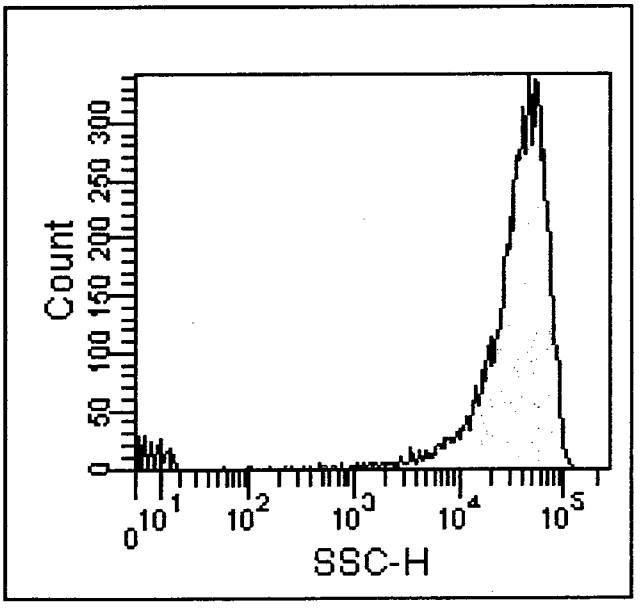

B

Figure 4.5 Histogram for side scattering and number of events for bacteria culture **(A)**, and bacteria mixed with phage-coated beads **(B)**

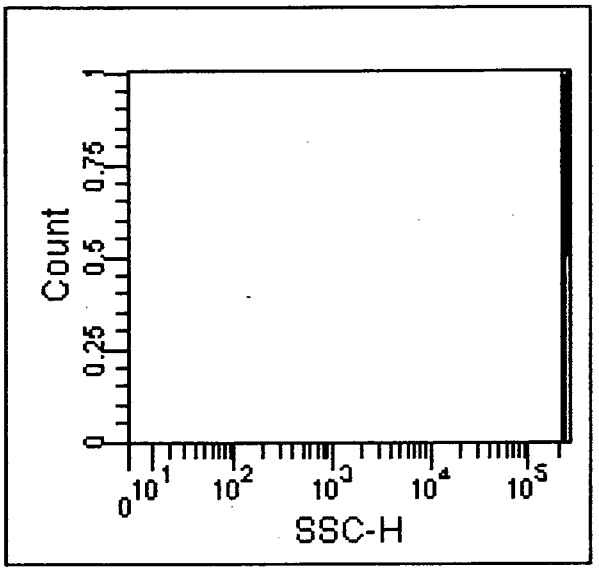

A

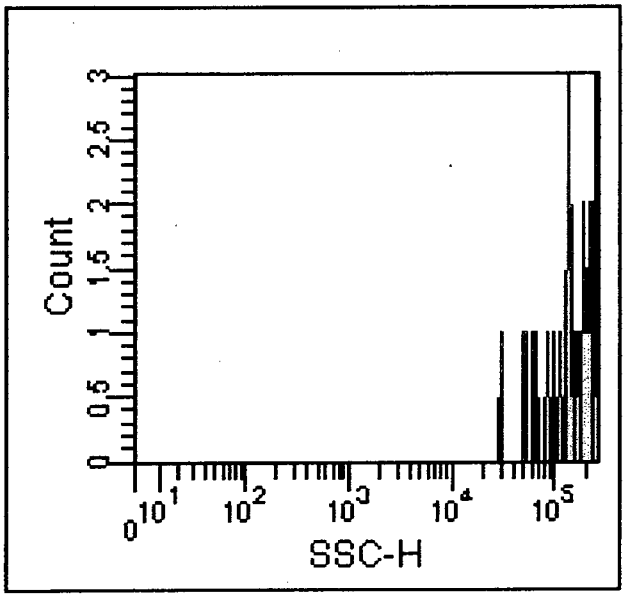

B

Figure 4.6 Histogram for side scattering and number of events for SM media only **(A)**, and bacteria mixed with beads and phages (not immobilized) **(B)**

4.3.4 Integrating the impedimetric sensor system with a magnetic field manipulation system

One of the important aims of this work is to address the specificity and rapidity of the biosensor for the detection of bacteria. In chapter 2, our detection limit for bacteria detection was determined to be 10^4 cfu/mL. As illustrated in Figure 4.7, one of the problems with the impedimetric detection is that the majority of bacteria are initially far from the immobilized phages on the electrode surface. The surface-captured bacteria may already undergo lysis as the diffusing intact bacteria are gradually reaching the surface.

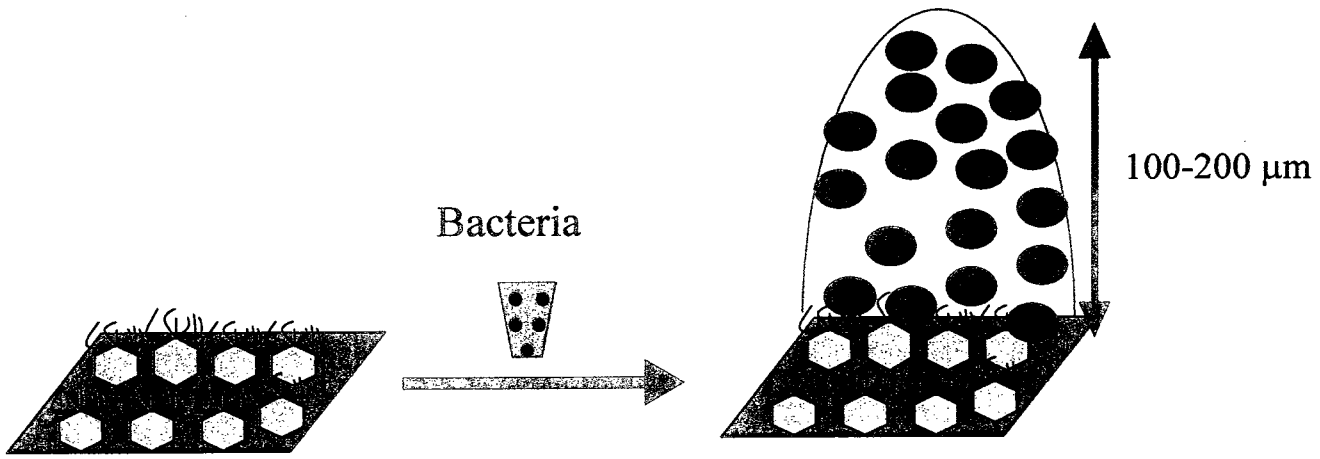

Figure 4.7 Diffusion limited transport of bacteria to the phage-modified surface

In order to solve this problem, an attempt was made to integrate the impedimetric sensor with a magnetic manipulation technique, to enhance the capture of bacteria by the immobilized phages as recognition receptors on the sensor surface. This integration is intended to improve the detection limit by a few orders of magnitude, shorten the analysis

time to a few minutes, and reduce the non- specific binding that cause false results. The detection setup using magnetic manipulation is shown in Figure 4.8. In the setup, the electrode surface of the chip was functionalized with the phages as specific binding agents, and a commercially available rare-earth (Neodymium-Iron-Boron) magnet was used to apply the magnetic field. As shown in Figure 4.8, a plastic base-plate was machined to incorporate piano wires, reproducing the pattern of 8 working electrodes of the screen-printed sensor array. The base-plate was used to effectively channel the magnetic field force lines and focus them right underneath the sensing electrodes

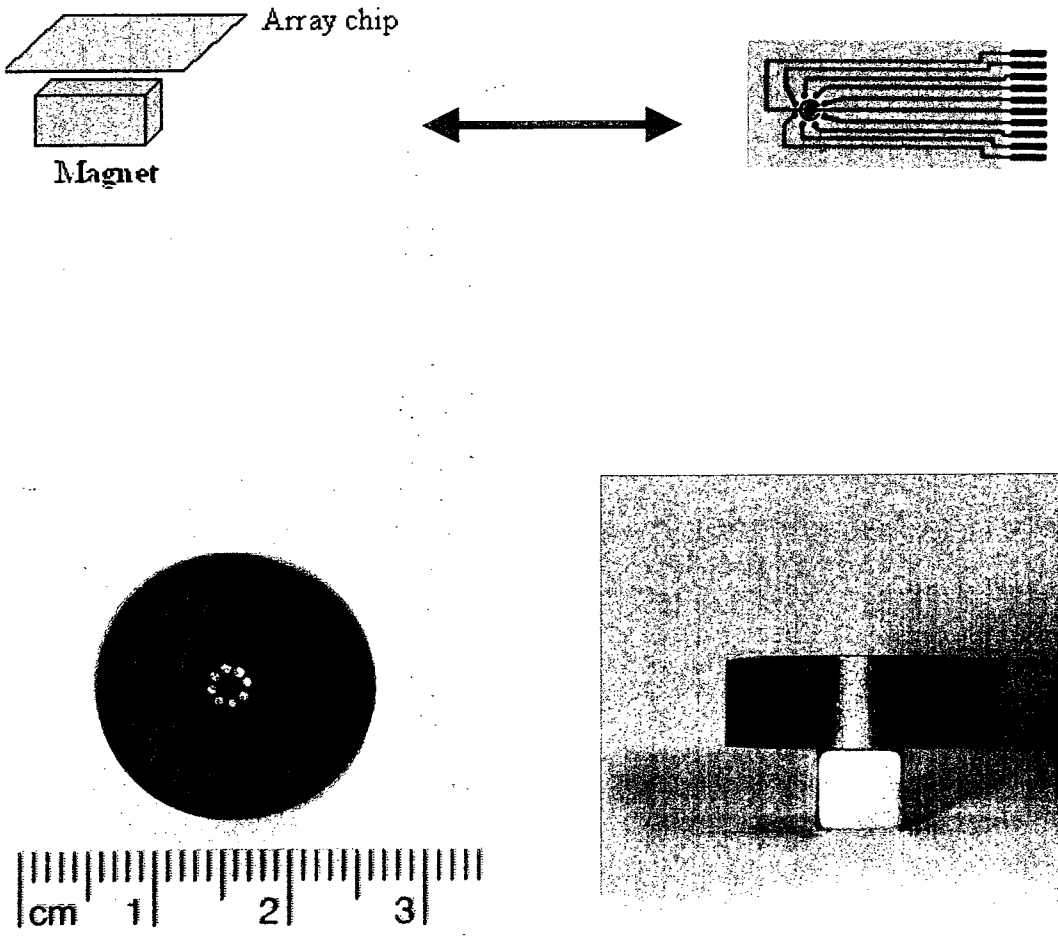

Machined base-plate: top view **Magnet with base-plate: side view**

Figure 4.8 Magnetic manipulation system setup

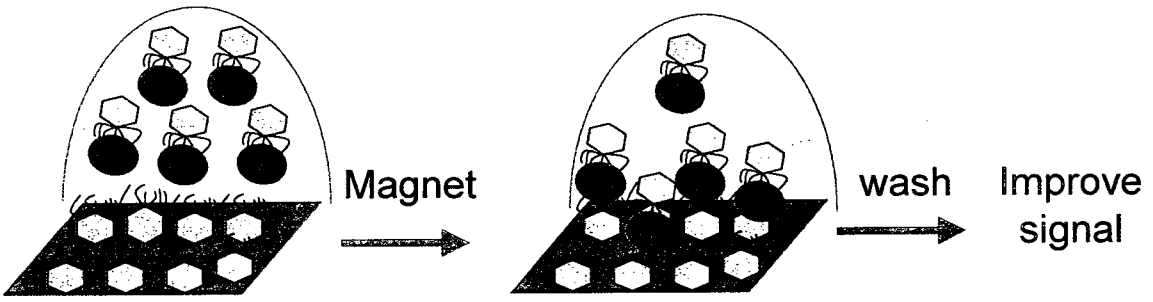

Figure 4.9 Illustration of the sensor with integrated magnetic field

The binding assay process will be performed in 3 steps (as illustrated in Figure 4.9):

Step 1: Magnetic beads covered with the specific phages and field samples are introduced in the array wells containing the electrodes coated with the phages;

Step 2: Magnet is placed under the chip to attract the magnetic beads, along with the captured analytes (bacteria in our case), to the sensor surface. As a result, the response of the sensor (impedance) changes due to the added bacteria captured by the phage.

Step 3: Remove the magnet and wash the surface, which causes the unbound magnetic beads to move away from the sensor.

4.3.5 Impedimetric detection of bacteria with magnetic manipulation

After immobilizing the phages onto the magnetic beads, the beads are mixed with the bacteria sample for 10 minutes, the mixture is then added to the electrode surface, and the magnet for applied 1-2 minutes.

Figure 4.10 presents the Bode impedance plots (impedance versus frequency) observed for different concentrations of *E. coli K12* ranging from 10^3 to 10^8 cfu/mL. It can be seen that the impedance spectra of the bacteria suspensions vary significantly with the different concentrations, in the low frequency domain from (10^2 Hz to 10^4 Hz), whereas the impedance spectra show no significant difference in the high frequency domain (10^4 Hz to 10^5 Hz).

At frequencies ranging from 10^2 Hz to 10^4 Hz the impedance spectra are sensitive to changes in the resistance [61], and therefore they reflect the contribution to the impedance coming from all the resistive components in the electrochemical detection system, including Zw, Rct, and Rs. The observation of increasing impedance with increasing bacterial cell concentration is in good agreement with the expected increase in resistance caused by the greater amount of bacteria being captured at the electrode surface, as the concentration is increased. The bacteria cell membrane is highly insulating, having a conductivity of approximately 10^{-7} S/m [205]. In addition, the combination of the bacteria and the phage-coated beads produce large bead-bacteria complexes, which also contributes to increase the resistive behavior of the system.

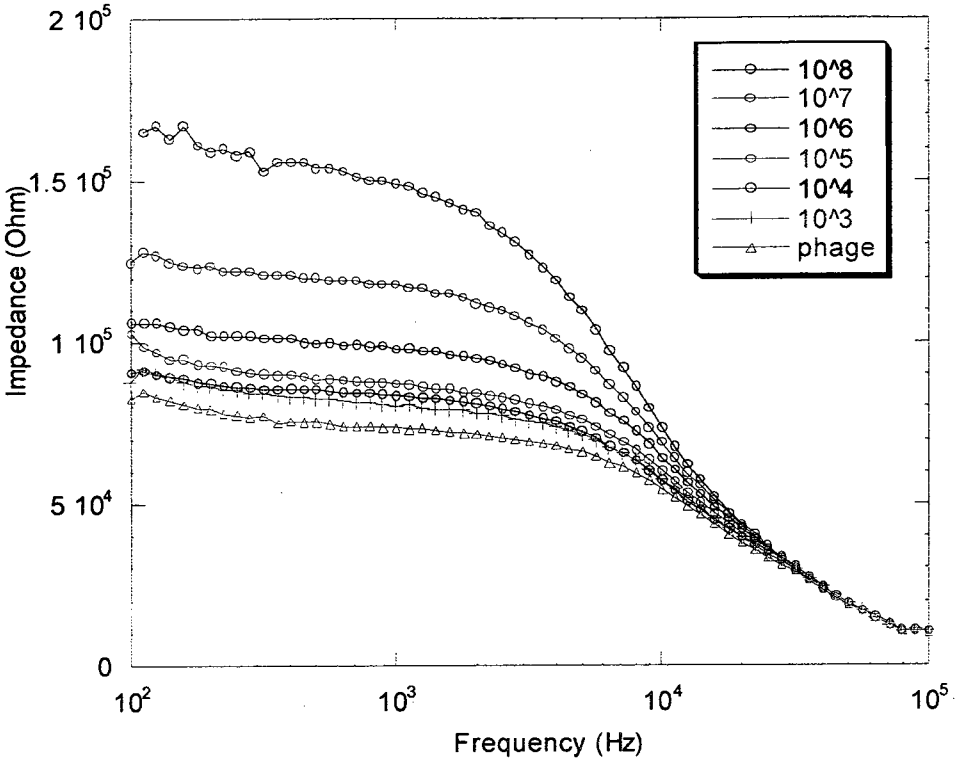

Figure 4.10 Bode impedance plots for live bacteria at different concentrations

As a control, the same series of experiments were performed with lysed bacteria. The mixture of bacteria and phage-coated beads was left to incubate for two hours (ensuring complete lysis of the bacteria), and then the mixture was tested with the impedimetric system. Figure 4.11 shows the Bode plots of lysed cells originating from the different intact bacteria concentrations, ranging from 10^3 to 10^8 cfu/mL. An increase in impedance

with increasing concentrations is also observed with the lysed cells but, in this case, the variation is much less pronounced compared to that of intact cells, and can be attributed to the adsorption of lysed material at the electrode surface.

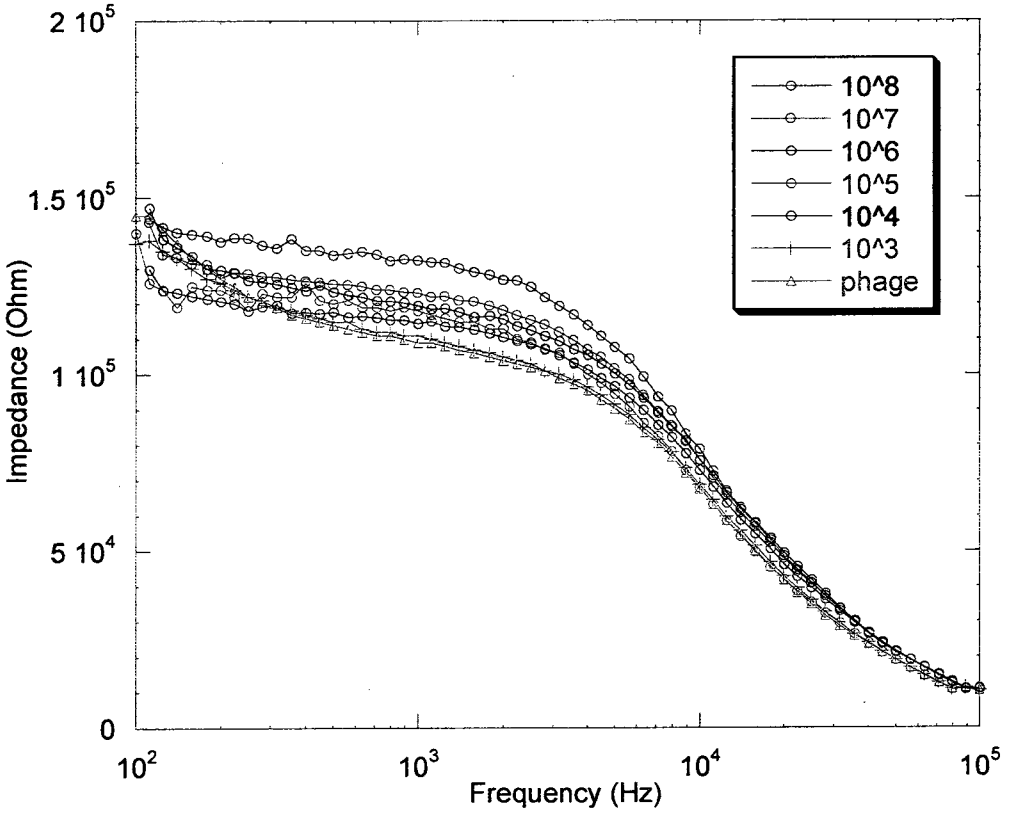

Figure 4.11 Bode impedance plots for lysed bacteria at different initial intact bacteria concentrations

Two other control experiments were performed. One that involved acquiring the Bode plots for the detection of *E. coli* under the same conditions as those used for the measurements shown in Figure 4.10, but in the absence of the magnetic field. These results are shown in Figure 4.12 where it is seen that very little shift in impedance occurs, even in going to the higher concentrations of bacteria, indicating the important impact and direct necessity of applying the magnetic field in order to get the proper detection response.

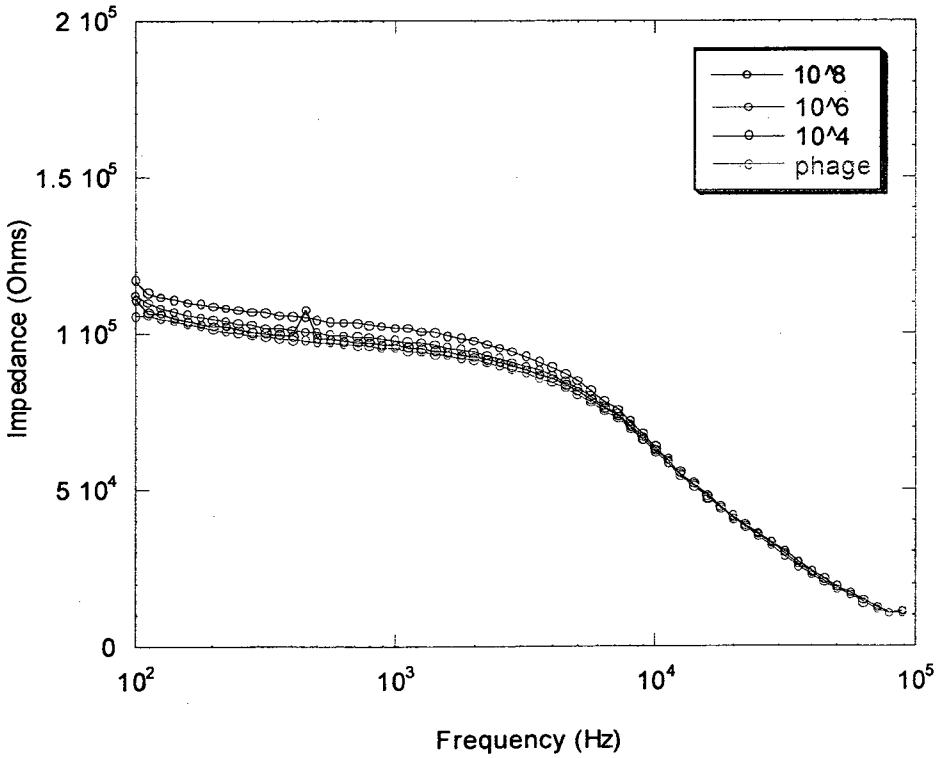

Figure 4.12 Bode plots for the control experiment performed without applying the magnetic field

The other control experiment involved testing the detection system while in the presence of non-target bacteria. Figure 4.13 presents the Bode plots for the detection of *Salmonella* which gives much less significant impedance shifts, compared to those observed for target *E. coli* bacteria (Figure 4.10), even at the higher concentrations. These smaller shifts can again be attributed to adsorption of bacteria onto the electrode surface.

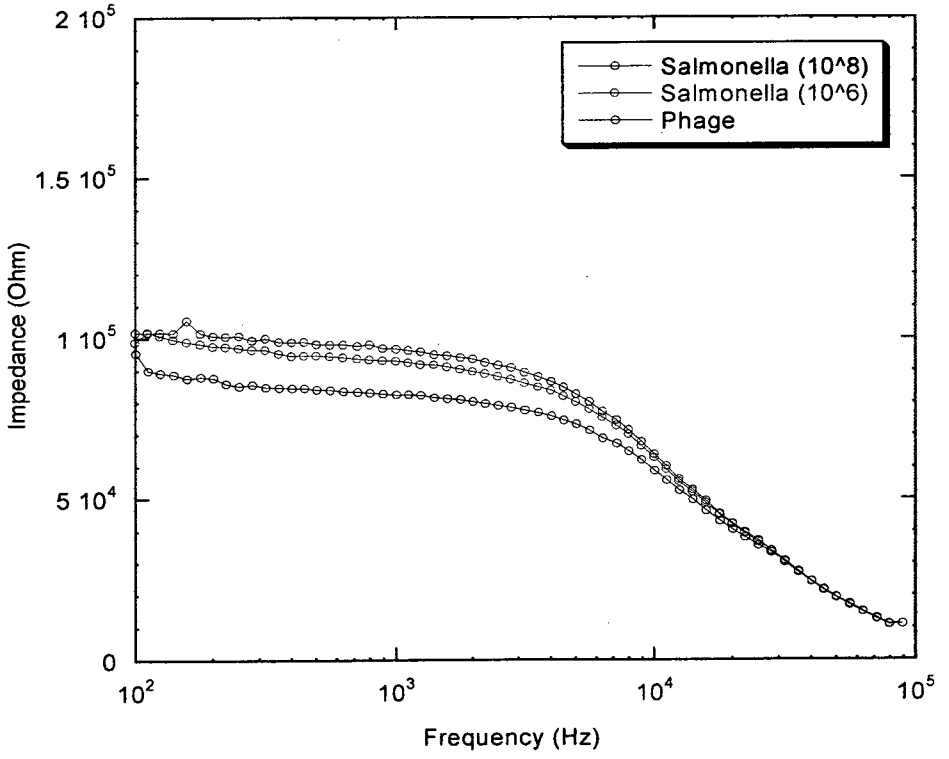

Figure 4.13 Bode plots for the control experiment performed with non-target bacteria

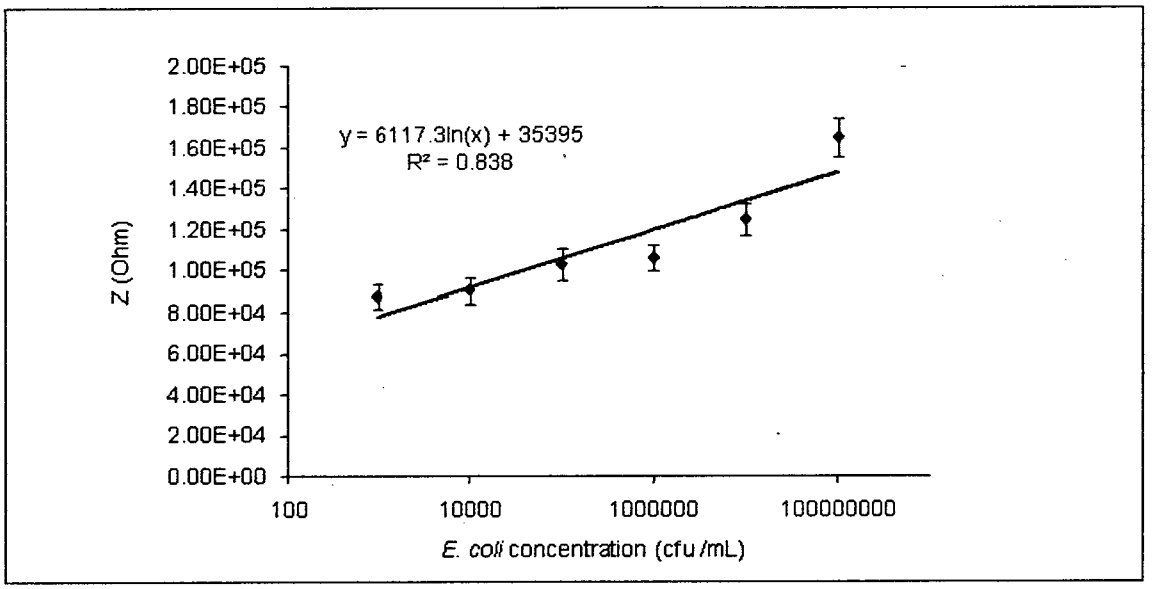

Figure 4.14 Impedance as a function of the bacteria concentration, with standard deviations

Figure 4.14 presents the variation in impedance (values taken from Figure 4.10, in the low frequency range) as a function of bacteria concentration. The standard deviations were obtained from 3 measurements performed at each of the concentrations. The detection limit, as calculated following the same procedure described in previous chapters (see, for example, Equation 3.2), was determined to be 10^3 cfu/mL, which is a one order of magnitude improvement over what was obtained for the detection *E. coli* without the use of magnetic manipulation (see Chapter 2).

4.3.6 Separation of bacteria from milk using magnetic beads, followed by detection

In order to demonstrate the potential of the technique for the capture/enrichment and detection of bacteria present in more complex media, milk samples (milk 2%) were inoculated with *E. coli K12* and *Salmonella typhimurium*. Then, T4 phage-coated beads were used to specifically separate *E. coli* cells from the mixture using a magnet, as shown in Figure 4.15.

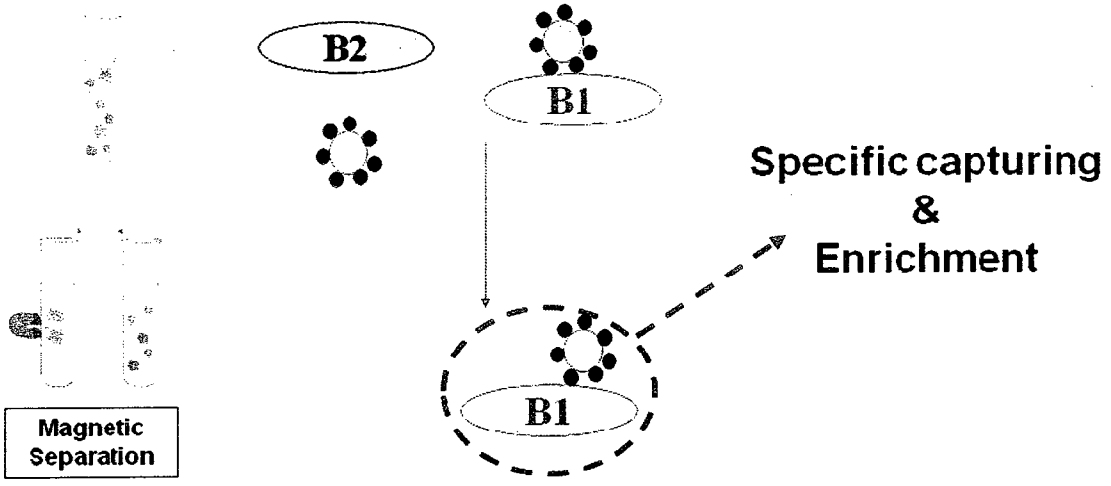

Figure 4.15 Schematic presentation of the separation of specific bacteria from a complex mixture using T4 phage-coated magnetic beads (B1 = *E. coli*, B2 = *Salmonella*)

Figure 4.16 shows the Bode plots (impedimetric detection with and without magnetic field) observed for *E. coli* only (10^8 cfu/mL) and a mixture of *E. coli* (10^8 cfu/mL) and *Salmonella* (10^8 cfu/mL) cells suspended in 2% milk, following magnetic separation. It should be emphasized here that the separation step consists in the removal of the beads from the milk sample using a magnet (as illustrated in Figure 4.15), which is separate from the impedance measurements performed with the sensor in the presence or absence of a magnetic field (set up shown in Figure 4.8). In Figure 4.16, the *E. coli*-magnetic bead complexes extracted from milk samples inoculated with *E. coli* only, show the trend expected when impedance measurements with the sensor are performed with and without applied magnetic field (i.e. significant increase in signal when the field is applied). This is also indicative of the effectiveness of the method in separating the target analyte from a more complex, real life sample (milk). More importantly, the results presented in Figure 4.16 for magnetic beads separated from milk samples containing both *E. coli* and *Salmonella*, also show a significant increase in the impedance signal when the measurement is performed in the presence of an applied magnetic field. It should be noted however that the curves obtained in the presence of *Salmonella*, without and with applied magnetic field (the green and black curve, respectively), compared to the result obtained with only *E. Coli* without applied field (red curve), indicate that the *Salmonella* is also contributing to increase the impedance in the lower frequency range. Not-withstanding the contribution to impedance shifts caused by non-specific adsorption due to the greater concentration of bacteria in the mixed samples, these results clearly indicate

the effectiveness of the protocol in providing selectivity for bacterial detection in more complex, real life, samples.

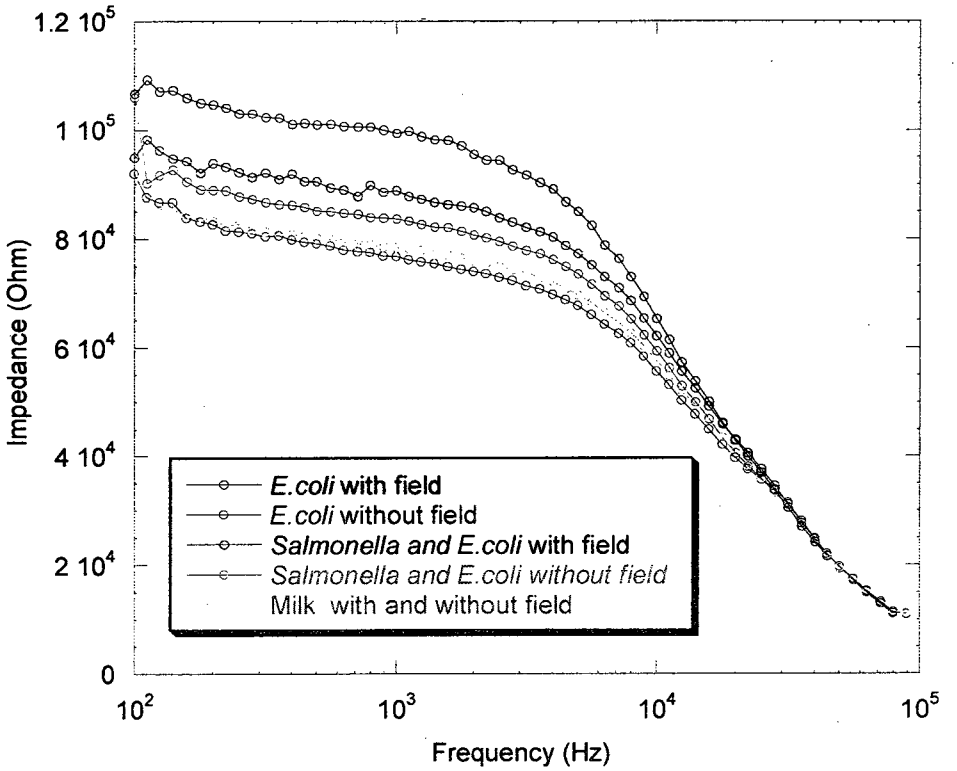

Figure 4.16 Bode impedance plots obtained following magnetic separation from milk samples containing *E. coli,* and a mixture of *E. coli* and *Salmonella* (all at 10^8 cfu/mL). Impedimetric measurements performed with and without magnetic field

4.4 Conclusion

In conclusion, we have demonstrated the feasibility of integrating the impedimetric sensor with a magnetic manipulation system for improving the sensitivity of the device. We have been able to show through fluorescence and flow cytometry measurements that the surface modification of the magnetic beads, with phages, and binding with the bacteria were successful. We have also demonstrated that the detection of bacteria was specific, it enables the operator to account for non-specific adsorption, and can be used to analyse more complex (real) samples. Finally, we have demonstrated that the sensitivity is improved (by one order of magnitude) through the use of a simple magnetic manipulation system.

CHAPTER 5

CONCLUDING REMARKS AND FUTURE CONSIDERATIONS

In chapter one, the structures/functions of bacteriophages and bacteria were described. Also, a range of methods that can be used for bacteria detection were reviewed, pointing out their limitations and advantages. Although conventional methods remain reliable, the development of novel biosensor technologies is expanding with the hope of providing more rapid, specific, and convenient methods for bacteria identification. Different types of biosensors based on the use of different transducers were described, with emphasis being placed on optical and electrochemical biosensors because of their growing use and simplicity of operation.

Impedimetric sensors, in particular, are now emerging as excellent candidates to fulfill the current needs in the area of specific and rapid detection of bacteria, for preventative and therapeutic applications. They also carry the potential to meet and resolve additional technological concerns related to biosensor miniaturization and portability. It should be noted however, that single cell detection still remains a daunting challenge. Since the infectious dosage of pathogens such as *Salmonella* or *E. coli* O157:H7 is 10 cells/100mL, the biosensor should be able to detect as low as one bacteria, with a rapid analysis time and low cost.

In this work, starting at chapter two, a novel method was presented for the specific and direct detection of bacteria using bacteriophages as recognition receptors immobilized covalently onto functionalized screen-printed carbon electrode (SPE) microarrays. The SPE networks were functionalized through electrochemical oxidation in acidic media of 1-ethyl-3-(3-dimethylaminopropyl)-carbodiimide (EDC) by applying a potential of +2.2 V to the working electrode. Immobilization of T4 bacteriophage onto the SPEs was achieved via EDC by formation of amide bonds between the protein coating of the phage and the electrochemically generated carboxylic groups at the carbon surface. The surface functionalization with EDC, and the binding of phages, was verified by time-of-flight secondary ion mass spectrometry. The immobilized T4 phages were then used to specifically detect *E. coli* bacteria. The presence of surface bound bacteria was verified by scanning electron and fluorescence microscopies. Impedance measurements (Nyquist plots) show shifts of the order of 10^4 Ohms due to the binding of *E. coli* bacteria to the T4 phages. No significant change in impedance was observed for control experiments using immobilized T4 phage in the presence of *Salmonella*. Impedance variations as a function of incubation time show a maximum shift after 20 minutes, indicating onset of lysis, as also confirmed by fluorescence microscopy. Concentration-response curves yield a detection limit of 10^4 cfu/mL for 50 μL samples.

In the third chapter, the carbon electrodes were initially functionalized through cyclic-voltammetric reduction of a nitro-aryl diazonium moiety, followed by further reduction of nitro groups to amino groups, and finally by treatment with glutaraldehyde. Functionalization of the carbon electrodes and the binding of *Gamma* phage were verified

by x-ray photoelectron spectroscopy and time-of-flight secondary ion mass spectrometry, respectively. The *Gamma* phage-modified microarrays were then used to detect *B. anthracis Sterne* bacteria in aqueous electrolyte media. Faradaic impedimetric detection of bacteria in KCl solution containing the ferri/ferro cyanide redox couple shows a gradual increase in Z_r values, taken from the extrapolation of the linear portion of Nyquist plots in the low frequency range, for sensors placed in contact with increasing concentrations of *B. anthracis*. ΔZ_r values vary approximately from 700 to 5300 Ohms for bacteria concentrations ranging from 10^2 to 10^8 cfu/mL, respectively. These shifts in Z_r are attributed to a decrease in diffusion controlled charge transport to the electrode surface (the $2\ \sigma^2\ C_d$ contribution, which is related to the mass transfer-dependent component of the equivalent circuit (i.e. Warburg impedance)), following capture of intact *B. anthracis*. No comparatively significant change in impedance was observed for control experiments using *E. coli K12* as a non-specific target, even at a concentration of 10^8 cfu/mL. Concentration-response curves yield a detection limit of 10^3 cfu/mL for 40 μL samples.

In chapter four, the possibility of reducing the detection time and detection limit of the system was demonstrated by integrating the impedance sensor with a magnetic bead manipulation system. Also demonstrated was the ability of the magnetic bead approach to effectively isolate/remove specific bacteria from more complex (real) samples, for detection purposes.

In general, the impedimetric system developed herein possesses the versatility for the development and commercialization of biosensors for the direct (label-free) and simultaneous detection (multiplexed) of different bacteria present in a single sample. However, some of its characteristics that still deserve further attention are sensitivity and overall performance. Here are some aspects to be considered in future improvement/development:

1. Chemical functionalization of carbon using a dendritic linker

Recent reports have shown that functionalization of substrates with dendrimers leads to the fabrication of more sensitive and highly stable DNA microarrays, based on the detection of fluorescent-labeled target oligonucleotides[206-208]. The dendrimers are nanometric spherical structures that initiate from a central core and have branches that extend outward.

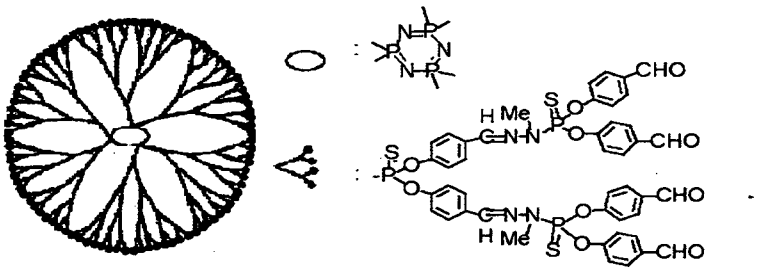

Figure 5.1 Illustration of dendrimer formation up to generation 4 [207]

In their outer sphere, they possess a high number of a specific functional group such as an amine, aldehyde, epoxide, thiol, etc, a number which is proportional to the branch units[207] (Figure 5.1). Commercially available polyamidoamine starburst dendrimers (PAMAM, from Aldrich) can be used, which offer 64 primary amino groups in their outer sphere, and are perfectly adapted for activation by reaction of the amino groups with glutaraldehyde.

An another interesting approach to consider is using a dendrimer that possesses aldehyde groups as previously described[209]. Generation 4 of this dendrimer has a diameter size of about 75 Å, and contains 96 aldehyde functional groups. The efficiency of binding of phage probes on the aldehyde functions of the dendrimer should be investigated, with the expectation of enhanced sensitivities using these dendrimer-modified surfaces (Figure 5.2).

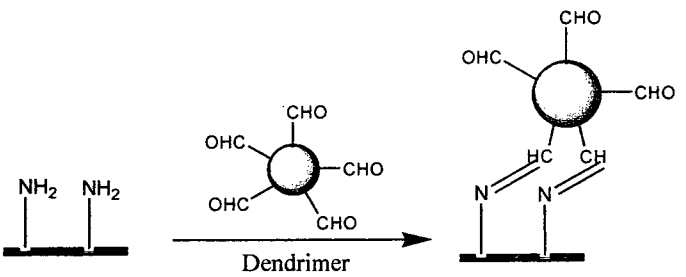

Figure 5.2 Surface activation to immobilize dendrimers

2. Developing the impedimetric sensor system for simultaneous multiplex detection

Electrode arrays could be designed to perform multiplex measurements to test specificity in the presence of a number of different bacteria, at different concentrations, simultaneously. The fabrication of screen-printed carbon microelectrode networks is well suited for mass production, and is more easily and cost effectively amenable to the design of versatile array configurations. Once it has been demonstrated that the biosensor detection is working for multiple bacteria, one can proceed to design a multiplex (multi phage) microarray capable of probing a single sample for the presence of a variety of bacteria, in a single assay. One can easily envisage scaling up this approach to go from ten (the current configuration) to a hundred array elements (electrodes), to provide more versatile chips for diagnostic purposes when dealing with complex samples.

References

(1) Twort, F. W. **1915**, *Lancet, II*, 1241-1243.
(2) Kutter, E.; Sulakvelidze, A. *Bacteriophages: biology and applications*, First ed.; CRC press: Washington, 2004.
(3) Maniloff, J.; Ackerman, R.-W.; Janis, A.; Webster, R. G.; Granoff, A. *A Bacteriophage Taxonomy and Classification*, 1994.
(4) Birge, E. A. *Bacterial and bacteriophage genetics*, 5th ed.; Springer Science: New York, 2006.
(5) Maloy, S. R.; Cronan, J. E.; Freifelder, D. **1994**.
(6) Prescott, L. M.; Harley, J. P.; Klein, D. A. *Microbiology*; Wm.C. Brown: Dubuque, IA, 1990.
(7) Tanji, Y.; Furukawa, C.; Na, S.-H.; Hijikata, T.; Miyanaga, K.; Unno, H. *Journal of Biotechnology* **2004**, *114*, 11-20.
(8) http://micro.magnet.fsu.edu/cells/bacteriacell.html.
(9) Deisingh, A. K.; Thompson, M. *The Analyst* **2002**, *127*, 567-581.
(10) Greenwood, D.; Slack, R.; Peutherer, J. *Medical Microbiology*, 15th ed.; Churchill Livingstone,: London, 1997.
(11) http://www.microbiologybytes.com.
(12) Rowe, P. C.; Orrbine, E.; Lior, H.; Wells, G. A.; Yetisir, E.; Clulow, M.; McLaine, P. N. *The Journal of pediatrics* **1998**, *132*, 777-782.
(13) Shangkuan, Y. H.; Lin, H. C. *Journal of Applied Microbiology* **1998**, *85*, 693-702.
(14) Ivnitski, D.; Abdel-Hamid, I.; Atanasov, P.; Wilkins, E. *Biosensors & Bioelectronics* **1999**, *14*, 599-624.
(15) Rossi, T. M.; Warner, I. M. *Applied Spectroscopy* **1985**, *39*, 949-959.
(16) Quinlan, J. J.; Foegeding, P. M. *Applied and Environmental Microbiology* **1997**, *63*, 482-487.
(17) Zhou, B.; Wirsching, P.; Janda, K. D. *Proceedings of the National Academy of Sciences of the United States of America* **2002**, *99*, 5241-5246.
(18) Beverly, M. B.; Basile, F.; Voorhees, K. J.; Hadfield, T. L. *Rapid Communications in Mass Spectrometry* **1996**, *10*, 455-458.
(19) Fox, A.; Black, G. E.; Fox, K.; Rostovtseva, S. *Journal of Clinical Microbiology* **1993**, *31*, 887-894.
(20) Goodacre, R.; Shann, B.; Gilbert, R. J.; Timmins, E. M.; McGovern, A. C.; Alsberg, B. K.; Kell, D. B.; Logan, N. A. *Analytical Chemistry* **2000**, *72*, 119-127.
(21) Fergenson, D. P.; Pitesky, M. E.; Tobias, H. J.; Steele, P. T.; Czerwieniec, G. A.; Russell, S. C.; Lebrilla, C. B.; Horn, J. M.; Coffee, K. R.; Srivastava, A.; Pillai, S. P.; Shih, M.-T. P.; Hall, H. L.; Ramponi, A. J.; Chang, J. T.; Langlois, R. G.; Estacio, P. L.; Hadley, R. T.; Frank, M.; Gard, E. E. *Analytical Chemistry* **2004**, *76*, 373-378.
(22) Huang, J.; Li, Y.; Slavik, M. F.; Tao, Y.; Huff, G. R. *Transactions of the ASAE* **1999**, *42*, 267-273.
(23) Prosser, J. I.; Killham, K.; Glover, L. A.; Rattray, E. A. *Critical reviews in biotechnology* **1996**, *16*, 157-183.
(24) Dickinson, B. *Introduction to Flow Cytometry: A Learning Guide.*
(25) Boye, E.; Loebner-Olesen, A. *Research in Microbiology* **1991**, *142*, 131-135.
(26) Thevenot, D. R.; Toth, K.; Durst, R. A.; Wilson, G. S. *Pure and Applied Chemistry* **1999**, *71*, 2333-2348.

(27) Turner, A. P. F.; Karube, I.; Wilson, G. S. *Biosensors: Fundamentals and Applications*; Oxford Univ. press: New York, 1987.
(28) Sethi, R. S. *Biosensors & Bioelectronics* **1994**, *9*, 243-263.
(29) Shabani, A.; Mak, A. W. H.; Gerges, I.; Cuccia, L. A.; M.F., L. *Talanta* **2006**, *70*, 615-623.
(30) Lenigk, R.; Carles, M.; Ip, N. Y.; Sucher, N. J. *Langmuir* **2001**, *17*, 2497-2501.
(31) Lee Jennifer, F.; Stovall Gwendolyn, M.; Ellington Andrew, D. *Current opinion in chemical biology* **2006**, *10*, 282-289.
(32) Awais, R.; Fukudomi, H.; Miyanaga, K.; Unno, H.; Tanji, Y. *Biotechnology Progress* **2006**, *22*, 853-859.
(33) Olsen, E. V.; Sorokulova, I. B.; Petrenko, V. A.; Chen, I. H.; Barbaree, J. M.; Vodyanoy, V. J. *Biosensors & Bioelectronics* **2006**, *21*, 1434-1442.
(34) Shabani, A.; Zourob, M.; Allain, B.; Marquette, C. A.; Lawrence, M. F.; Mandeville, R. *Analytical Chemistry* **2008**, *80*, 9475-9482.
(35) Barak, O.; Treat James, R.; James William, D. *Advances in dermatology* **2005**, *21*, 357-374.
(36) Williams, D. D.; Benedek, O.; Turnbough, C. L., Jr. *Applied and Environmental Microbiology* **2003**, *69*, 6288-6293.
(37) Lee, T. C.; Yusoff, K.; Nathan, S.; Tan, W. S. *Journal of Virological Methods* **2006**, *136*, 224-229.
(38) Ivnitski, D.; Abdel-Hamid, I.; Atanasov, P.; Wilkins, E.; Stricker, S. *Electroanalysis* **2000**, *12*, 317-325.
(39) Swenson, F. J. *Sensors and Actuators, B: Chemical* **1993**, *B11*, 315-321.
(40) Schneider, B. H.; Edwards, J. G.; Hartman, N. F. *Clinical Chemistry (Washington, D. C.)* **1997**, *43*, 1757-1763.
(41) Raether, H. *Surface plasmons on smooth and rough surfaces and on gratings*; Springer Verlag: Berlin, 1988.
(42) Taylor, A. D.; Yu, Q.; Chen, S.; Homola, J.; Jiang, S. *Sensors and Actuators, B: Chemical* **2005**, *B107*, 202-208.
(43) Fratamico, P. M.; Strobaugh, T. P.; Medina, M. B.; Gehring, A. G. *Biotechnology Techniques* **1998**, *12*, 571-576.
(44) Taitt, C. R.; Anderson, G. P.; Ligler, F. S. *Biosensors & Bioelectronics* **2005**, *20*, 2470-2487.
(45) Ko, S.; Grant, S. A. *Biosensors and Bioelectronics* **2006**, *21*, 1283-1290.
(46) Geng, T.; Morgan, M. T.; Bhunia, A. K. *Applied and Environmental Microbiology* **2004**, *70*, 6138-6146.
(47) Liu, Y.; Ye, J.; Li, Y. *Journal of food protection* **2003**, *66*, 512-517.
(48) Suleiman, A. A.; Guilbault, G. G. *Analyst* **1994**, *119*, 2279-2282.
(49) Marco, M.-P.; Barcelo, D. *Measurement Science & Technology* **1996**, *7*, 1547-1562.
(50) Si, S.-H.; Li, X.; Fung, Y.-S.; Zhu, D.-R. *Microchemical Journal* **2001**, *68*, 21-27.
(51) Pathirana, S. T.; Barbaree, J.; Chin, B. A.; Hartell, M. G.; Neely, W. C.; Vodyanoy, V. *Biosensors & Bioelectronics* **2000**, *15*, 135-141.
(52) Koenig, B.; Graetzel, M. *Analytical Letters* **1993**, *26*, 1567-1585.
(53) Plomer, M.; Guilbault, G. G.; Hock, B. *Enzyme and Microbial Technology* **1992**, *14*, 230-235.
(54) Prusak-Sochaczewski, E.; Luong, J. H.; Guilbault, G. G. *Enzyme and microbial technology* **1990**, *12*, 173-177.
(55) Ben-Dov, I.; Willner, I.; Zisman, E. *Analytical Chemistry* **1997**, *69*, 3506-3512.

(56) Neufeld, T.; Schwartz-Mittelmann, A.; Biran, D.; Ron, E. Z.; Rishpon, J. *Analytical Chemistry* **2003**, *75*, 580-585.
(57) Brooks, J. L.; Mirhabibollahi, B.; Kroll, R. G. *Journal of Applied Bacteriology* **1992**, *73*, 189-196.
(58) Gehring, A. G.; Crawford, C. G.; Mazenko, R. S.; Van Houten, L. J.; Brewster, J. D. *Journal of Immunological Methods* **1996**, *195*, 15-25.
(59) Gehring, A. G.; Patterson, D. L.; Tu, S. I. *Analytical biochemistry* **1998**, *258*, 293-298.
(60) Ercole, C.; Del Gallo, M.; Pantalone, M.; Santucci, S.; Mosiello, L.; Laconi, C.; Lepidi, A. *Sensors and Actuators, B: Chemical* **2002**, *B83*, 48-52.
(61) Yang, L. *Talanta* **2008**, *74*, 1621-1629.
(62) Limited, D. W. S.; www.dwscientificco.uk, 1999.
(63) Owicki, J. C.; Parce, J. W. *Biosensors & Bioelectronics* **1992**, *7*, 255-272.
(64) Bard, A. J.; Faulkner, L. R. *Electrochemical Methods:fundamentals and applications*; Wiley: New York, 2001.
(65) Ehret, R.; Baumann, W.; Brischwein, M.; Schwinde, A.; Stegbauer, K.; Wolf, B. *Biosensors & bioelectronics* **1997**, *12*, 29-41.
(66) Tahir, Z. M.; Alocilja, E. C.; Grooms, D. L. *Biosensors & Bioelectronics* **2005**, *20*, 1690-1695.
(67) Ruan, C.; Yang, L.; Li, Y. *Analytical Chemistry* **2002**, *74*, 4814-4820.
(68) Yang, L.; Li, Y.; Erf, G. F. *Analytical Chemistry* **2004**, *76*, 1107-1113.
(69) Park, I.-S.; Kim, W.-Y.; Kim, N. *Biosensors & Bioelectronics* **2000**, *15*, 167-172.
(70) Koubova, V.; Brynda, E.; Karasova, L.; Skvor, J.; Homola, J.; Dostalek, J.; Tobiska, P.; Rosicky, J. *Sensors and Actuators, B: Chemical* **2001**, *B74*, 100-105.
(71) Meeusen, C. A.; Alocilja, E. C.; Osburn, W. N. *Transactions of the ASAE* **2005**, *48*, 2409-2416.
(72) Radke, S. M.; Alocilja, E. C. *Biosensors & Bioelectronics* **2005**, *20*, 1662-1667.
(73) Boehm, D. A.; Gottlieb, P. A.; Hua, S. Z. *Sensors and Actuators, B: Chemical* **2007**, *B126*, 508-514.
(74) Arora, K.; Chand, S.; Malhotra, B. D. *Analytica Chimica Acta* **2006**, *568*, 259-274.
(75) Zourob, M.; Elwary, S.; Turner, A. *Principles of Bacterial Detection: Biosensors, Recognition Receptors and Microsystems*; Springer Science: New York, 2008.
(76) Lazcka, O.; Del Campo, F. J.; Munoz, F. X. *Biosensors & Bioelectronics* **2007**, *22*, 1205-1217.
(77) Yang, L.; Bashir, R. *Biotechnology Advances* **2008**, *26*, 135-150.
(78) *Golder Associates Ltd, Interim report on hydrogeological assessment, well integrity testing, geophysical surveys and land use inventory, bacteriological impacts, Walkerton town wells, Municipality of Brockton, County of Bruce, Ontario*: London, ON, 2000.
(79) Doyle, M. P.; Zhao, T.; Meng, J.; Zhao, S. *Escherichia coli O157:H7. In Food Microbiology Fundamentals and Frontiers.*; American Society for Microbiology: Washington D.C, 1997.
(80) Beran, G. W.; Shoeman, H. P.; Anderson, K. F. *Dairy Food Environ.Sci* **1991**, *11*, 189.
(81) Mead, P. S.; Slutsker, L.; Dietz, V.; McCaig, L. F.; Bresee, J. S.; Shapiro, C. *Emerging Infectious Diseases* **1999**, *5*, 607-625.
(82) Hobson, N. S.; Tothill, I.; Turner, A. P. F. *Biosensors & Bioelectronics* **1996**, *11*, 455-477.
(83) Bailey, J. S. *Journal of Food Protection* **1998**, *61*, 792-795.
(84) Belgrader, P.; Benett, W.; Hadley, D.; Richards, J.; Stratton, P.; Mariella, R., Jr.; Milanovich, F. *Science* **1999**, *284*, 449-450.

(85) Higgins, J. A.; Nasarabadi, S.; Karns, J. S.; Shelton, D. R.; Cooper, M.; Gbakima, A.; Koopman, R. P. *Biosensors & Bioelectronics* **2003**, *18*, 1115-1123.
(86) Edelstein, R. L.; Tamanaha, C. R.; Sheehan, P. E.; Miller, M. M.; Baselt, D. R.; Whitman, L. J.; Colton, R. J. *Biosensors & Bioelectronics* **2000**, *14*, 805-813.
(87) Gau, J., Jr.; Lan, E. H.; Dunn, B.; Ho, C.-M.; Woo, J. C. S. *Biosensors & Bioelectronics* **2001**, *16*, 745-755.
(88) Carbonnelle, E.; Beretti, J.-L.; Cottyn, S.; Quesne, G.; Berche, P.; Nassif, X.; Ferroni, A. *Journal of Clinical Microbiology* **2007**, *45*, 2156-2161.
(89) Pignone, M.; Greth, K. M.; Cooper, J.; Emerson, D.; Tang, J. *Journal of Clinical Microbiology* **2006**, *44*, 1963-1970.
(90) Grossman, H. L.; Myers, W. R.; Vreeland, V. J.; Bruehl, R.; Alper, M. D.; Bertozzi, C. R.; Clarke, J. *Proceedings of the National Academy of Sciences of the United States of America* **2004**, *101*, 129-134.
(91) Seo, K. H.; Brackett, R. E.; Frank, J. F.; Hilliard, S. *Journal of Food Protection* **1998**, *61*, 812-816.
(92) Yousef, A.; Carlstrom, C. *Food microbiology: A Laboratory Manual*; John Wiley and Sons, Inc: Hoboken, 2003.
(93) Meng, J.; Zhao, S.; Doyle, M. P.; Mitchell, S. E.; Kresovich, S. *International Journal of Food Microbiology* **1996**, *32*, 103-113.
(94) Inatomi, K. I.; Izuo, S. I.; Lee, S. S. *Letters in applied microbiology* **2006**, *43*, 296-300.
(95) Xia, N.; Hunt, T. P.; Mayers, B. T.; Alsberg, E.; Whitesides, G. M.; Westervelt, R. M.; Ingber, D. E. *Biomedical Microdevices* **2006**, *8*, 299-308.
(96) D'Souza, S. F. *Biosensors & Bioelectrronics* **2001**, *16*, 337-353.
(97) Wadkins, R. M.; Golden, J. P.; Pritsiolas, L. M.; Ligler, F. S. *Biosensors & Bioelectronics* **1998**, *13*, 407-415.
(98) Pyun, J. C.; Beutel, H.; Meyer, J. U.; Ruf, H. H. *Development of a biosensor for E. coli based on a flexural plate wave (FPW) transducer*, 1998.
(99) Koenig, B.; Gratzel, M. *Analytical Letters* **1993**, *26*, 2313-2328.
(100) Abdel-Hamid, I.; Ivnitski, D.; Atanasov, P.; Wilkins, E. *Biosensors & Bioelectronics* **1999**, *14*, 309-316.
(101) Abdel-Hamid, I.; Ivnitski, D.; Atanasov, P.; Wilkins, E. *Analytica Chimica Acta* **1999**, *399*, 99-108.
(102) Medina, M. B.; Van Houten, L.; Cooke, P. H.; Tu, S. I. *Biotechnology Techniques* **1997**, *11*, 173-176.
(103) Perkins, E. A.; Squirrell, D. J. *Biosensors & Bioelectronics* **2000**, *14*, 853-859.
(104) Zourob, M.; Mohr, S.; Brown, B. J. T.; Fielden, P. R.; McDonnell, M. B.; Goddard, N. J. *Analytical Chemistry* **2005**, *77*, 232-242.
(105) Watts, H. J.; Lowe, C. R.; Pollard-Knight, D. V. *Analytical Chemistry* **1994**, *66*, 2465-2470.
(106) Ferreira, A. P.; Werneck, M. M.; Ribeiro, R. M. *Biotechnology Techniques* **1999**, *13*, 447-452.
(107) DeMarco, D. R.; Saaski, E. W.; McCrae, D. A.; Lim, D. V. *Journal of Food Protection* **1999**, *62*, 711-716.
(108) King, K. D.; Anderson, G. P.; Bullock, K. E.; Regina, M. J.; Saaski, E. W.; Ligler, F. S. *Biosensors & Bioelectronics* **1999**, *14*, 163-170.
(109) Anderson, G. P.; King, K. D.; Gaffney, K. L.; Johnson, L. H. *Biosensors & Bioelectronics* **2000**, *14*, 771-777.

(110) Rowe, C. A.; Tender, L. M.; Feldstein, M. J.; Golden, J. P.; Scruggs, S. B.; MacCraith, B. D.; Cras, J. J.; Ligler, F. S. *Analytical Chemistry* **1999**, *71*, 3846-3852.
(111) Sipe, D. M.; Schoonmaker, K. P.; Herron, J. N.; Mostert, M. J. *Proceedings of SPIE-The International Society for Optical Engineering* **2000**, *3913*, 215-222.
(112) Ur, A.; Brown, D. F. *Journal of medical microbiology* **1975**, *8*, 19-28.
(113) Cady, P.; Dufour, S. W.; Lawless, P.; Nunke, B.; Kraeger, S. J. *Journal of clinical microbiology* **1978**, *7*, 273-278.
(114) Yang, L.; Ruan, C.; Li, Y. *Biosensors & Bioelectronics* **2003**, *19*, 495-502.
(115) Brewster, J. D.; Gehring, A. G.; Mazenko, R. S.; Van Houten, L. J.; Crawford, C. J. *Analytical Chemistry* **1996**, *68*, 4153-4159.
(116) Perez, F. G.; Mascini, M.; Tothill, I. E.; Turner, A. P. F. *Analytical Chemistry* **1998**, *70*, 2380-2386.
(117) Call, D. R.; Brockman, F. J.; Chandler, D. P. *International Journal of Food Microbiology* **2001**, *67*, 71-80.
(118) Katz, E.; Willner, I. *Electroanalysis* **2003**, *15*, 913-947.
(119) Zhao, Y. D.; Pang, D. W.; Hu, S.; Wang, Z. L.; Cheng, J. K.; Qi, Y. P.; Dai, H. P.; Mao, B. W.; Tian, Z. Q.; Luo, J.; Lin, Z. H. *Analytica Chimica Acta* **1999**, *388*, 93-101.
(120) Elsholz, B.; Woerl, R.; Blohm, L.; Albers, J.; Feucht, H.; Grunwald, T.; Juergen, B.; Schweder, T.; Hintsche, R. *Analytical Chemistry* **2006**, *78*, 4794-4802.
(121) Farabullini, F.; Lucarelli, F.; Palchetti, I.; Marrazza, G.; Mascini, M. *Biosensors & Bioelectronics* **2007**, *22*, 1544-1549.
(122) Balasubramanian, S.; Sorokulova, I. B.; Vodyanoy, V. J.; Simonian, A. L. *Biosensors & Bioelectronics* **2007**, *22*, 948-955.
(123) Neufeld, T.; Mittelman, A. S.; Buchner, V.; Rishpon, J. *Analytical Chemistry* **2005**, *77*, 652 -657.
(124) Thomas, J. H.; Kim, S. K.; Hesketh, P. J.; Halsall, H. B.; Heineman, W. R. *Analytical Chemistry* **2004**, *76*, 2700-2707.
(125) Gervais, L.; Gela, M.; Allain, B.; Tolba, M.; Brovko, L.; Zourob, M.; Mandeville, R.; Griffiths, M.; Evoy, S. *Sensors and Actuators B* **2007**, *125*, 615–621.
(126) Nanduri , V.; Sorokulova , I. B.; Samoylov , A. M.; Simonian , A. L.; Petrenko , V. A.; Vodyanoy , V. *Biosensors & Bioelectronics* **2007**, *22*, 986–992.
(127) Corgier, B. P.; Marquette, C. A.; Blum, L. J. *Journal of the American Chemical Society* **2005**, *127*, 18328-18332.
(128) Sambrook, J.; Russell, D. W. *Molecular Cloning: A Laboratory Manual*, 2nd ed.; Cold Spring Harbor Laboratory Press: New York., 1989.
(129) Marquette, C. A.; Lawrence, M. F.; Blum, L. J. *Analytical Chemistry* **2006**, *78*, 959-964.
(130) Nygren, H.; Hagenhoff, B.; Malmberg, P.; Nilsson, M.; Richter, K. *Microscopy Research and Technique* **2007**, *70*, 969-974.
(131) Goodridge, L.; Chen, J.; Griffiths, M. *International Journal of Food Microbiology* **1999**, *47*, 43-50.
(132) Goodridge, L.; Chen, J.; Griffiths, M. *Applied and Environmental Microbiology* **1999**, *65*, 1397-1404.
(133) Van Poucke, S. O.; Nelis, H. J. *Journal of Microbiological Methods* **2000**, *42*, 233-244.
(134) Oda, M.; Morita, M.; Unno, H.; Tanji, Y. *Applied and Environmental Microbiology* **2004**, *70*, 527-534.
(135) Deisingh, A. K.; Thompson, M. *Canadian Journal of Microbiology* **2004**, *50*, 69-77.
(136) *North Atlantic Treaty Organization, NATO Handbook on the Medical Aspects of NBC Defensive Operations, part II*: P-6(B), 1996.

(137) Bhunia, A. K. **2006**, *1*, 109-149.
(138) Sanderson, W. T.; Stoddard, R. R.; Echt, A. S.; Piacitelli, C. A.; Kim, D.; Horan, J.; Davies, M. M.; McCleery, R. E.; Muller, P.; Schnorr, T. M.; Ward, E. M.; Hales, T. R. *Journal of Applied Microbiology* **2004**, *96*, 1048-1056.
(139) Jernigan Daniel, B.; Raghunathan Pratima, L.; Bell Beth, P.; Brechner, R.; Bresnitz Eddy, A.; Butler Jay, C.; Cetron, M.; Cohen, M.; Doyle, T.; Fischer, M.; Greene, C.; Griffith Kevin, S.; Guarner, J.; Hadler James, L.; Hayslett James, A.; Meyer, R.; Petersen Lyle, R.; Phillips, M.; Pinner, R.; Popovic, T.; Quinn Conrad, P.; Reefhuis, J.; Reissman, D.; Rosenstein, N.; Schuchat, A.; Shieh, W.-J.; Siegal, L.; Swerdlow David, L.; Tenover Fred, C.; Traeger, M.; Ward John, W.; Weisfuse, I.; Wiersma, S.; Yeskey, K.; Zaki, S.; Ashford David, A.; Perkins Bradley, A.; Ostroff, S.; Hughes, J.; Fleming, D.; Koplan Jeffrey, P.; Gerberding Julie, L. *Emerging infectious diseases* **2002**, *8*, 1019-1028.
(140) Kaufmann, A. F.; Meltzer, M. I.; Schmid, G. P. *Emerging infectious diseases* **1997**, *3*, 83-94.
(141) Shah, J.; Wilkins, E. *Electroanalysis* **2003**, *15*, 157-167.
(142) Cooney, S. *Nature Medicine (New York, NY, United States)* **2001**, *7*, 1265.
(143) Higgins, J. A.; Ibrahim, M. S.; Knauert, F. K.; Ludwig, G. V.; Kijek, T. M.; Ezzell, J. W.; Courtney, B. C.; Henchal, E. A. *Annals of the New York Academy of Sciences* **1999**, *894*, 130-148.
(144) Lee, M. A.; Brightwell, G.; Leslie, D.; Bird, H.; Hamilton, A. *Journal of Applied Microbiology* **1999**, *87*, 218-223.
(145) Makino, S. I.; Cheun, H. I.; Watarai, M.; Uchida, I.; Takeshi, K. *Letters in Applied Microbiology* **2001**, *33*, 237-240.
(146) McBride, M. T.; Masquelier, D.; Hindson, B. J.; Makarewicz, A. J.; Brown, S.; Burris, K.; Metz, T.; Langlois, R. G.; Tsang, K. W.; Bryan, R.; Anderson, D. A.; Venkateswaran, K. S.; Milanovich, F. P.; Colston, B. W., Jr. *Analytical Chemistry* **2003**, *75*, 5293-5299.
(147) Patra, G.; Sylvestre, P.; Ramisse, V.; Therasse, J.; Guesdon, J.-L. *FEMS Immunology and Medical Microbiology* **1996**, *15*, 223-231.
(148) Uhl James, R.; Bell Constance, A.; Sloan Lynne, M.; Espy Mark, J.; Smith Thomas, F.; Rosenblatt Jon, E.; Cockerill Franklin, R., 3rd *Mayo Clinic proceedings* **2002**, *77*, 673-680.
(149) De, B. K.; Bragg, S. L.; Sanden, G. N.; Wilson, K. E.; Diem, L. A.; Marston, C. K.; Hoffmaster, A. R.; Barnett, G. A.; Weyant, R. S.; Abshire, T. G.; Ezzell, J. W.; Popovic, T. *Emerging Infectious Diseases* **2002**, *8*, 1060-1065.
(150) Longchamp, P.; Leighton, T. *Journal of Applied Microbiology* **1999**, *87*, 246-249.
(151) Phillips, A. P.; Martin, K. L. *The Journal of applied bacteriology* **1988**, *64*, 47-55.
(152) Phillips, A. P.; Martin, K. L.; Broster, M. G. *Journal of clinical microbiology* **1983**, *17*, 41-47.
(153) Smith, P. A.; MacDonald, S. *Journal of Chromatography, A* **2004**, *1036*, 249-253.
(154) Arakawa Edward, T.; Lavrik Nickolay, V.; Datskos Panos, G. *Applied optics* **2003**, *42*, 1757-1762.
(155) Speight, S. E.; Hallis, B. A.; Bennett, A. M.; Benbough, J. E. *Journal of Aerosol Science* **1997**, *28*, 483-492.
(156) Song, J. M.; Culha, M.; Kasili, P. M.; Griffin, G. D.; Vo-Dinh, T. *Biosensors & Bioelectronics* **2005**, *20*, 2203-2209.
(157) Farrell, S.; Halsall, H. B.; Heineman, W. R. *Analyst* **2005**, *130*, 489-497.
(158) Borthwick, K. A. J.; Love, T. E.; McDonnell, M. B.; Coakley, W. T. *Analytical Chemistry* **2005**, *77*, 7242-7245.

(159) King, D.; Luna, V.; Cannons, A.; Cattani, J.; Amuso, P. *Journal of Clinical Microbiology* **2003**, *41*, 3454-3455.
(160) Bruno, J. G.; Yu, H. *Applied and Environmental Microbiology* **1996**, *62*, 3474-3476.
(161) Gatto-Menking, D. L.; Yu, H.; Bruno, J. G.; Goode, M. T.; Miller, M.; Zulich, A. W. *Biosensors & Bioelectronics* **1995**, *10*, 501-507.
(162) Stopa, P. J. *Cytometry* **2000**, *41*, 237-244.
(163) Park, T. J.; Park, J. P.; Seo, G.-M.; Chai, Y. G.; Lee, S. Y. *Journal of Microbiology and Biotechnology* **2006**, *16*, 1713-1719.
(164) Floriano, P. N.; Christodoulides, N.; Romanovicz, D.; Bernard, B.; Simmons, G. W.; Cavell, M.; McDevitt, J. T. *Biosensors & Bioelectronics* **2005**, *20*, 2079-2088.
(165) Rongzhang, H.; Dianbing, W.; Xian'en, Z.; Guomin, Z.; Hongping, W.; Ruifu, Y.; Zhiping, Z.; Zhenxing, C.; Yongchao, G.; Zongqiang, C.; Yafeng, Z. *Biosensors and Bioelectronics* **2009**, *24*, 1330-1335.
(166) Wan, J.; Johnson, M. L.; Guntupalli, R.; Petrenko, V. A.; Chin, B. A. *Sensors and Actuators, B: Chemical* **2007**, *B127*, 559-566.
(167) Huang, S.; Hu, J.; Wan, J.; Johnson, M. L.; Shu, H.; Chin, B. A. *Materials Science & Engineering, C: Biomimetic and Supramolecular Systems* **2008**, *28*, 380-386.
(168) Johnson, M. L.; Wan, J.; Huang, S.; Cheng, Z.; Petrenko, V. A.; Kim, D.-J.; Chen, I. H.; Barbaree, J. M.; Hong, J. W.; Chin, B. A. *Sensors and Actuators, A: Physical* **2008**, *A144*, 38-47.
(169) Campbell, G. A.; Mutharasan, R. *Biosensors & Bioelectronics* **2006**, *21*, 1684-1692.
(170) Campbell, G. A.; deLesdernier, D.; Mutharasan, R. *Sensors and Actuators, B: Chemical* **2007**, *B127*, 376-382.
(171) Campbell, D. P.; Gottfried, D. S.; Scheffter, S. M.; Beck, M. C.; Halpern, M. D. *Abstracts of Papers, 226th ACS National Meeting, New York, NY, United States, September 7-11, 2003* **2003**, ENVR-085.
(172) Rowe-Taitt, C. A.; Golden, J. P.; Feldstein, M. J.; Cras, J. J.; Hoffman, K. E.; Ligler, F. S. *Biosensors and Bioelectronics* **2000**, *14*, 785-794.
(173) Rowe-Taitt, C. A.; Hazzard, J. W.; Hoffman, K. E.; Cras, J. J.; Golden, J. P.; Ligler, F. S. *Biosensors and Bioelectronics* **2000**, *15*, 579-589.
(174) Tims, T. B.; Lim, D. V. *Journal of Microbiological Methods* **2004**, *59*, 127-130.
(175) Hang, J.; Sundaram, A. K.; Zhu, P.; Shelton, D. R.; Karns, J. S.; Martin, P. A. W.; Li, S.; Amstutz, P.; Tang, C.-M. *Journal of Microbiological Methods* **2008**, *73*, 242-246.
(176) Zourob, M.; Mohr, S.; Brown, B. J. T.; Fielden, P. R.; McDonnell, M.; Goddard, N. J. *Sensors and Actuators B: Chemical* **2003**, *90*, 296-307.
(177) Zourob, M.; Mohr, S.; Brown, B. J. T.; Fielden, P. R.; McDonnell, M. B.; Goddard, N. J. *Lab on a Chip* **2005**, *5*, 1360-1365.
(178) Zourob, M.; Hawkes, J. J.; Coakley, W. T.; Brown, B. J. T.; Fielden, P. R.; McDonnell, M. B.; Goddard, N. J. *Analytical Chemistry* **2005**, *77*, 6163-6168.
(179) Yemini, M.; Levi, Y.; Yagil, E.; Rishpon, J. *Bioelectrochemistry* **2007**, *70*, 180-184.
(180) Pal, S.; Ying, W.; Alocilja, E. C.; Downes, F. P. *Biosystems Engineering* **2008**, *99*, 461-468.
(181) Pal, S.; Alocilja, E. C.; Downes, F. P. *Biosensors & Bioelectronics* **2007**, *22*, 2329-2336.
(182) Pal, S.; Alocilja, E. C. *Biosensors and Bioelectronics* **2009**, *24*, 1437-1444.
(183) Brooksby, P. A.; Downard, A. J. *Langmuir* **2004**, *20*, 5038-5045.
(184) Allongue, P.; Delamar, M.; Desbat, B.; Fagebaume, O.; Hitmi, R.; Pinson, J.; Saveant, J.-M. *Journal of the American Chemical Society* **1997**, *119*, 201-207.
(185) Cho, Y.; Ivanisevic, A. *Journal of Physical Chemistry B* **2004**, *108*, 15223-15228.

(186) Zhang, F.; Srinivasan, M. P. *Langmuir* **2004**, *20*, 2309-2314.
(187) Hall Robert, H. *Microbes and infection* **2002**, *4*, 425-432.
(188) Vasavada, P. C. *Food Testing & Analysis* **1997**, *3*, 18-20, 22-23, 47.
(189) Van Der Zee, H.; In't Veld, H. J. H. *Journal of AOAC International* **1997**, *80*, 934-940.
(190) Swaminathan, B.; Feng, P. *Annual Review of Microbiology* **1994**, *48*, 401-426.
(191) Krt, B. *FEMS Immunology and Medical Microbiology* **1999**, *24*, 293-297.
(192) Ekong, T. A. N.; McLellan, K.; Sesardic, D. *Journal of Immunological Methods* **1995**, *180*, 181-191.
(193) Pitt, M. L. M.; Little, S. F.; Ivins, B. E.; Fellows, P.; Barth, J.; Hewetson, J.; Gibbs, P.; Dertzbaugh, M.; Friedlander, A. M. *Vaccine* **2001**, *19*, 4768-4773.
(194) Hale, M. L.; Stiles, B. G. *Toxicon* **1999**, *37*, 471-484.
(195) Valdivieso-Garcia, A.; Riche, E.; Abubakar, O.; Waddell, T. E.; Brooks, B. W. *Journal of Food Protection* **2001**, *64*, 1166-1171.
(196) Varshney, M.; Li, Y. *Biosensors & Bioelectronics* **2007**, *22*, 2408-2414.
(197) Varshney, M.; Li, Y.; Srinivasan, B.; Tung, S. *Sensors and Actuators B: Chemical* **2007**, *128*, 99-107.
(198) Yang, L.; Li, Y. *Journal of Microbiological Methods* **2006**, *64*, 9-16.
(199) Liu, R. H.; Yang, J.; Lenigk, R.; Bonanno, J.; Grodzinski, P. *Analytical Chemistry* **2004**, *76*, 1824-1831.
(200) Varshney, M.; Li, Y.; Nanapanneni, R.; Johnson, M. G.; Griffis, C. L. *Journal of Rapid Methods and Automation in Microbiology* **2003**, *11*, 111-131.
(201) Bennett, A. R.; MacPhee, S.; Betts, R. P. *Letters in applied microbiology* **1996**, *22*, 237-243.
(202) Che, Y. H.; Yang, Z.; Li, Y.; Paul, D.; Slavik, M. *Journal of Rapid Methods and Automation in Microbiology* **1999**, *7*, 47-59.
(203) Yang, L.; Ruan, C.; Li, Y. *Journal of Rapid Methods and Automation in Microbiology* **2001**, *9*, 229-240.
(204) Gitis, V.; Adin, A.; Nasser, A.; Gun, J.; Lev, O. *Water Research* **2002**, *36*, 4227-4234.
(205) Pethig, R.; Markx, G. H. *Trends in Biotechnology* **1997**, *15*, 426-432.
(206) Oh, S. J.; Ju, J.; Kim, B. C.; Ko, E.; Hong, B. J.; Park, J.-G.; Park, J. W.; Choi, K. Y. *Nucleic Acids Research* **2005**, *33*, 10 e90.
(207) Le Berre, V.; Trévisiol, E.; Dagkessamanskaia, A.; Sokol, S.; Caminade, A. M.; Majoral, J. P.; Meunier, B.; François, J. *Nucleic Acids Research* **2003**, *31*, 16 e88.
(208) Benters, R.; Niemeyer, C. M.; Drutschmann, D.; Blohm, D.; Wöhrle, D. *Nucleic Acids Research* **2002**, *30*, 2 e10.
(209) Le Berre, V.; Trévisiol, E.; Dagkessamanskaia, A.; Sokol, S.; Caminade, A. M.; Majoral, J. P.; Meunier, B.; François, J. *Nucleic Acids Research* **2003**, *31*, 16 e88.